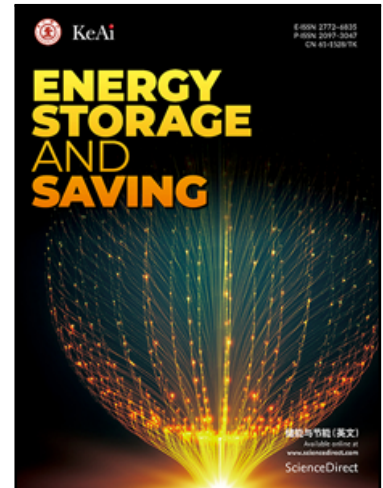


Journal Pre-proof

Review on Thermal Management Technologies for Electronics in
Spacecraft Environment

Yi-Gao Lv , Y Yi-Gao Lv , Yao-Ting Wang , Tong Meng ,
Qiu-Wang Wang , Wen-Xiao Chu

PII: S2772-6835(24)00013-X
DOI: <https://doi.org/10.1016/j.enss.2024.03.001>
Reference: ENSS 70



To appear in: *Energy Storage and Saving*

Received date: 1 November 2023
Revised date: 16 March 2024
Accepted date: 27 March 2024

Please cite this article as: Yi-Gao Lv , Y Yi-Gao Lv , Yao-Ting Wang , Tong Meng ,
Qiu-Wang Wang , Wen-Xiao Chu , Review on Thermal Management Technologies
for Electronics in Spacecraft Environment, *Energy Storage and Saving* (2024), doi:
<https://doi.org/10.1016/j.enss.2024.03.001>

This is a PDF file of an article that has undergone enhancements after acceptance, such as the addition of a cover page and metadata, and formatting for readability, but it is not yet the definitive version of record. This version will undergo additional copyediting, typesetting and review before it is published in its final form, but we are providing this version to give early visibility of the article. Please note that, during the production process, errors may be discovered which could affect the content, and all legal disclaimers that apply to the journal pertain.

© 2024 The Authors. Published by Elsevier B.V. on behalf of KeAi Communications Co. Ltd.
This is an open access article under the CC BY-NC-ND license
(<http://creativecommons.org/licenses/by-nc-nd/4.0/>)

Manuscript for *Energy Storage and Saving*

Review on Thermal Management Technologies for Electronics in Spacecraft Environment

Yi-Gao Lv^a, Y Yi-Gao Lv^a, Yao-Ting Wang^b, Tong Meng^b, Qiu-Wang Wang^a, Wen-Xiao Chu^{a,*}

^a Key Laboratory of Thermo-fluid Science and Engineering, Ministry of Education, Xi'an Jiaotong University, Xi'an, Shaanxi 710049, China

^b Xi'an Institute of Space Radio Technology, No. 504 Chang'an Eastern Street, Xi'an, Shaanxi 710100, China

*Corresponding author: Wen-Xiao Chu, E-mail address: wxchu84@xjtu.edu.cn

Authors checklist

Yi-Gao Lv, Writing – original draft

Yao-Ting Wang, Conceptualization, Supervision

Tong Meng, Writing – original draft

Qiu-Wang Wang, Supervision

Wen-Xiao Chu, Conceptualization, Supervision, Writing – review & editing

Abstract

Due to the rapid development of the space industry, ever higher demands are being made for the optimization and improvement of spacecraft thermal management systems. Thermal control technology has become one of the key bottlenecks that restrict the level of spacecraft design. In this paper, the thermal management technologies (TMTs) for spacecraft electronics are reviewed according to the different heat transfer processes, including heat acquisition, heat transport, and heat rejection. The researches on efficient heat acquisition include the utilization of high thermal conductance materials, the development of novel package structure based on micro-/nano-electromechanical system (MEMS/NEMS) technologies, and advanced near-junction microfluidic cooling techniques. For the heat transport process, various heat pipes and mechanical pumped fluid loops (MPFLs) are widely implemented to transport heat from heat generation components to the ultimate heat sinks. The heat pipes are divided into two categories based on their structure layout, i.e., separated heat pipes and unseparated heat pipes. The merits and demerits of these heat pipes and MPFLs (including the single-phase MPFL and the two-phase MPFL) are discussed and summarized respectively. In terms of the heat rejection for spacecraft, thermal radiators are normally the sole option due to the unique space environment. To meet the requirements of large heat dissipation power and fluctuated thermal environment, research efforts on the radiators mainly focus on the development of deployable radiators, variable emissivity radiators, and the combination with other techniques. Due to the fluctuated characteristics of the heat power of internal electronics and the

outer thermal environment, the phase change materials (PCMs) exhibit great advantages in this scenario and have attracted a lot of research attention. This review aims to serve as a reference guide for the development of thermal management system in the future spacecraft.

Keywords: *Thermal management; electronics; spacecraft; heat pipe; mechanically pumped fluid loop; radiator; phase change material*

Journal Pre-proof

Nomenclature

APG	annealed pyrolytic graphite
ACCS	Active CryoCubeSat
CCHP	constant conductance heat pipe
CFRP	carbon fiber reinforced polymer
CHF	critical heat flux
CPL	capillary pumped loop
CTE	coefficient of thermal expansion
DARPA	Defense Advanced Research Projects Agency
DMLS	direct metal laser sintering
HEMT	high-electron-mobility transistor
HLHP	hybrid loop heat pipe
HS	heat spreader
ICED	impingement cooled embedded diamond
k	thermal conductivity, $\text{W}\cdot\text{m}^{-1}\cdot\text{K}^{-1}$
LHP	loop heat pipe
LMTA	low melting temperature alloy
MEMS/NEMS	micro-electromechanical system/nano-electromechanical system
MPFL	mechanical pumped fluid loop
NCG	Non-condensable gas
NJTT	Near-Junction Thermal Transport
OHP	oscillating heat pipe
PCM	phase change material
PTC	pulse tube cryocoolers
R	thermal resistance, $\text{cm}^2\cdot\text{K}\cdot\text{W}^{-1}$
SHP	sorption heat pipe
TEC	thermoelectric cooler
TESU	thermal energy storage unit
TIM	thermal interface material
TMT	thermal management technology
VC	vapor chamber
VCHP	variable conductance heat pipe

Subscripts

xy	in plane direction
z	through-plane direction

1. Introduction

In recent years, the evolution of spacecraft technology provides tremendous conveniences and support to space exploitation, telecommunications, scientific observation, weather monitoring, navigation, and data-relay services, etc. However, the operation of electronics in spacecraft environment has to overcome many extraordinary challenges [1-3]. Among these are the effects of micro-gravity, atmospheric drag, the degradation of external surfaces by atomic oxygen, complications generated by a vacuum which leads to material degassing and cold soldering phenomena, as well as the harsh conditions of potent solar and cosmic radiation, space debris, and energized particles [4]. In this regard, a variety of targeted design and measures must be taken to ensure the stable and efficient operation of the in-orbit equipment where the thermal management technologies (TMTs) play significant roles. Studies have shown that, beyond its threshold junction temperatures of approximately 80 to 90 °C, the dependability of a silicon chip may diminish by roughly 10% with every increase of 2 °C [5, 6]. Depending on the spacecraft functions, various types of spacecraft are launched such as space stations, manned and cargo spacecrafts, space probes and various man-made satellites, etc. Especially, a diversity of satellites presents rapid increasing market demands in recent years [7]. Regarding the satellites in-orbit, various electronic devices are implemented, such as electrical propulsion units, transmit/receive (T/R) modules of spaceborne radars, cameras, sensors and plenty of low power multi-output DC/DC converters, etc. Each of these components is designed with a specific temperature tolerance to satisfy both survival and functional criteria throughout every stage of the mission.

Due to the special operating environment of spacecrafts, some unique constraints should be considered when designing thermal management systems. A typical illustration of the thermal challenges faced in orbit is that one side of a spacecraft can be subjected to direct sunlight, while the opposing side is shrouded in darkness and the extreme cold of space. This scenario results in sharp temperature gradients that can compromise the dependability and precision of onboard transponders. Besides, microgravity or weightlessness effect might reduce the temperature controlling precision of components, e.g., heat pipes, while the features may not be revealed during the ground testing process [8]. The main reason is the startup problems in the two-phase component where the vapor bubble migration and stagnation occur. What makes the thermal management system complex in space missions is the fact that the sole heat rejection component is the radiator where the heat is released to the ambient space environment via thermal radiation. The mechanical shock and high-vibration concerns should also be considered from the mechanical integrity point of view. On the other hand, with the demand of high-speed processing characteristics, the heat generation of electronics in spacecraft environment rises rapidly. Accordingly, the increasingly local high heat flux necessitates the development of

novel, effective and reliable TMTs [9]. Moreover, smaller satellites are promising to provide more advanced capabilities, indicating extra challenges to the applications of TMTs [10]. The integration of numerous temperature-sensitive electronic elements within T/R modules means that any temperature increase beyond the junction threshold could significantly degrade the output of excitation currents. Furthermore, it may adversely affect the electromagnetic capabilities of antennas. Fluctuating temperatures can lead to thermal deformation and result in temperature-related deviations in the myriad of electronic components in T/R modules [11, 12]. Moreover, within a full daylight and eclipse operation period in-orbit, there are strong variations in the radiant energy received from the sun and other celestial bodies. Besides, the on-board radar electronic power-on and off operation could yield drastic temperature variations and large thermal gradients which can apparently affect the devices reliability and even cause device failure [13]. Consequently, considering both the harsh operating environment and the high heat flux density on-board, as shown in Fig. 1, the thermal management technologies applied to electronics in spacecraft environment become increasingly challengeable. For overcoming the above challenges and maintaining the temperature within ideal ranges, large number of modern TMTs and carefully designed systems were proposed over the last decades [14-16].

This paper presents a review on the TMTs for electronics in spacecraft environment based on heat transfer processes, including heat acquisition, heat transport, and heat rejection, as summarized in Fig.2. In section 2, recent investigations on efficient heat acquisition are detailly discussed, including the utilization of high thermal conductance materials, development of novel package structures based on the MEMS/NEMS technologies and advanced near-junction microfluidic cooling techniques. Then, the development of various kinds of heat pipe and mechanical pumped fluid loop (MPFL) for the heat transport process are introduced. The merits and demerits are also summarized with the application of heat pipes and phase change materials (PCMs). In section 3, efforts on developing advanced radiators for ultimate heat rejection are discussed, including the development of deployable radiators and variable emissivity radiators and those combining with other techniques. Eventually, section 4 concludes the main concerns, dominant constrains as well as the candidate breakthrough techniques of the next-generation TMTs for future spacecrafts.

2 TMTs for heat acquisition and transport processes

In this section, both passive and active methods for the processes of heat acquisition and heat transport are discussed, including applications of efficient heat conduction materials, heat pipes, MPFLs and advanced microchannel, microjet impingement and spray cooling techniques. Consequently, studies on the PCMs which are usually applied with the combination of above-mentioned TMTs are also reviewed.

2.1 Efficient heat conduction technologies

2.1.1 Material-based solutions

In order to effectively transport the heat from the originated place to the ultimate heat sink, advanced materials with excellent thermal conduction performance are usually implemented. Generally, heat spreaders (HSs) and thermal interface materials (TIMs) play crucial roles to efficiently smooth the heat transfer path. Over the last decades, a large variety of novel materials were developed. As shown in Fig. 3, according to Silverman et al. [17], the evolution of materials designed for spacecraft thermal management reflects a shift from isotropic metals like aluminum, proceeding to carbon-reinforced polymers, and moving forward to advanced materials including carbon-carbon composites and annealed pyrolytic graphite (APG). Typically, composites are composed of at least two disparate substances. A primary substance acts as a host matrix, whereas another serves as the reinforcement, commonly in the form of fibers embedded in the matrix. With thermosetting compounds such as epoxy, bismaleimide, and polyimide often employed as standard matrix materials, both ceramic and metal matrix composites have garnered considerable interest for use in the aerospace sector in recent years due to their weight saving feature as well as the high-temperature capability/oxidation resistance characteristics [18]. Table 1 summarizes the advanced materials reported in literatures. It is evident that the carbon-based composites predominate because of their high thermal conductivity and lightweight features. Note that their thermal properties are almost completely anisotropic, potentially limiting their extensive application.

Various carbon fiber materials have been developed and are considered as the most advantageous candidates, which always exhibit low coefficient of thermal expansion (CTE), ultra-high-thermal conductivity and low-density characteristics. For spacecraft where mass reduction is paramount, carbon-polymer composites are increasingly favored over aluminum for use as thermal radiator materials, primarily due to their reduced weight. This preference not only leads to considerable cost reductions by eliminating the necessity for heat pipes integration but also facilitates overall spacecraft design. Subsequent developments saw the advent of carbon-carbon composites that promise to boost thermal efficiency with their superior z-directional thermal conductivity relative to their polymer-based counterparts. Although recent studies have highlighted the extensive benefits of carbon-carbon composites in space technology, the high cost of production and extensive lead times associated with the intricate carbonization and densification processes could hinder their widespread implementation [18]. In addition to the above conventional carbon-based composites, APG also emerges as a promising candidate, presenting as a highly ordered crystalline material with the thermal conductivity exceeding $1500 \text{ W}\cdot\text{m}^{-1}\cdot\text{K}^{-1}$ [17]. However, the brittle nature of APG's strength properties poses significant challenges to its direct application in electronic cooling.

To tackle this issue, the Northrop Grumman Space Technology (NGST) verified and applied an innovative encapsulated APG concept [17]. The ingenuity of this material lies in its design, where an encapsulant such as aluminum or carbon-polymer composite is mechanically isolated from the APG core by a zero-shear interface, which enhances the thermal effectiveness of the assembly up to five times that of standard aluminum. This separation permits tailored optimization of the individual materials; hence, the encapsulation materials control attributes like robustness, rigidity, and thermal expansion, while the embedded APG dictates the thermal conduction. As a consequence, the encapsulated APG facilitates a more economical fine-tuning of the whole system. Concurrently, the K Technology Corporation developed a distinctive patented process for embedding APG within a durable frame [19], a technique implemented in diverse applications from extensive radiator plates to compact electronic bases. Despite these advancements, the heat spreading capabilities of APG in these roles are yet to reach their peak. Introduction of thermal vias has been a solution to increase the effective cross-plane conduction; for instance, with a copper/tungsten shell, the thermal vias can elevate the conductivity from a mere $10 \text{ W}\cdot\text{m}^{-1}\cdot\text{K}^{-1}$ to a substantial $230 \text{ W}\cdot\text{m}^{-1}\cdot\text{K}^{-1}$.

On the other hand, the adoption of TIMs plays a significant role in improving the heat transfer performance by filling the gap between contact surfaces of electronic devices [20]. Within the scope of the Defense Advanced Research Projects Agency's (DARPA) portfolio for Thermal Management Technologies, particularly under the Nano Thermal Interfaces initiative, the prime goal is to engineer TIMs utilizing micro and nano-scale technologies. These TIMs are envisioned to deliver a substantial decrease in thermal resistance at the interface layer, situated between the rear surface of an electronic device and the subsequent packaging layer, which could either function as a heat spreader or a heat sink. The developed TIMs comprise materials such as copper nanosprings, which offer superior compliance, along with laminated solder and flexible graphite films, as well as multi-walled carbon nanotubes with layered metallic bonding materials, and open-ended carbon nanotubes to enhance adhesion and conduction [21, 22]. Within the space environment, these TIMs are exposed to high doses of Gamma radiation and the thermal contact resistance of the TIM can be adversely affected due to the significant radiation exposure with typical design lifetimes of 5 to 10 years. Sayer et al. [23] investigated the effect of radiation-induced aging on the thermal contact conductance of various widely used thermally conductive yet electrically insulating interface materials in satellite systems. The findings revealed that such aging from radiation caused a significant surge in thermal contact resistance in the samples evaluated. Moreover, this could enhance the fragility of the interface materials, leading to cracks or peeling of the TIM, which might contaminate the system.

Moreover, the theoretical thermal conductivity of carbon nanotubes reaching $6000 \text{ W}\cdot\text{m}^{-1}\cdot\text{K}^{-1}$ has provided a compelling choice for thermal conductive material. Ever since their inception in 1991, carbon nanotubes have

captivated considerable interest due to their unique electrical, mechanical, and thermal characteristics, paving the way for a myriad of applications. A particularly notable application is their potential as TIMs [24]. Despite the remarkable properties of individual carbon nanotubes in terms of strength, conductivity, and heat transfer, composites made from aggregated carbon nanotubes often face challenges like anisotropic thermal properties and elevated inter-junction resistance. Puneet et al. [25] presented a concise review of scalable production techniques that hold the promise of integrating carbon nanotubes into TIMs, structural reinforcements, and ancillary power systems like energy-storage devices, particularly for use in aerospace domains. Beyond carbon nanotubes, other innovative nanomaterials such as copper nanosprings are also making transformative strides in advanced thermal management for aerospace high-power electronic systems. Barako et al. [26] discussed the potential and obstacles of systematically embedding nanomaterials throughout the thermal resistance pathway, from high-heat-flux sources to the system-level heat dissipation. They advocated for a “materials-by-design” strategy for the deliberate creation of nanostructures with tailored properties on demand. Fig. 4 depicts a holistic model for incorporating nanomaterials into an integrated thermal management scheme; from co-designing electronic and thermal layouts at the nanoscale to managing heat at the system level, purpose-built nanomaterials have the potential to exhibit exceptional heat transport qualities. Yet, there remain sizeable challenges, including enhancing understanding of the foundational science, refining production processes for scale, and engineering nanomaterials to fulfill their latent capabilities.

2.1.2 Micro/nano technology-based solutions

In addition to the development of aforementioned thermal conductive materials, the applications of novel package structures and advanced manufacture processes have also been developed to achieve efficient near-junction thermal transport [27]. For example, the GaN high-electron-mobility transistor (HEMT) technology attracts great attention for microprocessors, power semiconductor lasers and radar amplifiers, with particular focus on the thermal resistance challenges present at the levels of the device, substrate, package, and overall system. Chao et al. [28] delineated recent advancements in the fabrication of GaN-on-diamond HEMTs utilizing a low-temperature device-transfer methodology. The devices were initially crafted using a GaN-on-SiC epitaxial wafer, then separated from the SiC substrate and bonded onto a diamond base with superior thermal conductivity at a reduced temperature. Performance assessments of the $12 \times 50 \mu\text{m}$ GaN-on-diamond HEMTs revealed top-tier electrical operation. These units not only showed marginally lower channel temperatures compared to the GaN-on-SiC counterparts but also produced radio frequency power that was 3.6 times greater within the identical active area. Additionally, the transfer technique for the GaN devices was shown to conserve the inherent electrical performance typical of GaN-on-SiC transistors while benefiting from the

excellent thermal properties of the diamond substrates. Meanwhile, Radway [29] examined a wafer bonded GaN-on-SiC HEMTs, as a thermally advantageous substitute for traditional growth configurations. Illustrated by Fig. 5, the dual wafer bonding technique for GaN-on-SiC HEMTs is revealed. The findings suggested that this novel bonded approach holds promise for crafting cutting-edge GaN HEMTs, producing performance on par with GaN-on-diamond technology. However, it was also noted that additional advancements in the fabrication process were necessary. Bar-Cohen et al. [30, 31] summarized the accomplishments of the DARPA Near-Junction Thermal Transport (NJTT) program alongside contemporary findings from the active DARPA Intra-Chip Embedded Cooling (ICECool) program. The process of cultivating or bonding diamond to GaN epitaxy has facilitated a threefold to fivefold enhancement in the power management capacity for each unit area of a transistor. The DARPA NJTT project set a benchmark for participating groups to showcase an increase in surface output power from a GaN transistor that exceeds three times the performance of a standard GaN transistor in the industry. Furthermore, innovative technologies, such as diamond grown on GaN, diamond grown in thermal vias as well as GaN bonded to diamond, were also introduced. Nonetheless, while the GaN composite with high-thermal-conductivity substrates such as SiC and diamond are promising, the thermal resistances at GaN-substrate interfaces should be paid more attention. Cho et al.[32] conducted a thermal analysis on GaN-on-SiC and GaN-on-diamond substrates by applying a mix of picosecond time-domain thermo reflectance and DC Joule heating methods. The results revealed that thermal interface resistances in the GaN-diamond composites were comparably higher than those found in the GaN-on-SiC samples. Consequently, diminishing the thermal interface resistance associated with GaN-on-diamond could substantially improve the cooling efficiency of HEMT-on-diamond devices.

The necessity for lightweight and compact design, alongside low-power consumption and closely integrated electronics, renders MEMS-based electronic devices exceedingly attractive for minimizing the size and weight of spacecraft without sacrificing functionality [33]. Recently, the near-junction embedded cooling technology has caught the eyes of scientists. It was reported that the embedded cooling, which is applied in power electronic component packages based on MEMS technology, can improve the heat flux by 3 to 10 times higher depending on the added high thermal conductivity medium [16]. Recent embedded cooling efforts were funded by DARPA Microsystems Technology Office and have focused on reducing the near-junction thermal resistance. The diamond substrates as well as efficient heat removal technologies with convective and evaporative microfluidics were applied. As the result, higher heat removal capability was achieved by replacing the solid heat transfer medium with two-phase working fluid. Won et al.[34] delved into the foundational and ultimate cooling constraints associated with junction-to-fluid cooling, facilitated by cutting-edge thermal management technologies such as GaN-diamond composites and nano-engineered heat sinks.

Usually, the near-junction thermal transport with fluid is also named microfluidic cooling. Either cold plates or evaporators were regarded as the near-junction cooling devices, which are integrated in a single-phase or two-phase mechanical pumped fluid loop (MPFL). The more detailed discussions will be presented in Section 2.3.

2.2 Heat pipes

With the rapid increase of heat flux of electronic devices onboard spacecrafts, traditional heat conduction methods involving metal or carbon-based composites often fall short in heat dissipation for certain applications. In response to this challenge, a kind of passive two-phase heat transfer device, named as heat pipe, has been developed and commonly adopted in the spacecraft TMS due to its excellent heat transfer capabilities, minimal weight contribution, absence of maintenance requirements, and high reliability. In 2015, Shukla [35] presented an overview of heat pipes for aerospace applications, reviewing the historical perspectives, principles of operation and various functional heat pipe. At present, there are a variety of heat pipes with different shapes, configurations and filling mediums available in the market. Considering the structural layouts, heat pipes used for space missions can be divided into two categories, i.e., unseparated heat pipes and separated heat pipes. The main distinction between the two types is the presence of separated vapor line and liquid line. Generally, the separated heat pipes include the loop heat pipe (LHP), capillary pumped loop (CPL), hybrid loop heat pipe (HLHP), etc. In contrast, the unseparated heat pipes include the cylindrical heat pipe, oscillating heat pipe (OHP) and flat heat pipe which is also called vapor chamber (VC), etc.

2.2.1 Unseparated heat pipes

Over the last decades, various unseparated heat pipe have been developed, as summarized in Table 2. It can be observed that the variable conductance heat pipe (VCHP) has been widely used since 1970s. Then, constant conductance heat pipe (CCHP) employing diverse working fluids, wick structure and materials has progressed to fulfill specific operational requirements. Primarily, the large heat transfer capacity and high operation reliability are the main design objective.

As shown in Fig. 6, the VCHP operates similarly to conventional heat pipes but distinguishes itself by incorporating a reservoir charged with noncondensable gas (NCG), like argon or helium, at the condenser segment. The effective conductance of the VCHP is modulated by adjusting the active length of the condenser, that is, the condenser surface area available for condensation, thereby indirectly regulating the evaporator temperature. As the thermal load escalates, the working fluid's temperature-responsive saturation pressure rises, causing the NCG to be compressed into the reservoir. In contrast, when the saturation pressure of the working fluid declines, the NCG is permitted to return into

the condenser, expanding within the space [36]. In the earlier time, Mock et al. [37] designed a VCHP system to provide thermal control for a transmitter experiment package aboard a communication satellite. Results showed that the VCHP system could provide effective heat rejection during power-on operation and minimize the heat leak during power-down operation. Moreover, the VCHP could also be used in combination with other thermal control devices. Cleary et al. [38] evaluated the efficiency of a VCHP in combination with a thermoelectric cooler (TEC) for precision temperature regulation of photonic elements, aiming to reduce power usage. They measured the power consumption of a TEC-VCHP assembly and contrasted it with that of a TEC-CCHP configuration. The findings indicated that the VCHP provided satisfied temperature management across varying heat loads at a fixed ambient temperature. Furthermore, it was observed that the maximum power consumption of the TEC within the TEC-VCHP assembly was cut by over 40%.

Moreover, it has been shown through terrestrial experiments that an innovative VCHP with a hot reservoir can offer significantly more precise passive thermal control than a traditional VCHP equipped with a cold-biased reservoir. Recently, NASA have tested a novel hot reservoir VCHP on the International Space Station in 2017. However, the microgravity testing failed though the ground testing was successful. ACT Inc., in collaboration with Case Western Reserve University, embarked on a detailed and foundational research project to gain a deeper understanding of the intricate multi-species transport phenomena within a hot reservoir VCHP. Based on this study, they proposed a new loop hot reservoir VCHP design, aimed at bolstering the reliability of the VCHP in both terrestrial and microgravity operations. Fig. 7 shows the schematic that contrasts the traditional VCHP with this new loop configuration, featuring a hot reservoir VCHP paired with two NCG tubes [39]. The internal tube coming out from the NCG reservoir and enters the evaporative section of the heat pipe, while an external tube connects the condenser's end back to the reservoir. This configuration anticipates that the secondary fluid flow (with the vapor considered as the "primary" flow) will help purge and move through the loop in a favorable direction, moving from the reservoir through the internal tube to the condenser (as indicated by the black arrows). The detailed information on the development of this novel hot reservoir VCHP with advanced fluid management features, including both numerical and experimental efforts, can be found in Ref. [40].

Given the significant impact of wick structure and materials on the thermal efficacy of heat pipes, considerable research has been directed toward developing novel capillary wicks. Typically, hybrid wick heat pipes feature a porous wick in the evaporator section, complemented by a grooved wick design throughout the adiabatic and condenser sections. The sintered powder metal wick in the evaporator is adept at operating against gravity and can manage higher heat fluxes. The grooved wick in the condenser and adiabatic sections enables the heat pipe to perform effectively in the vacuum of space, transferring heat over long distances. In a recent initiative, ACT Inc., in collaboration with NASA's

Marshall Space Flight Center and Johnson Space Center, has planned to undertake testing and validation of the hybrid wick VCHPs featuring warm reservoirs in Low-Earth Orbit on the International Space Station [36]. Preliminary tests indicated that the heat flux might increase to more than $50 \text{ W}\cdot\text{cm}^{-2}$ by using the hybrid wick that containing screen mesh or sintered evaporator wicks for the evaporator region, as shown in Fig. 8. These findings highlight the promise of hybrid capillary wicks in managing the high heat fluxes that next-generation spacecraft are likely to encounter. It should be noted that the manufacturing process is pivotal, the emergence of 3D-printed wicks has garnered significant interest due to their cost-efficiency and reliability [41].

To provide efficient cooling performance for spacecrafts with distributed heat sources, some novel heat pipe configurations have been developed. Tang et al. [42] proposed a heat pipe with multi-heat source and double-end cooling. In this approach, multiple heat sources were situated at the midsection of an ordinary heat pipe, and two condenser sections were installed at both ends of the heat pipe. Results showed that this novel configuration of multi-heat source and double-end cooling in a heat pipe considerably enhanced the thermal performance. Mashaei et al. [43] performed a two-dimensional analysis to evaluate the thermal performance of a cylindrical heat pipe with multiple heat sources with Al_2O_3 nanofluid as the working fluid. Results showed that a significant reduction could be achieved in the thermal resistance and size of heat pipe when nanofluid was used. Besides, for cases with higher heat loads, more pronounced effects on the heat transfer rate augmentation and temperature reduction of satellite equipment were obtained. It can be attributed to the thermal properties of working fluids, which showing considerable influence on the performance of heat pipes. In practice, the working fluids are meticulously selected to match the operating temperature range of devices. Heat pipes with water are extensively used in on-earth applications, which are disregarded in larger satellites because of their invalid operation when ambient temperature lowering down to $0 \text{ }^\circ\text{C}$. However, this property might be turned into an advantage if the heat pipe acts as a heat switch. More recently, the space community has shown increasing interest in copper-water heat pipes. These heat pipes are capable of absorbing excess heat from high-power chips and dissipating it over a broader area into a more manageable heat flux, at the interface where the payload is connected to the spacecraft. Brouwer [44] conducted research on the feasibility of utilizing water heat pipes within CubeSats, focusing on performance evaluation and their integration into the CubeSat platform. Transient start-up, repetitive freeze/thaw cycle tests and the heat pipe integration experiments were performed. The findings revealed that commercial water heat pipes are a dependable solution for the heat dissipation issues faced by high-performance CubeSat missions on the horizon. Capable of passively managing heat loads that can reach up to 10 W , the copper-water heat pipes are well-suited for upcoming next-generation CubeSat developments. Since their initial flight with NASA in 2017, ACT Inc. has collaborated with the space agency to establish testing procedures and define criteria for

qualification. The results indicated that the space-grade copper-water heat pipes could efficiently handle high heat fluxes from electronic devices and channel them to the radiator panels. Furthermore, they have demonstrated resilience against the rigors of static and dynamic freeze/thaw cycles, as well as cold starts, thus ensuring reliability for extended space missions [45].

The cylindrical heat pipes, commonly discussed thus far, are predominantly designed for transferring heat from sources to sinks. Moreover, the VCs, which can transfer heat along planar geometries, have also been widely used for minimizing the temperature gradient of electronic devices. Over the last decades, many types of VC have been developed to offer better thermal performance with a smaller footprint for space applications. Semenov et al. [46] fabricated a titanium-water VC measuring 95.3 mm by 95.3 mm with a thickness of 1.0 mm. Titanium was the material of choice due to its low weight and compatibility with water. The assembly weighed in at 26.3 grams, resulting in an effective density of $2900 \text{ kg}\cdot\text{m}^{-3}$. The thermal resistance was demonstrated as low as $0.9 \text{ K}\cdot\text{W}^{-1}$ under a heat flux of $40 \text{ W}\cdot\text{cm}^{-2}$, successfully tested up to heat flux levels of $60 \text{ W}\cdot\text{cm}^{-2}$. Oshma et al. [47] developed and successfully validated a polymer-based VC with a thickness on the order of 1 mm. Liquid-crystal polymer films with copper-filled thermal vias were employed for the casing. A specially crafted wicking structure, which combines copper micropillars with a woven mesh, was developed to enhance heat transfer during evaporation and condensation, as well as to ensure consistent liquid delivery to the evaporator. The tests showed that the VC was capable of functioning efficiently at a heat flux of $11.94 \text{ W}\cdot\text{cm}^{-2}$, achieving an effective thermal conductivity ranging from 650 to $830 \text{ W}\cdot\text{m}^{-1}\cdot\text{K}^{-1}$. An important advantage of this VC is its flexibility, provided by the liquid-crystal polymer, which allows for seamless integration into printed circuit boards or flexible electronic assemblies, aiding in the thermal management of heat-generating components. The ACT Inc. developed a novel VC product named HiK™ or high conductivity plate [36]. This product features an assembly of heat pipes embedded within a single plate to efficiently transfer heat from one point to another. The effective thermal conductivities of these plates ranged from 500 to $1200 \text{ W}\cdot\text{m}^{-1}\cdot\text{K}^{-1}$. In some spacecraft applications, the effective thermal conductivity could be reached as high as $2500 \text{ W}\cdot\text{m}^{-1}\cdot\text{K}^{-1}$.

To meet the high-power density demands of CubeSat systems, the Rocco LLC. developed a flat, lightweight and conformable heat strap FlexCool, which could also be regarded as a ultra-thin VC [48, 49]. The FlexCool strap was constructed using casings of $50.8 \mu\text{m}$ -thick copper foils, accompanied by finely woven copper meshes that serve as wicks, and coarse copper meshes that function as vapor cores. The acetone was applied as the working fluid, yielding an average effective thermal conductivity of $2149 \text{ W}\cdot\text{m}^{-1}\cdot\text{K}^{-1}$. Moreover, the total thickness of heat strap was controlled within 0.86 mm , which is able to withstand the internal vapor pressures up to 930 kPa .

Recently, the Boyd Corporation [50] developed the ultra-thin titanium VCs, which offer the added benefits of

enhanced structural integrity, weight minimization, and ease of assembly. These titanium VCs are thermally on par with 0.3mm-thick graphite alternatives but offer greater design flexibility. The use of Titanium allows for even thinner solutions under the highest performance, showing potential for use in small satellite applications. Nesterov et al. [51] experimentally investigated two flat T-shaped heat pipes (copper–water and titanium-acetonitrile). The innovative T-shaped configuration of the heat pipes facilitates effective heat transfer across surfaces that intersect at right angles, enhancing thermal distribution between perpendicularly aligned components. Results indicated that the titanium-acetonitrile heat pipes could provide heat transfer under the heat loads with 2~3 times lower in comparison to that with the copper-water heat pipe. However, the weight of the titanium heat pipe was much smaller.

In addition, great efforts were also taken to advance the applicability of OHPs in space environment. An experimental assessment of a flat-plate OHP was carried out in a variety of gravity conditions during a parabolic flight campaign [52]. The device under test was a molybdenum plate featuring 14 milled rectangular channels, each with a cross-section of $3 \times 3 \text{ mm}^2$, and was equipped with a sapphire window. It was tested in a vertical orientation with ethanol employed as the working fluid. In both normal and hyper-gravity conditions, characterized by a nucleate boiling regime, the OHP functioned similarly to a looped thermosyphon. However, upon transitioning to microgravity conditions, changes in flow patterns were observed, shifting to a slug regime with thin film evaporation due to the absence of buoyancy. Additionally, hydrodynamic instabilities, accompanied with short-term periods of emergence of nucleate boiling under microgravity, were also observed during several parabolic flight tests.

2.2.2 Separated heat pipes

The unseparated heat pipes mentioned previously encounter limitations due to the relatively small heat transport capacity and the thermal conductance attenuation along the longitudinal direction. The liquid and vapor transport in opposite direction and meet each other within the same enclosure, which may depress the two-phase transport efficiency. To overcome this, a system that segregates the capillary-driven flow from the vapor transport can achieve superior performance. In this section, the heat pipes having individual liquid and vapor lines are defined as separated heat pipes, including the widely used capillary pumped two-phase loops, sorption heat pipes (SHP) [53] and gravity-assisted heat-driven two-phase fluid loop which was first applied successfully for the thermal management of the Jade Rabbit rover of Chang'E-3 [54], etc. The capillary pumped two-phase loops include the loop heat pipe (LHP), capillary pumped loop (CPL) and the hybrid loop heat pipe (HLHP), as summarized in Table 3 [55]. Among these, the LHP is most prevalently deployed in spacecraft. A salient distinction between the CPL and LHP could be found in the reservoir positioning — typically external to the coolant loop in CPLs, while incorporated internally within LHP loops [56].

Research within the last few decades has predominantly concentrated on separated heat pipes, aiming to fulfill the evolving cooling requirements of spacecraft. Mishkinis et al. [57] summarized the use of thermal control systems based on two-phase loops with capillary pump for space applications. The current and future trends of the technology for the aerospace sector were also discussed.

Wang et al. [58] conducted a comprehensive review of the advancements in LHP technology within Canada, which encompassed aspects such as hardware development, different applications, performance evaluations, analytical prediction, and numerical modeling. They highlighted that given the intricate nature of the physical processes taking place within two-phase capillary-driven systems, developing mathematical models with an acceptable accuracy remains a challenging task for engineers. Table 4 summarized various types of separated heat pipes in spacecraft applications. Researches mainly focus on the development of multi-evaporator/multi-condenser loop structures, miniature or micro LHPs, and cryogenic heat pipes.

(1) Capillary pumped loop (CPL)

As the key structure of the CPLs, the porous wick organizes the heat transfer in the evaporator and circulation of the working fluid around the loop via the capillary force. In general, the main factors dictating the choice of wick material for the porous structure are the wettability and compatibility with the working fluids used. Additionally, the performance of a CPL is highly influenced by the particular characteristics of the wick itself, such as pore size, porosity, and permeability. A wick with an ideal pore configuration permits efficient fluid transport and distribution within the CPL, thus directly affecting its heat transfer capacity. Mishra et al. [59] performed experimental trials to develop a porous wick that exhibits high porosity featuring interconnected pores with an average diameter smaller than $5\ \mu\text{m}$, a high aspect ratio, and permeability exceeding $10^{-14}\ \text{m}^2$. They utilized loose carbonyl nickel powders, with particle sizes ranging from 2 to $7\ \mu\text{m}$, which were sintered within a graphite mold under hydrogen atmosphere at varying temperatures to fine-tune the porosity, pore size, and permeability of the wick structure, thereby ensuring enhanced capillary performance for CPLs.

(2) Loop heat pipe (LHP)

In practical, heat sources onboard spacecrafts are often located at a relatively large distance from each other and display different capacity. Besides, radiators facing deep space usually shows high radiative heat transfer performance, however, they might locate remote from the heat sources. Accordingly, the LHPs are particularly well-suited for this task due to their ability to provide a long-distance connection between evaporators to the heat eventual destination. Maydanik et al. [60] developed a $1\ \text{m}$ long ammonia ramified LHP with two cylindrical evaporators and two condensers as pipe-in-pipe heat exchangers, which were tested under different orientations. Results showed that the LHP was

capable of functioning effectively under conditions of both symmetrical and asymmetrical heat load distributions among the evaporators, as well as across various temperatures of the condensers. A noted limitation was the drop in maximum capacity on the occasions when only one condenser was actively cooled — a result of the penetration of a large quantity of vapor into the liquid line. Nagano et al. [61] developed a miniature LHP with multiple evaporators and multiple condensers and the gravity effect on heat transport characteristics was also evaluated. It was indicated that the gravity might affect the loop's natural operating temperature, the maximum heat transport capability, and the thermal conductance. With the development of advanced MEMS technology, more miniature or micro LHPs are developed and tested. Cytrynowicz et al. [62] developed a silicon-based LHP, featuring a design where the condenser could be integrated on-chip or, more typically, situated at a considerable distance, linked through tubing connecting the back to the wick structure. The core innovation resided in the development of a coherent porous silicon wick, a creation entailing vast arrays of uniformly sized micrometer-scale through-holes, all etched simultaneously and perpendicularly to the surface of the silicon wafer or chip. Subsequently, SiO₂ capillary tubes were then grown inside the pipes or pores, which demonstrated impressive capillary forces. The theoretical cooling capability of this system was projected to exceed 300 W·cm⁻².

To meet the more complicated thermal control requirement for spacecrafts, the LHPs are often used in combination with other thermal control devices. Guo et al. [63] recently tested a co-designing cryogenic system consisting of two pulse tube cryocoolers and two neon cryogenic LHPs operating at a temperature around 35 K. A novel integrated multifunctional heat exchanger proposal was put forward to facilitate heat exchange between the cold head of a pulse tube cryocooler and the condenser of a cryogenic LHP. This innovation aims to synergize the functions of both cooling systems, potentially improving efficiency and performance in cryogenic temperature control. This co-designing cryogenic system was capable of operating at temperatures approximately around 35 K, with a heat transport length over 500 mm. The maximum heat transfer capacities of the two systems were 1.9 W and 2.05 W, with equivalent thermal conductivities of 13881 W·m⁻¹·K⁻¹ and 8390 W·m⁻¹·K⁻¹, respectively.

Yang et al. [64] presented a temperature-controlled LHP structure which was different from the traditional LHP structure to provide accurate temperature control of the distributed CCD devices of the GF-9 satellite remote sensor. In addition to the electric heaters installed in contact with the evaporator and the preheating plate, a cold plate assembly containing multiple cold plate units was specially designed to control the temperature of the distributed heat sources. Another concern for LHPs is the high-cost manufacture. The largest expense in the production process arises from the manufacture of the primary wick, which necessitates several stages of machining in addition to the application of a knife-edge seal. Richard et al. [65, 66] developed a 3D printed LHP evaporator, utilizing a Direct Metal Laser Sintering

(DMLS) technique for the construction of the primary wick. Through this approach, the overall manufacturing costs could be significantly diminished by eliminating the need for numerous machining processes, and the potential for failure associated with the knife-edge seal could also be substantially reduced. Their research included detailed studies on the optimization of pore radius and permeability aimed at improving the DMLS method and its parameters specifically for crafting porous wicks. Additionally, the prototype withstood vibration testing, affirming the durability of the 3D-printed wick. The advent of 3D printing technology in this context enables the unified printing of the LHP evaporator's components, encompassing both the wick structure and its encapsulating envelope, as a solitary piece.

According to Table 4, the most widely used working fluid in LHPs is ammonia. However, due to its low freezing temperature at $-78\text{ }^{\circ}\text{C}$, the condenser design must prevent such a condition, some other working fluids such as propylene and acetone are also considered. Meanwhile, the safety concern, geometric limitations, as well as the use of less hazardous working fluids should also be considered when using ammonia and propylene as working fluids. Dutra et al. [67, 68] designed a LHP and test it with acetone as the working fluid to manage up to 70 W of heat transfer rate. Experimental tests showed that though acetone presented lower thermal efficiency than ammonia, it could be used as working fluid at low power levels by avoiding freezing concerns. On the other hand, the addition of nanoparticles such as graphene nanoparticles to conventional heat transfer fluid is also thought to be a good approach to improve the thermal performance due to the increased thermal conductivity of the nanofluid [35, 69].

Over the past few years, extensive ground tests have revealed some peculiar behaviors inside the LHP such as temperature overshoot during start-up and temperature hysteresis. In general, the LHP usually operates at fixed operating temperature for the case with steady heat load. When the heat load and/or the sink temperature changes, the operating temperature will change accordingly and reaches another steady state. However, it was also observed that the loop operating temperature not really reaches a truly steady state but oscillates indefinitely under some certain conditions. Ku et al. [70] comprehensively examined the temperature oscillation phenomenon within a miniature LHPs, with ammonia serving as the working fluid. They pinpointed that this oscillatory behavior arose when there was a dynamic movement of the vapor front, back and forth, in proximity to the condenser exit. Additionally, it was discovered that all components of the loop, including the evaporator, condenser, and compensation chamber, were interconnected both thermally and hydrodynamically. Such temperature oscillations were observed to ripple throughout the system. Furthermore, they noted that external forces—specifically acceleration—could induce or eliminate these temperature swings. Bearing in mind that the operational temperature of an LHP is contingent on the temperature within the compensation chamber, as well as on thermal leakage and the subcooling degree of the returning liquid. In this regard, strategic control of the compensation chamber temperature using heaters was suggested as a possible strategy to

quell the phenomenon of temperature oscillations. Ku et al. [71] further proposed to install a TEC on the compensation chamber and the hot side of the TEC was connected to the evaporator through a copper strap, as shown in Fig. 9 (a). It was demonstrated that the LHP delivered robust loop operation in all tests where the heat load varied between 0.5 W and 140 W, and the sink temperature varied between 243 K and 293 K. The TEC was able to control the compensation chamber temperature within ± 0.3 K under all test conditions with minimal additional power requirement (less than 1 W). To meet the temperature control precision requirement of the GF-7 laser altimeter and ensure the stable operation of the LHP, Huang et al. [72] adopted an auxiliary heater installed on the LHP capillary pump, as shown in Fig. 9 (b). It was demonstrated that the temperature oscillation of the key components could be maintained within ± 0.3 K. This strategy potentially mitigates the temperature oscillation issue by offering direct heating to counteract unwanted fluctuations.

(3) Hybrid loop heat pipe (HLHP)

As aforementioned, LHPs and CPLs do have some inherent shortcomings. For example, a lengthy startup procedure is needed for CPLs before heat is imposed to the evaporator. As for the LHP, the effective thermal conductance is not as high as that of CPL though it does not require a preconditioning process. Thus, a novel concept, which is called HLHP, is proposed to incorporate their strengths while avoiding their weaknesses. A proof-of-concept testbed of the HLHP was put together and tested at the Naval Research Laboratory [73]. The objective of this new design was to manage the heat leak across the evaporator pump wick with a secondary wick. By managing the heat leak with the secondary wick, return liquid subcooling is not needed. Thus, allowing for a more compact radiator, leading to weight savings. For the validation of multi-evaporator HLHP technology, single-, dual-, and quad-evaporator breadboard test loops were designed, fabricated, and tested by Bugby et al. [55].

Breadboard components included cylindrical Teflon wick evaporators for low control power, counter-flow condensers for freeze tolerance, a back-pressure regulator for heat load sharing, a co-located flow regulator for radiator switching, a cold-biased heat exchanger for temperature control, and a secondary evaporator/reservoir for core sweepage. The breadboard configuration for the thermal control system comprised a collection of components designed to enhance its performance under various operating conditions. It included cylindrical Teflon wick evaporators, which are chosen for their efficiency with low control power. Counter-flow condensers were utilized due to their ability to tolerate freezing temperatures, allowing for continued functionality even in cold environments. A back-pressure regulator was installed to facilitate heat load sharing. Accompanying this was a co-located flow regulator, which is critical for switching between different radiator panels as needed. To maintain temperature control, a cold-biased heat exchanger was incorporated into the setup. Additionally, a secondary evaporator/reservoir system was included for the

purpose of core sweepage. Yun et al. [74] further advanced multi-evaporator HLHP technology, and successfully tested a multi-evaporator HLHP which incorporated a liquid cool shield, engineered to safeguard the liquid return line against unwanted parasitic heat absorption. During testing, the loop demonstrated reliable start up, cool down to sub-ambient temperature, and sustained operation at saturation temperatures that could reach as low as 30 °C below the local ambient temperature. The implementation of the liquid cool shield proved pivotal in affording the multi-evaporator cooling system with the robustness required to handle transient fluctuations in thermal load. It showcased the ability to convey a heat load as considerable as 600 W at a saturation temperature of - 3 °C. Moreover, they employed a commercially available temperature controller to achieve precise temperature regulation within a narrow margin of ± 0.2 °C.

(4) Sorption heat pipe (SHP)

The SHP is a new thermal control device proposed by Vasiliev and Jr., which can be used as either a sorption cooler or a heat pipe [53, 75]. The SHP is an innovative integration of a separate heat pipe and a solid sorption cooler, featuring a noteworthy interplay between these two components, as depicted in Fig. 10. This apparatus combines the superior heat and mass transfer capabilities characteristic of conventional heat pipes with the sorption phenomena of a sorbent bed situated within. The SHP encompasses a sorbent bed at one extremity, with a condenser and an evaporator at the opposite end. Functionally versatile, the SHP not only operates as an LHP but is also applicable as a cryogenic cooler. It is particularly suited for the cryogenic storage of fluids at low pressure and ambient temperature. Moreover, within the realm of space operations, the SHP can be an integral element of active thermal control systems—such as cold plates employed in the infrared observation of Earth or other cosmic entities—serving as an effective cooling device for electronic components aboard spacecraft. Vasiliev et al. [75] experimentally compared the thermal performance of LHPs and SHPs, employing varied porous wick architectures manufactured from titanium sintered powder within the evaporator. Their findings demonstrated that LHPs, when using ammonia and water as the working fluids, could achieve heat transfer coefficient of up to $4500 \text{ W}\cdot\text{m}^{-2}\cdot\text{K}^{-1}$. Notably, they observed that SHPs could deliver a minimum of threefold enhancement in heat transfer efficiency in comparison to LHPs with identical evaporators, showcasing the SHP's superior performance in thermal management applications.

2.3 Mechanically pumped fluid loops (MPFLs)

When inadequate capillary force is provided, the dry-out phenomenon might occur which limit the application of aforementioned heat pipes under high-power loads. Hence, the mechanically pumped fluid loop (MPFL) is another

widely used technology for thermal management of spacecrafts. By forcing the working fluid to circulate in the MPFL via an active pumping system, heat might be collected from the heat generation components and then transferred to the cold end and eventually dissipated via the thermal radiator. Compared to the passive thermal management solution via heat pipes, the active MPFL technology can provide superior stability, flexible configuration, long transmission distance and high temperature control precision, thus attracting lots of research attentions over the past few years. Moreover, the MPFL system also features properties like quick and straightforward startup process, wide operational temperature range and strong environmental adaptability. In contrast, there are still some disadvantages of the MPFL system, such as the need of power consumption to drive the pumps and the potential for mechanical failures due to the presence of moving parts. With the fast-growing demand for multiple capabilities of spacecrafts with high-density electronic devices, the cooling load for future spacecrafts is dramatically increasing. In this regard, the passive thermal management solution via heat pipes is no longer adequate to cope with the high heat flux and provide stable and precise temperature control. The MPFL technology is regarded as the best solution for scenarios where the payloads are multiple, distributed and of high heat flux. In general, the MPFLs can be divided into two categories based on whether the working fluid undergoes a phase change, i.e., the single-phase MPFL and the two-phase MPFL, which usually consist of the heat acquisition unit such as cold plate and evaporator, pump, accumulator, control valves, and the radiator. Table. 5 presents the typical loop architecture and features of the single-phase MPFL and two-phase MPFL highlighting a comparison of their benefits and drawbacks to assist in determining the right system for specific spacecraft thermal management applications.

2.3.1 Single-phase MPFLs

Up to now, the single-phase MPFL technology has seen successful deployment across a range of spacecraft such as the space station, manned and cargo spacecraft, and different types of satellite, etc. Within a single-phase MPFL system, the working fluid in liquid phase may not undergo phase transition as it circulates through the cold plate. A mechanical pump is used to sustain the fluid flow from the heat acquisition unit to the thermal radiator, as shown in Table 5. The bypass assembly is commonly integrated to assist in temperature control, thereby accommodating fluctuating operational conditions. Over the last years, great efforts have been dedicated to the development of single-phase MPFL system for thermal management of spacecrafts (especially the satellite). Camañes et al. [76] presented a report which provided the state of the art of the most relevant components of an MPFL. They investigated the cooling needs for current and future satellites. The information gathered was used to perform a trade-off for cooling systems design and component selection in the next phase of the IMPACTA project, which was launched for the thermal management of

high-power communication satellites equipped with active phased array antennae. Based on the comparison of different thermal management solutions, the MPFL was thought to be the preeminent choice for such applications.

Many novel loop structures were developed in combination with advanced technologies to cope with the increasing thermal dissipation and the negative effects of the future spacecrafts [77]. The European Space Agency initiated the development of a single-phase MPFL which was one of the two heat transfer element options for the large Alphas deployable radiator [78]. The purpose of the project was to develop and qualify the key components such as pumps and valves of a single-phase MPFL for extended payload power ranging from 3 to 6 kW. Yet, the design process faces considerable hurdles including severe operational temperature bounds, reliability, and longevity, with special regard to bearings, the pump motor, and the coolant selection. Subsequently, a valve-less single-phase MPFL concept was advanced to leverage the east and west panels of geostationary satellites as supplementary radiator surfaces [79]. In a strategic arrangement whereby the payload loop was segmented into two series-connected parts aligned with the east and west radiators, the need for flow-control valves was eliminated. To forecast the thermal-hydraulic behavior and orbital temperature stability of this valve-less MPFL system, a mathematical model was constructed. The results derived from both transient thermal analysis and full-scale loop laboratory testing indicated that the payload's orbital temperature stability was maintained within a ± 5.5 °C range under fluctuating heat load conditions. Therefore, this innovative system design was advocated for use in large geostationary satellites due to its contribution to a more compact structural design, efficient utilization of the east and west radiator panels, and enhanced overall system reliability.

Recently, under the NASA Small Spacecraft Technology Program, the Center for Space Engineering at Utah State University and NASA's Jet Propulsion Laboratory jointly took efforts to develop an active thermal control system for cryogenic instrumentation in future CubeSat platforms [80]. The project is named Active CryoCubeSat (ACCS) and includes two development phases. The first stage consists of a single-phase MPFL that circulates a moderate temperature coolant between the cryocooler's cold plate heat exchanger and a radiator, while the second stage consists of a miniature cryocooler for sub 100 K detector thermal management. Then, Anderson et al. [81] presented the design update for the Active Thermal Architecture project. This update, part of a series of progressive efforts, integrates a pumped fluid loop and a radiator, initially established by ACCS. The project's specialized attention was directed toward evolving and refining a two-stage deployable radiator, which utilized a rotationally flexible joint, a solar tracking system for the deployed radiator, and a system to passively isolate vibrations. Fig. 11 shows a 1U terrestrial model of an active thermal control subsystem with a single-phase, two-stage mechanically pumped fluid loop. This was meticulously engineered for CubeSat platforms of the 6U category. The system employs a micro-pump to circulate the

working fluid through an integrated heat exchanger and the aforementioned tracking radiator. Further, a miniature cryocooler provided the necessary cryogenic cooling for the instruments carrying the payload.

With continuous miniaturization of space-borne devices, more powerful payloads are anticipated to be integrated in small satellites. Consequently, the compactness and miniaturization of the thermal control system is a significantly important development tendency. Es et al. [82] proposed an innovative concept for thermal management utilizing a mini single-phase MPFL tailored to regulate the temperatures of small satellites, notably those with issues in power dissipation, and to make their thermal conditions orbit-agnostic. The architecture of the mini MPFL accounts for the specific needs of CubeSats and their subsystems, thus guaranteeing adaptability with small spacecraft on diverse mission profiles. The heart of the system, which provided a low mass mechanically pumped loop solution with high reliability, is the multi-parallel micro-pump developed by the Netherlands Aerospace Centre, as shown in Fig. 12. The pump was made of titanium through laser additive manufacturing technology. The design featuring several micro-pumps in parallel, ranging from 10 to 30, was engineered to address the risk of single-point failure that is typical in traditional micro-pumps. While the mini MPFL operated on a single-phase loop principle, the accumulator was deployed as a two-phase accumulator to enhance functionality. By sustaining the accumulator's temperature above a predetermined saturation point, the system's internal pressure was consistently regulated. Thus, more robust for launch vibrations and easy future upgrades can be achieved to the mini two-phase MPFL for greater heat removal capabilities. Basically, as the key component of the active liquid cooling system, the performance and reliability of the micropump directly determine the operational performance of the thermal control system, which have attracted considerable interests and become the highlighted area of research, particularly for microfluidic applications. Mohith et al. [83] reviewed the contemporary research and advancements in micropump technologies, paying special attention to mechanical micropumps. They delved into key aspects that influence mechanical micropump efficiency, including actuation methods, dimensions, functional parameters, principles of flow rectification, and materials and fabrication methods. An analytical survey, supported by numeric and illustrative evidence, was offered to explore the strengths and shortcomings of various actuation methods used in mechanical micropumps, focusing on their impact on flow rates and the resultant back pressure.

In addition to the development of loop structure and advanced devices for the single-phase MPFL, the transient simulation and experimental tests are vital to improving the operational performance of the system such as the dynamic response to the environmental change and the temperature control precision and stability [84]. To improve the thermal control adaptability of spacecraft under variable external space environment, Wang et al. [85] proposed a novel single-phase MPFL thermal control system. The temperature control was realized by utilizing the automatic flow rate

and temperature proportional regulation characteristic of the temperature-sensing wax-based temperature control valve. A mathematical model employing the lumped parameter method was constructed to analyze the dynamic response performance to different operational parameters of the thermal control system. It was found that the valve configuration and the temperature-response characteristics of the wax indicate apparent effect on the dynamic performance of the thermal control system. When adopting the conventional single-phase MPFL in spacecraft thermal control system, as shown in Fig. 13 (a), some problems are encountered, including (1) the high energy consumption, (2) suboptimal temperature control precision for each cold plate which is thermally coupled to distributed heat sources, and (3) dependency of the entire system's function on the reliability of three-way valves, necessitating their redundant deployment which, in turn, enlarges system bulk and mass. To tackle these problems, Wang et al. [86] further proposed a novel single-phase MPFL by using highly self-adaptive cold plates where the paraffin-actuated thermal control valves were integrated, as shown in Fig. 13 (b). In each branch of the system, a thermal control valve equipped with a paraffin-actuated mechanism situated at the forefront of each corresponding cold plate was utilized. The valve harnessed the volumetric expansion that occurs during the phase change from solid to liquid, delicately regulating the flow of the coolant and the cold plate's heat removal capability, directly in response to the thermal load affecting the cold plate. Thus, the operating economy could be remarkably enhanced since the rare energy consumption in the flow control process and the thermal control system could be simplified by integrating the sensor, controller and actuator systems. The validated prototype was established and the temperature control performance under various operating conditions was tested. Results demonstrated that this novel system could provide stable temperature control with sufficient fast transient responses and sufficient small steady-state errors. Moreover, in order to avoid the adverse effect of water hammer on the pipes and facilities of single-phase MPFL used in spacecraft, Huang et al. [87] built a mathematical model to simulate the water hammer effects on the system by using characteristics method. Based on the transient analysis of a single-phase MPFL with parallel branches, the relationship between the valve on-off state and the water hammer effect was obtained and some countermeasures were proposed to suppress the water hammer effect.

2.3.2 Two-phase MPFLs

When utilizing the single-phase MPFL for thermal management, the temperature of the working fluid is subject to considerable variation along the flow path. Though the temperature difference can be reduced by increasing the working fluid flow rate, higher pumping power is needed simultaneously. Consequently, this necessitates larger component sizes and, ultimately, a heavier system [88]. As the advantages and disadvantages of the single-phase MPFL and the two-phase MPFL were presented in Table 5, a pump is also required to circulate the working fluid in a two-phase MPFL.

Downstream of the pump, the fluid first flows to the evaporator where liquid is evaporated, and absorbing the generated heat from the payloads. Then the resultant vapor flows to a condenser where it is condensed back into liquid. Typically, a heat exchanger is adopted to preheat the cold liquid to near saturation temperature by absorbing heat from the vapor/liquid downstream the evaporator, thus saving power budget in cold orbits. Furthermore, an accumulator is necessary to accommodate the fluid density fluctuations as a result of evaporation and condensation. The saturation pressure and the saturation temperature in the system is adjusted by the accumulator. When the accumulator is accurately controlled, the evaporator is controlled simultaneously. Compared with the single-phase MPFL, the two-phase MPFL system has the characteristics of light weight, low power consumption, high temperature uniformity and the ability to transfer a large amount of heat at a lower mass flow rate. Therefore, it's increasingly deemed a suitable candidate for spacecraft thermal management, particularly for applications demanding high power capacity and long heat transfer distances, such as cooling for spaceborne active phased array antennas that encounter high local heat fluxes (up to $20\text{W}\cdot\text{cm}^{-2}$ at amplifier interface) and stringent temperature stability and uniformity requirements [89].

Yet the two-phase MPFL is not often used in spacecrafts due to its relatively complex structure and low technology maturity. It was reported that the first two-phase MPFL operating in space is the thermal bus on board the Russian segment of the International Space Station used for removing and distributing the heat generated in the internal single-phase loop. The system had a capacity of 30 kW with ammonia as working fluid [76]. The technology readiness level of the two-phase MPFL is not as high as that of the single-phase MPFL and further development of the two-phase MPFL is highly dependent on the technical maturity. In 2011, a two-phase MPFL with CO_2 as working fluid was developed for the Alpha Magnetic Spectrometer (AMS-02) silicon tracker to remove the wasted heat of about 150 W from the tracker front-end electronics to the space, and keep the tracker in a stable and uniform thermal environment [90]. A centrifugal pump was adopted to provide driving force and the temperature fluctuation was controlled within $\pm 0.2\text{ }^\circ\text{C}$.

Meanwhile, to address the thermal management requirements of forthcoming high-power telecommunication satellites equipped with active antennas, the Thales Alenia Space collaborated with the French National Centre for Space Studies to engineer a two-phase MPFL. This advanced system was capable of transporting substantial heat dissipated from an active antenna (up to 4kW) to dedicated large deployable radiators. The system-level design revealed that the two-phase MPFL could proficiently manage varying heat flux from the antenna while maintaining the isothermicity of $5\text{ }^\circ\text{C}$ across all traveling wave tubes, ensuring thermal consistency. Moreover, it effectively minimized the thermal gradient between the onboard equipment and the radiator, thus safeguarding the radio frequency antenna performances [91, 92]. In response to the challenges highlighted in NASA's Thermal Management Systems Roadmap,

specifically Technology Area 14, the ACT Inc. innovated an active two-phase MPFL system. This inventive system propelled a two-phase flow using a single-phase liquid pump that circulates through an array of heat sources and sinks arranged both in parallel and sequentially. Meanwhile, the momentum term of working fluid was utilized to provide phase management. The pump efficiently deals with large pressure drops using minimal power consumption, effectively transferring waste heat across substantial spans. In practice, the system's prototype demonstrated proficiency in managing close to 3 kW of thermal load across three cold plates, while keeping the surface temperature gradient below 2 °C [93]. Very recently, funded by the European Union, the IMPACTA project was launched to develop a two-phase MPFL for active antennas of communication satellites, aiming to achieve a technical readiness level of 6. The two-phase MPFL was thought to be a key building block in the next generation telecommunications satellites. The preliminary design of such a two-phase MPFL was presented. The feasibility of this preliminary design was validated via the measurements on evaporator samples and an excellent performance was obtained [76, 94].

In practice, some other thermal management technologies combined with the two-phase MPFL were developed to further improve the performance.

Zuo et al. [95] designed a combined loop configuration that merges features from both passive and active thermal loop systems for the removal of high heat fluxes from substantial heat input regions, as depicted in Fig. 14. This hybrid loop comprised a two-phase cycle alongside an additional liquid loop. The two-phase loop included the evaporator, condenser, vapor conduit and return line for the condensed fluid. The evaporator's generated vapor pressure, similar to that in LHP, acted as the propelling force for the vapor flow. The supplementary liquid loop incorporated a pump, a reservoir, and conduits to connect the elements. The pump's function was to direct fluid to the evaporator, with a fraction of it vaporizing upon heat absorption, thus transferring the heat to the condenser through the two-phase loop. The excess liquid might return to the reservoir through the capillary wick structure in the evaporator. Significantly, the system operated without the need for valves or other regulatory devices. An inventive porous wick structure was introduced to effectuate the segregation of liquid and vapor phases within the evaporator. Testing of the prototype manifested its efficacy in removing heat flux surpassing $350 \text{ W}\cdot\text{cm}^{-2}$ across heat input areas beyond 4 cm^2 . The hybrid loop managed to perform consistently in a wide range of heat flux inputs without any manual modulation. The excess liquid could be passively collected and circulated back to the reservoir via the wick structure. Moreover, the hybrid loop technology was eligible to operate effectively at all orientations. Then, they further proposed the multiple-evaporator operation of the novel loop [96]. The study revealed that the expected interplay between dual evaporators when subject to uneven heat distribution had negligible impact on the overall performance and functionality of the loop.

Furst et al. [97] unveiled a novel two-phase MPFL where a mechanical pump and bypass line was added to make a

pump-assisted CPL, as shown in Fig. 15. Noted that the mechanical pump was placed with its inlet close to the accumulator and its outlet directed towards the evaporator. The bypass line was situated in parallel with the evaporator line, such that it connected the pump outlet directly to the condenser outlet. It was pointed that the bypass line could also be further terminated closer to the evaporator outlet to enhance certain system capabilities. Compared to the conventional two-phase MPFL, this novel loop architecture provides some benefits, such as the region of two-phase flow is much smaller and the pressure drop is less for a given heat load. Preliminary testing indicated the system's stable operation over heat loads ranging from 30 W to 850 W, along with the capability of handling a heat flux of up to $13 \text{ W}\cdot\text{cm}^{-2}$. The evaporator maintained isothermality within $0.5 \text{ }^\circ\text{C}$ for heat loads up to 100 W and within $3 \text{ }^\circ\text{C}$ for heat loads up to 325 W. To obtain high-quality science data and achieve the NASA's planetary science objectives, Sunada et al. [98] developed a reference mission of the two-phase MPFL thermal management system to accommodate future heat fluxes on the order of $5 \text{ W}\cdot\text{cm}^{-2}$ while maintaining isothermicity and temporal stability to reduce thermally driven noise. The tradeoffs of the thermal/fluid architecture and system configuration were highlighted considering the key component and system sensitivities and critical environmental drivers.

Similarly, the most important component of the two-phase MPFL is also the pump. A pump failure can directly result in the system malfunction. Jeong et al. [99] experimentally evaluated the performance of a two-phase MPFL for thermal control of a laser equipment with high heat flux source using an electrohydrodynamic conduction pump. The electrohydrodynamic conduction pump was defined as the device which pumps dielectric fluids utilizing heterocharge layers formed by imposition of electrostatic fields. It was demonstrated that recovery from the evaporator dryout condition could be realized by increasing the applied voltage to the pump. Besides, test results showed that this electrohydrodynamic conduction pump was applicable for stand-alone system under high heat flux thermal control. Wits et al. [100] investigated the design of a reliable, leak-tight, low-weight and high-pressure micro-pump used in a two-phase MPFL for small satellite thermal control. The micro-pump used a piezoelectric disk to create a pressure head and drive the working fluid. Titanium alloy (Ti6Al4V) was selected to produce the micro-pump via the selective laser melting metal additive manufacturing technique, while Galden HT-90 was used as the working fluid. The rarely moving parts valves and passive check valves were investigated as micro-pump valve designs. The developed prototypes weighed about 300 g showed promising pump capacities when applying cross type check microvalves. Following the previous single-phase modeling of a mini-pumped loop presented above, Es et al. [101] further investigated a micro two-phase MPFL using a multi-parallel micro pump which has been presented in Fig. 12. The system featured a heat switch capability, offering the option to dissipate heat from payloads with varying hot spots effectively. Additionally, its design was highly adaptable and could address thermal control issues for CubeSats ranging from 3U to 16U sizes.

Overall, micro-pumps like the ones described above are considered as having considerable potential for future space missions, especially in harsh environmental conditions.

Usually, the temperature stability of the target devices is crucial to ensure the operational performance. To increase the imaging indexes of space remote sensors, Meng et al. [102-104] constructed a two-phase MPFL setup to investigate the dynamic operating behaviors caused by the multiple distributed heat sources of the core optical detector assembly for the load-on and load-off status. The temperature control component of the system consisted of a two-phase thermal-controlled accumulator integrated with passive cooling and a shield centrifugal pump to provide the driving force. The thermodynamic behaviors in the accumulator were analyzed based on the test data, and the method for decreasing the system instability was proposed. In addition, the operating behaviors of the main loop and the accumulator during the power change of the heat source were investigated. Results showed that the temperatures of the multi-evaporators presented excellent temperature stability and uniformity, indicating good boundary conditions for the stabilization imaging of the space camera. The system stability during the phase change process was influenced by the loading power on the pre-heater.

Bejarano et al. [105] conducted experimental research to improve the cold-start problem inherent in a pump-assisted, capillary-driven, two-phase cooling loops. They focused on characterizing the system's thermal efficiency employing active flow regulation to ameliorate the initiation process during cold starts. The technique involved a proportional-integral algorithm for fine-tuning the phase transition in the evaporator from pool boiling to thin-film boiling and managing the system's back pressure when starting up under low thermal loads. This active management proved to reduce thermal resistance by 50% at low heat inputs, in contrast with a constant flow approach, and yielded a significant reduction in pumping power by 56%. Additionally, the application of a dedicated proportional-integral algorithm efficiently mitigated the temperature overshoot, ensuring a more consistent start-up with smaller temperature fluctuations. In addition to the flow and temperature instability problem of such two-phase system, there are also potential risks on evaporator dryout and vapor lock resulting from the uncondensed vapor bubble in the micropump.

2.4 Microchannel, microjet impingement and spray cooling

The progression of manufacturing technology has culminated in the advent of advanced thermal management strategies with enhanced heat removal capacity. Prominently, the microchannel, microjet impingement and spray cooling technologies have attracted great attentions over the last decades [14]. Fig. 16 shows the schematic of the three cooling technologies. Typically, the three technologies discussed in this section are usually integrated in a MPFL to

function as a heat acquisition unit, i.e., cold plate and evaporator. The implementation of these cooling methods is realized in MEMS applications. Compared to conventional MPFL systems, the MEMS-based MPFL can not only extend the effectiveness and flexibility of the cooling system, but also realize more precise temperature regulation.

2.4.1 Microchannel cooling

In terms of the microchannel cooling, liquid might flow across the multi-arranged microchannels and absorb heat from the devices via either single-phase forced convection or flow boiling. The hydraulic diameter of the microchannel typically ranges from 1 μm to 1000 μm , contributing to the compact system size and challenges of high heat dissipation capacity.

At the Jet Propulsion Laboratory, Birur et al. [106] investigated a MEMS-based single-phase MPFL. The setup involved utilizing a micro-pump to drive the working fluid through microchannels. Silicon was the material of choice for fabricating the first-generation microchannel heat exchangers, featuring microchannels that were 50 μm deep and varied in width from 50 to 100 μm . Then, the thermal-hydraulic performance was evaluated in simulated micro spacecraft thermal loads using deionized water as the working fluid. Furthermore, comprehensive investigations into different microchannel layouts, working fluids, and micro-pump designs were performed. The findings pointed to the single-phase MPFL's proficiency in dissipating heat fluxes exceeding $25 \text{ W}\cdot\text{cm}^{-2}$ from spaceborne electronics. For the last few years, the DARPA launched the Thermal Management Technologies portfolio to tackle the thermal impediments brought by the utilizing of GaN semiconductor devices. The main effort of the NJTT thrust was directed towards employing substrates with high thermal conductance like diamond, alongside transitional layers compatible with devices and a hybrid of active and passive cooling techniques. This approach aimed to reduce the thermal resistance from the junction to the case [21]. Within the scope of DARPA's Intrachip/Interchip Embedded Cooling initiative, Bar-Cohen et al. [107] provided an expansive review and update on the current endeavors, focusing particularly on the projects pertaining to GaN power amplifiers. The options, inherent challenges, and the advanced methodologies in crafting embedded microfluidic solutions for thermal management were discussed. In this program, therma-electrical-mechanical co-simulation and modeling tools were implemented to facilitate the analysis and design of radio frequency power amplifiers and digital integrated circuits, aiming ambitiously to enhance electronic performance by more than threefold through the adoption of cutting-edge embedded cooling strategies. The microfabrication of cooling channels and two-phase thermofluid transport were included [108]. Altman et al. [109] delved into the design of an intra-chip cooling system, which utilized a combination of GaN-on-diamond and embedded micro-channels supplied by a silicon-based fluid distribution manifold, as illustrated in Fig. 17. This layout eliminated

the need for traditional heat spreaders, sinks, and thermal interface layers, instead integrating microfluidic cooling adjacent to the device junction. Their approach optimized conjugate heat transfer performance, while concurrently minimizing the electrical and mechanical interference typically caused by fluidic cooling near the electrically active regions. This was achieved through a thermal-electrical-mechanical codesign strategy tailored to the integrated circuit features. To bring this innovative structure to fruition, they developed some new micro-fabrication techniques targeting the creation of GaN-on-diamond composite substrates and the advancement of diamond micro-channel technology. These techniques were investigated to fabricate channels with an average width of 25 μm and depth of 191 μm . Indeed, the technological advancements nurtured by DARPA-funded projects, primarily tailored for terrestrial high heat flux electronic devices such as active phased array antennas, possess significant potential for aerospace applications. As the functional demands of electronic equipment onboard spacecraft continue to expand, and the associated heat fluxes escalate, these robust terrestrial technologies present a vital research avenue for adaptation to space environments.

The flow boiling heat transfer in the microchannels of a two-phase MPFL system exhibits much higher cooling capacity. Yu et al. [110] developed a two-phase MPFL with a diamond micro-channel evaporator to meet the heat dissipation requirement of high-power payloads such as laser and radar using in spacecraft. The loop structure and key components were designed and a prototype was manufactured and tested via the on-board and terrestrial experiments. The system operated stably and displayed pronounced cooling capacity at 271 $\text{W}\cdot\text{cm}^{-2}$. The device temperature could be precisely controlled by utilizing the accumulator. Besides, the gravity-independent design of the system which was critical for space applications was also verified.

Huang et al. [111] recently conducted experimental research into the flow boiling heat transfer characteristics when employing ammonia within diamond microchannel heat sinks. The heat sink consisted of 37 V-shaped microchannels with hydraulic diameters of 280 μm and channel lengths of 45 mm. The effects of heat flux, mass flux, vapor quality, inlet subcooling, and saturation temperature on the flow boiling heat transfer characteristics were analyzed. Moreover, their investigation encompassed not only saturated flow boiling experiments but also an exploration into the subcooled flow boiling experiments. As buoyancy effects could impede the performance of such microchannel-based two-phase MPFL systems in space by hindering bubble detachment and unfavorable flow regime development. Alam et al. [112] recently utilized the flow boiling silicon nanowires microchannels to regulate two-phase flow regimes and enhance the heat transfer performance, aiming to promote such gravity insensitive two-phase heat sinks in a MPFL for space applications. The research involved extensive tests within a forced convection loop across a broad range of heat and mass fluxes with HFE-7100 as working fluid. The high-speed flow visualization method was employed at up to 70000 frames per second (fps) to understand the boiling mechanism in terms of bubble dynamics, flow patterns, and flow

regime developments for silicon nanowires microchannels. The findings suggested that these engineered channels could significantly enhance thermal management by improving liquid renewal and nucleate boiling, reducing bubble departure diameter, smoothing flow transition, increasing thin film evaporation by flow separation by minimizing intermittent flow regimes, ultimately leading to an excellent improvement in system performance.

2.4.2 Microjet impingement cooling

In a jet impingement cooling system, the liquid or vapor coolant might eject from the nozzle and impact on the target surface to achieve relatively stronger heat transfer compared to convective flow behavior [113, 114]. The jet size usually ranges from several microns to hundreds of microns, which is called as MEMS-based microjet cooling. Compared with the microchannel cooling, the microjet impingement cooling might provide more uniform and stable temperature control, especially for scenarios where there is a large spatial variation in the heat generation [115]. To the best of the authors' knowledge, there have been no publicly reported cases of the successful application of microjet impingement cooling technology in the thermal management of electronic devices onboard spacecraft due to the peculiar constraints of the space environment. Nonetheless, considering the distinctive advantages of microjet impingement cooling, such as excellent heat dissipation capability and hotspot elimination, it remains a promising option for the thermal management of high-power spaceborne electronics. Consequently, several advanced microjet impingement cooling technologies developed for managing ground-based electronic devices with extremely high heat flux are introduced for technical reference.

Lin et al. [116] proposed a novel bottom-side microjet array cooling concept to meet the thermal management demands imposed by active radar systems, as shown in Fig. 18 (a). In this cooling system, liquid impingement was performed directly onto the bottom side of the package substrate. The thermal performance of the cooling system with different current package substrates and heat dissipation power was numerically investigated. Results demonstrated that this system was capable of dissipating high heat thermal power within uniform temperature distribution in chips. Similarly, Ditri et al. [117, 118] introduced an integrated cooling strategy designed to manage the thermal loads of high-power amplifiers. This technique involved the use of a microfluidic manifold which was bonded directly to the underside of the targeted devices, as can be seen in Figure 18(b). The manifold featured an intricate network composed of micro-sized impingement jets and flow channels which were fabricated using a flexible 3D additive photolithographic technique. Numerical studies were carried out to examine the impact of manifold design parameters, including the shape, size, and arrangement of the jets, on the system's heat dissipation capabilities and the associated pressure drops. Fig. 18 (c) showed the design concept of an innovative Impingement Cooled Embedded Diamond

(ICED), for radio frequency thermal management, which was proposed by Gambin et al. [119]. The heat generated by the transistors might dissipate via the liquid flowing through diamond-lined microchannels etched into the back of a GaN-on-SiC radio frequency die. This approach combined the superior heat spreading of high-conductivity diamond with the outstanding convection capability of impinging jets to manage high local heat fluxes. Meanwhile, the structural analysis was also performed to evaluate the ICED mechanical stress levels, including those imposed by diamond growth and hardware assembly. Similarly, Walsh et al. [120] developed a microjet cooler leveraging established silicon micro-fabrication techniques to gain deeper insights into the operation and effectiveness of a silicon-embedded microjet cooling apparatus. The configuration is shown in Fig. 18 (d). It's important to highlight that an array of microjets was produced within the jet plate, which was subsequently bonded directly onto the substrate of the electronic component. The fluid reservoir was constructed for flow entering the microjet orifices and exited through wider exhaust ports. A comprehensive exposition of the design philosophy behind the microjet cooler, along with specifics of its fabrication, numerical models to predict its behavior, and the results from experimental evaluations carried out to characterize the performance of the microjet-powered silicon cooling solution were also presented in detail.

Generally, the jet impingement cooling solution has been extensively researched and applied in the ground-based apparatus. However, future work is still required to theoretically understand of the heat transfer mechanism and technical bottleneck, and to develop precisely predictive models to guide the design of advanced cooling system under microgravity environment. Especially, the development of advanced micro-fabrication technologies, which are compatible to the next-generation semiconductor devices, is essential.

2.4.3 Spray cooling

In general, the operational mechanism of spray cooling is similar to that of jet impingement cooling system. The unique feature for spray cooling is that liquid injected into a nozzle should be finely pulverized into numerous fine liquid droplets by a strong pressure or atomization with air before reaching the target surface. The spray would form a sustainable liquid film where convection, evaporation, and boiling occur simultaneously, in responsibility for heat transfer enhancement. Compared to the jet impingement cooling, the spray cooling can provide higher cooling capacity and a more uniform temperature distribution [121].

Basically, the spray cooling technology has been practically applied in industry for several years [122]. However, the theoretical mechanism is still not clear due to the complex interaction between vapor and liquid droplet impact and the phase change process [121, 123]. While parameters such as flow pattern, spray management and regulation and control of the heat transfer process in a zero/micro gravity environment yield significant effect, rare research focused on

the spray cooling for space-based applications. Moreover, the incomprehension regarding the heat transfer process during spray under various gravitational fields prohibits its extensive space application [124]. In the earlier times, both the US Air Force and NASA have carried out exploratory studies on spray cooling used for thermal control of spacecrafts [125]. Rowden et al. [126] discussed the fabrication of a spray cooling system aimed at addressing issues such as heat flux capability, orientation, and volumetric packaging, pertinent to space applications. Silk et al. [127] presented a review on the spray cooling technology and assessment of future challenges for micro-gravity application. The terrestrial spray cooling investigations provided increased knowledge on the spray cooling process, heat flux enhancement techniques and reduced gravity effects upon spray cooling heat flux were reviewed. Finally, the NASA's goals and development direction, as well as the ongoing strategies and challenges associated with the implementation of this technology in the space environment was detailly discussed.

Currently, applications of spray cooling technology tailored for the space environment remain emergent, with a paucity of published articles addressing its utilization. Within the scope of the limited literature pertaining to space-oriented spray cooling technology, considerable research efforts have been dedicated to investigating the heat transfer performance and flow patterns in the unique contexts of the space environment, characterized by low environmental pressure and micro gravity [128]. Additionally, flow patterns subjected to various gravities and accelerations demonstrate distinct characteristics when compared to those observed under normal gravitational conditions [129, 130]. It was pointed that the presence of vapor within the pumps of closed spray cooling systems can lead to reduced pumping pressure and potentially disrupt system operation. Thus, to effectively operate the spray cooling system in the space environment, the concern for the pump malfunction needs to be properly addressed. Lin et al. [131] proposed a new closed two-phase loop that combined with a large area spray cooling unit to dissipate heat from current and future high-power directed energy devices for space-based applications. A magnetic gear pump which operated with an ejector unit was used to circulate the fluid (including FC-72 and water). An assembly featuring 48 miniature nozzles, organized in a multi-nozzle setup, was utilized, covering a spray cooling zone of 19.3 cm². The application of an ejector significantly augmented the maximal spray pressure drop across the nozzle at critical heat flux (CHF), leading to an elevation in the CHF for spray cooling by as much as 16%. Incorporating an ejector into the setup effectively precluded uncondensed vapors from intruding into the magnetic gear pump, thereby ensuring stable circulation of the two-phase fluid. Wang et al. [132] proposed an improved gravity-immune closed-loop spray cooling system, incorporating an ejector loop to boost the thermal protection platform for space-based laser wireless power transmission systems. As shown in Fig. 19 (a), the gravity-immunity features great reliability for upcoming in-orbit test and potential of the practical deployment in spacecraft thermal management. The innovation primarily resides in the

cohesive combination of a spray cooling loop and an ejector loop, which generates a low-pressure zone free of any rotating mechanical parts. The ejector functions as a fluid entrainment device that applied venturi effect to attain kinetic energy from pressure energy of the primary flow to draw the secondary flow, as shown in Fig. 19 (b). This allows for the consistent removal of the liquid-vapor mixture from the spray chamber, maintaining a high-pressure environment essential for high operational efficiency. Ground-based experiments validated that the system's operation mechanism is feasible, with findings indicating the maximum CHF could escalate to $705 \text{ W}\cdot\text{cm}^{-2}$ during sustained operation. Subsequently, they developed a hybrid cooling approach that merges a self-adjusting single-phase MPFL with a gravity-immune two-phase spray module specifically tailored for the thermal regulation of spacecraft [128]. The prototype was established on the basis of the optimal design method. To verify the synchronized functionality of the single-phase and two-phase components, three distinct setups involving parallel, cross, and nested arrangements were tested. The results revealed that the spray cooling segment could attain a peak heat flux of $468.8 \text{ W}/\text{cm}^2$ while operating at a superheat temperature of $70 \text{ }^\circ\text{C}$.

Recently, Wang et al. [133] provided an extensive review on the spray cooling research directed towards space applications. The effects of gravity, environmental pressure and acceleration and vibration on the flow patterns and heat transfer characteristics, and the development and verification of the spray cooling system for space applications were reviewed. Due to the extremely high experimental cost and the required validation conditions, the current research focusing on the space-oriented spray cooling technologies is still in its infancy. It was found that the influence of gravity on spray heat transfer and its flow field is still not clear as conclusions drawn from different studies sometimes contradicted each other. To narrow this knowledge gap of the spray cooling in space environment, the development of gravity-immune and acceleration-immune spray cooling system and affordable ground-based research methods may be the breakthrough in future investigations. Future studies should place emphasis on the development of advanced control algorithms to regulate mass flow rates in real-time, in response to heat load and thermal environment variations, achieving more precise and stable thermal management.

2.5 Phase change materials (PCMs)

During the eclipse and daylight periods as the spacecraft orbits the earth or moon, the power components on board might overcome the strongly varying ambient temperature difference. In this regard, the passive thermal management technology integrating PCMs present great advantages and has attracted great research interest. With the thermal storage during the phase transition process of PCMs, the design of the heat transport devices and the radiator can be determined based on the average thermal power rather than the peak power. Thus, the weight and size of the thermal

management system can be greatly reduced. Note that the mass saving due to the reduction of the radiator size is significant because the radiator account for a large proportion of the overall mass of the spacecraft. Besides, the PCMs can also function as a thermal buffer to be integrated in the thermal management system to improve the temperature stability of the target components and reduce the magnitude of temperature cycles as well as the severity of solder/bond line stresses in case of the accumulation of fatigue damage during cyclic operations [134].

Over the last decades, the PCMs have been widely implemented for space missions, especially for components that operate intermittently or periodically with varying duty, such as satellite propulsion systems, active antennas and other payloads. Table 6 summarizes the application of PCMs for spacecraft electronics thermal management. It can be found that the most widely adopted PCM is paraffin because of its favorable features such as light weight, low cost and stable properties. Note that the commercially available paraffins exhibit different ranges of melting temperatures due to impurities and/or the presence of multiple wax chemistries. Meanwhile, the low melting temperature alloy (LMTA) also presents great application prospect in the thermal management of spacecrafts with transiently high-power load [135]. In general, the researches utilizing PCMs for spacecrafts thermal management can be divided into two categories. One approach is encapsulating the PCMs in a casing into a heat storage panel, and the other approach is integrating the PCMs with other thermal control devices such as heat pipes.

When encapsulating PCMs in casings, the material of the casing should have high thermal conductivity and light weight features. In terms of the thermal management for large planar array antennas of future spaceborne radar in low earth orbit, it is important to maintain the temperature-sensitive electronic components warm during the eclipse period. Unlike the PCM thermal management systems applied in the ground-based apparatus [136-138], the PCM thermal management systems for spacecraft must adhere to stringent weight constraints. Consequently, carbon-based materials are commonly utilized to enhance the performance of PCM heat storage devices. Vrable et al. [139] utilized a lightweight and high thermal conductivity graphite foam material to encapsulate the PCM to exploit the large latent heat capacity for thermal energy storage, as shown in Fig. 20 (a). Owing to the high thermal conductivity of the carbon foam and cell geometric characteristics, efficient heat transfer was obtained during both the thermal energy storage and extraction processes. Test results indicated that this system apparently improved the temperature control performance with near isothermal operation of the antenna array during the entire orbit. Yamada et al. [140] proposed a thermal control device named heat storage panel to satisfy the thermal management requirements for the small, micro and nano satellites. The device consisted of PCM and a thin panel-shaped container. The container was made of a high-thermal-conductivity ($420 \text{ W}\cdot\text{m}^{-1}\cdot\text{K}^{-1}$ in plane) pitch-based carbon fiber reinforced polymer (CFRP) to enhance the heat dissipation, as shown in Fig. 20 (b). Compared to the other heat storage devices, the heat storage panel features

thinner shape, high specific strength and high thermal diffusivity. Especially, the heat storage panel is multi-functional and could be used as not only a heat storage device, but also as a honeycomb face sheet or a thermal doubler. Choi [141] developed the mini paraffin PCM packs to meet the temperature and thermal stability requirements imposed by the thermal environment changes and the instrument power on/off cycles on the IceCube. The mini paraffin packs were encased in a structure featuring an aluminum honeycomb core with fine pores, interwoven with K1100 carbon fibers, and were encased within an aluminum frame and outer face sheets. However, the fabrication of the packs was relatively costly and the dry mass was higher than the tolerated mass for many CubeSat applications. Then, Isaacs et al. [142] developed a PCM panel with aluminum casing to improve the thermal stability of the CubeSats, as shown in Fig. 20 (c). The DMLS additive manufacturing method was adopted to construct aluminum parts with integral internal structure that acts as load-bearing layer and as thermal conductivity enhancement layer. To identify the designs suiting the temperature stability and component weight requirements, the thermal performance evaluation models were developed and experimentally validated in the vacuum chamber. Desai [143] proposed a novel junction-level cooling technique that fills the PCMs in the micrometer-sized grooves etched in the semiconductor substrate to meet the heat dissipation challenges imposed by extremely high-power pulsed GaN devices, as shown in Fig. 20 (d). In the operational phase of the device, the PCM located close to the junction absorbed the waste heat, which was afterward conveyed to a heat sink during the inactive period of the device. To validate the viability of this concept, both computational simulations and experimental tests were conducted, leading to demonstrable decreases in junction temperature. The results indicated that DC and pulsed assessments of the innovatively designed PCM-integrated devices exhibited an enhancement of electrical performance up to 10% over standard GaN transistors, attributing this gain to the advanced thermal regulation. However, it was also pointed out that the optimization of the groove dimension, the determination of the PCM type and quantity and the leakage of melted PCM in the devices were critical that need further investigations.

The integration of PCMs with other devices, such as heat pipes, has become a prevalent solution for the thermal control of spaceborne electronics. Over the past few years, various thermal management systems combining PCMs with heat pipes have been developed. Izenson et al. [144] proposed a novel thermal control system that combines a LHP with thermal energy storage device utilizing PCMs, as shown in Fig. 21 (a). Usually, the thermal energy storage unit (TESU) was thermally coupled to the evaporator of the LHP to improve its thermal stability. In this system, the TESU could provide the heat flow path in parallel with the system radiator via the thermal coupling with the evaporator. When the generated heat exceeding the heat rejection capacity of the radiator, the excess of heat might be absorbed and stored in the TESU. Otherwise, the stored heat would flow from the TESU to the evaporator. Consequently, the thermal coupling between the TESU and the evaporator was required to improve the temperature stability in response to the dynamic

variations in heat load. Similarly, Madhav et al. [145] recently investigated the performance of a canister module filled with PCM to improve the operation time and reduce the peak temperature of spacecraft electronics with unsteady or cyclic heat loads. Fig. 21 (b) shows the module which was thermally coupled to an axially grooved heat pipe. A rectangular prism canister module was manufactured and filled with eicosane based on the geometrical parameters obtained from a thermal network model. Then, experiments were carried out to evaluate the thermal performance of the canister and validate the thermal network model. The evaluation of heat balance for the PCM canister and the heat pipe was also performed via theoretical analysis and experimental tests. On the other hand, the Cu-H₂O heat pipes coupling with PCM chamber were also used to spread the heat along the surface due to the poor thermal conductivity of PCMs, and transfer the heat from the source to the PCM chamber where the heat would be temporarily stored [146]. The ACT Inc. developed a novel heat exchanger that integrated PCMs within a vapor chamber to reduce the mass of onboard thermal management systems for NASA future space missions. As shown in Fig. 21 (c), the PCM-based heat exchanger consisted of multiple ultra-thin aluminum compartments infused with a substantial amount of PCM. Each compartment's outer surface was encased in a screen mesh that served as a wicking structure, providing the capillary action necessary to circulate the working fluid back to the heat generation zones. This apparatus functioned alternatively as a thermal capacitor or a two-phase heat exchanger with thermal storage capability, depending on the temperature of the heat sink. For instance, during the launch phase of a spacecraft, excessive heat conveyed by saturated vapor could be stored within the PCM, to subsequently be dissipated into the two-phase medium and dissipated from the heat exchanger while in orbit [147]. Then, the geometry and number of the such PCM-loaded drawers enclosed inside the heat exchanger's casing was further optimized [148]. This optimization was guided by factors like the mass proportion of PCM to the entire mass of the heat exchanger, limitations associated with additive manufacturing, and the overall thermal resistances affecting the system in both operational modes. The DMLS additive manufacturing method was used to develop a prototype. Similarly, Yun et al. [149] developed a novel PCM-based vapor chamber that consisted of a packed bed of microencapsulated PCM particles surrounded by two-phase working fluid, as shown in Fig. 21 (d). Within this setup, the microencapsulated PCM granules performed a dual function: they efficiently stored heat and simultaneously functioned as a wicking framework, enabling the capillary-driven movement of the two-phase working fluid, thus ensuring its effective recirculation. Thus, the uniform thermal boundary was provided to the microencapsulated PCM beads via the two-phase working fluid. Compared to the traditional PCM-based heat sinks, this novel vapor chamber eliminates the need for solid conduction enhancement materials such as high thermal conductivity metal fins or carbon foams.

In the above discussed applications, the paraffin is the most widely used PCM. However, the relatively small

thermal conductivity, volume expansion, leakage and gravitational effect can present challenges in practical applications. Recently, some other PCMs, such as LMTA and solid-to-solid PCM, have also attracted research interests. Hartsfield et al. [150] recently explored using gallium as an effective PCM for thermal management for transient high-power load on board the spacecraft. Tests results demonstrated that the gallium was capable of forming shallow thermal gradients under transient heat conditions and facilitating nearly isothermal transitions. Although gallium-based PCM devices offer numerous advantages, such as compact size, minor temperature variations across the device, and a substantial capacity for energy storage, the density of gallium is obviously higher than that of paraffins. Nevertheless, given that volume rather than mass is often the more critical constraint in managing the thermal load of small satellites, the utilization of low-melting-point metals and alloys holds significant potential for advancing thermal management solutions in spacecraft. Moreover, Raj et al. [151] filled the organo-metallic layered perovskite solid-solid PCM into a thermal control module for satellite avionics. The influence of fin configurations on the heat transfer effectiveness was numerically investigated. Subsequently, they further investigated the thermal performance of the novel tapered triangular finned heat sink, which was tamped with a new solid-solid PCM, nano-encapsulated gallium-indium eutectic metal alloy homogenized with an organometallic manganese layered perovskite. It was indicated that introducing just 5 wt% nanoalloy to the PCM could significantly enhance its thermal conductivity by 21.05%, and its charging and discharging enthalpy by 16.84% and 17.61%, respectively.

3 TMTs for heat rejection process: thermal radiator

In terms of the spacecraft thermal management system, three basic processes are involved, including the heat acquisition, heat transport and heat dissipation. TMTs of the first two heat transfer processes have been discussed in Section 2. Different from the commercial ground-based electronics systems where natural and forced convection air cooling have been routinely employed, heat in the spacecraft is ultimately rejected via thermal radiation. Thus, the design of the radiator is extremely important to the whole thermal management system. Due to the special operation environment, the radiator is required to have light weight, compact size, high heat dissipation capacity, good controllability and high reliability. Over the last few decades, literatures explored plenty of advanced thermal radiators for spacecrafts. The commonly used thermal radiator techniques are summarized in Table 7. It is well known that a radiator's heat dissipation capability is dependent on its surface area, absolute temperature, temperature distribution across the radiator and optical property of the radiator surface coating, etc. Thus, researches mainly focused on the performance improvement on the heat dissipation capacity and load matching under fluctuated thermal environment. Note that heat pipes and MPFLs discussed in Section 2 are widely adopted to transport heat from the heat sources to the

radiator. In general, the heat rejection capacity regulation of the radiator is usually achieved via the development of deployable radiators and novel variable emissivity devices.

3.1 Deployable radiator

The deployable radiator is capable of controlling the radiative heat flux by actively or passively modulating the effective radiator surface, exhibiting great advantages of lightweight, compact size and good adaptability compared to the conventional body mounted radiator. Note that weight is the key factor in space applications, thereby the mass-optimized radiator design is paramount. Galouye et al. [152] worked in Alcatel Space developed a lightweight and high performance deployable radiator with two LHPs. By embedding the LHP condenser in the honeycomb radiator panel and using corrugated flexible lines, a considerable mass improvement (about 20~30%) was achieved. The ground tests were carried out in a vacuum chamber with both uniform and non-uniform heat loads. Transient behaviors as the loop start up, shut down, regulation and interaction with environmental heat leaks or gains were also evaluated. The high thermal performance was obtained in terms of the heat rejection capability and the thermal gradient between the evaporator and the radiator. To meet the thermal management demand of future high-power small satellite where high-power components will inevitably be used, Hengeveld et al. [153] introduced several design concepts focusing on the high-efficiency, lightweight deployable radiating technologies. The thermal performance of these design revisions was analyzed and compared by using the same nominal 6U small satellite bus architecture and components. Results showed that the novel deployable radiator offered 220% more heat dissipation capacity than the conventional body-mounted radiator. Consequently, a thermal power of 200 W in a nominal 6U small satellite could be realistically dissipated by using this deployable radiator. Then, Yendler et al. [154] considered two types of deployable radiator, as shown in Fig. 22, including the rigid panel deployable radiator and the rollout deployable radiator. It was indicated that the inherently complex configuration attracts less attention in small satellites though the thermal resistance of the traditional rigid panel deployable radiator can be solved by integrating LHPs. In contrast, the rollout deployable radiator exhibits distinct advantages of small thermal resistance and compact layout. The analysis on the conceptual design of the rollout deployable radiator indicated that much higher mass and volume efficiency could be achieved in comparison to the conventional heat pipe radiator.

In addition to designing novel radiator structure, advanced materials such as shape memory alloys are also implemented to develop deployable radiators. Shape memory alloys are distinct metallic substances that can alter their form through a reversible phase transition that is sensitive to both temperature and stress, oscillating between two solid states: austenite and martensite [155]. Due to their unique properties, they are ideally suited for constructing deployable

radiators in which passive shape change happens without external power, control, or sensing instrumentation. Recently, Bertagne et al. [156] proposed a novel morphing radiator concept using temperature-dependent mechanical response of shape memory alloy to passively reconfigure the radiator shape, thus regulating the heat rejection rate in response to the temperature changes. Fig. 23 (a) illustrates the basic function of the morphing concept. The radiator transitions between two configurations is based on the temperature of the multi-material panel. The radiator will take an extended shape at hot state while it curls into a near full circle when sensor sufficiently cold changes. Furthermore, by using the high emissivity material at the top surface and the low emissivity material at the bottom surface, the turndown ratio of the radiator could be greatly improved. Fig. 23 (b) shows the array having proportional turndown response of such radiator panels in a parallel flow configuration. A sequence of discrete, transformable radiator panels was affixed consecutively along each conduit. The temperature of the fluid gradually diminished along the length of each tube as heat was rejected via radiation. Two benchtop prototypes were fabricated and the feasibility of the morphing design was demonstrated. A turndown ratio ranging from 12:1 to 35:1 was predicted via thermal modeling. Moreover, this design could reduce the system mass by approximately 25% by enabling a single-loop thermal control architecture. Then, Ueno et al. [157] developed a flexible re-deployable radiator to be integrated in the thermal management system for a micro-satellite. By utilizing the shape memory alloy, the deployment angle and the radiation area of the radiator could be changed depending on temperature. Bsibsi et al. [158] developed a variable effective surface radiator using an OHP as a heat switch. This switch was designed to decouple the electronics from the radiator when it is not in operation. Given that oscillation within the OHP would stop at lower temperatures, it became theoretically feasible to adjust the active surface area of the radiator based on the operating temperature. During warmer operational phases, heat dissipated from the electronics would be distributed from the radiator's core to its full surface area. Conversely, in cooler conditions, oscillations within the OHP ceased, thereby engaging only a limited section of the radiator. Experimental evaluations confirmed the OHP's capacity to act as a dynamic heat switch, modulating the heat transport from the heat-generating component to the radiator's surface. It's important to mention that a start-up failure was noted after long cold periods, due to unfavorable liquid-vapor distribution within the OHP tubing. Hence, the system was enhanced by integrating miniature reservoirs and heaters to re-establish proper liquid-vapor distribution before start-up, ensuring consistent performance.

3.2 Variable emissivity radiator

Based on the Kirchoff's law, the regulation of the heat rejection capability of the radiators can also be achieved by implementing novel variable emissivity devices and coatings. These methods can be categorized into the active scheme

and passive scheme.

The active scheme involves the modulation of a radiator surface's emissivity driven by electric signals, such as MEMS-based louver systems [159], electrostatic switches [160] and electrochromic devices [161], etc. MEMS-based louver systems are efficient ways to mechanically modulate the radiator surface emissivity by radiating less heat when cold by closing the louvers, and more heat when hot by opening the louvers. Osiander et al. [162] developed a MEMS-based radiator panel with variable emissivity surface for use in small satellite. The louver thermal controller was adopted where panels were mechanically positioned to modulate the effective radiator surface area, as shown in Fig. 24 (a). This system was composed of MEMS arrays of small shutters ($6 \mu\text{m} \times 150 \mu\text{m}$) exposing either bare-silicon substrate or gold-coated substrate. The arrays of shutters were produced through the Sandia Ultraplanner Multilevel MEMS Technology, which employs the multi-layer polycrystalline silicon surface micromachining technique. These shutters were engineered to function individually, thus permitting digital modulation of the system's effective emissivity. In the low-emissivity state, the light emitted by the high-emissivity substrate beneath was obstructed by both the shutter and its frame, preventing it from escaping the apparatus. Conversely, the shutter moved and allowed light to escape in the high-emissivity state. The possible emittance range of the first prototype reached up to 40%. Li et al. [163] performed a dynamic modeling and transient performance analysis of a LHP-MEMS thermal management system for spacecraft electronics. Similarly, a variable emittance radiator employing MEMS technologies was integrated in the system as a condenser, as shown in Fig. 24 (b). The panel was composed of an opened high-emissivity louver cell and closed low-emissivity louver cell. The heat dissipation capacity of the radiator could be regulated by controlling the open number of louver cells in the louver array. The electrostatic switch acted as the device controlling the gap between the high emissivity film surface and the low emissivity substrate surface by electrostatic force to regulate the emissivity. Ueno et al. [164] developed a parylene-based active micro space radiator that incorporates a thermal contact switch. This design, distinct from the conventional bulky thermal louvers or shutters, achieved a higher fill factor by deploying an array of electrostatically actuated micro diaphragms suspended with polymer tethers. A prototype with a relatively high fill factor at 61% was tested. It was indicated that this device could achieve a radiation heat flux enhancement up to 42%. Electrochromic devices operate by reversible optical property changes (absorbance, emissivity, transmittance) in the presence of an electric field. Demiryont et al. [165] designed an all-solid-state electrochromic device (Eclipse VEECDTM) for electronic variable emissivity control for thermal control of satellite. The device was composed of substrate, mirror electrode, active element and infrared radiation transparent electrode layers. It had the thermal control capacity of tuning reflection/emittance from $5 \mu\text{m}$ to $15 \mu\text{m}$ region with an activation voltage of about ± 1 V. The average reflectance/emittance modulation of the system from the 400 K to 250 K region was about 75%, while that at

room temperature (9.5 μm) reaching around 90%.

In the passive scheme, variable emissivity coatings are commonly adopted to passively adjust the heat rejection of the radiator in response to variations in the thermal load and environmental conditions, without the need for electrical input. The radiators painted with thermochromic coating are capable of passively changing their emittance based on radiator temperature. Compared to the active schemes, the thermochromic variable-emissivity radiator is an appealing option for variable heat rejection due to no electrical input and additional mass increment. When the radiator temperature is high, the radiator has high emittance to promote heat rejection. Conversely, when the radiator operates at low temperature, the emittance drops to minimize heat loss from the radiator to outer space. The dynamic change of the emissivity could be achieved by using thermochromic phase transition materials such as VO_2 and lanthanum strontium manganese oxide (LSMO). Taylor et al. [166] studied the dynamic heat rejection of a VO_2 -based nanophotonic variable-emittance coating. A significant augmentation in radiated heat flux was observed, from $136 \text{ W}\cdot\text{m}^{-2}$ at the onset of the VO_2 insulator-to-metal phase transition to $444 \text{ W}\cdot\text{m}^{-2}$ at the end. The research also focused on evaluating temperature stability in extreme conditions, ranging from the cryogenic temperature of $-196 \text{ }^\circ\text{C}$ up to high temperatures of $450 \text{ }^\circ\text{C}$. Moreover, the effect of the thermal cycling on the fabricated VO_2 films, as well as the hysteresis phenomena associated with VO_2 were also investigated. Results demonstrated that both the VO_2 thin films and the variable emitter sample maintained commendable thermal stability at both cryogenic and elevated temperatures, alongside durability against thermal cycling. Despite these positive attributes, the thermal coatings experienced outgassing and mass decreases from being in the harsh thermal vacuum conditions in space. Joshi et al. [167] carried out the high-vacuum tests on aluminum specimen with four different types of anodized coatings (chromic acid anodized, clear anodize with polytetrafluoroethylene polymer, and black- and brown-anodized coatings) varying in thickness to evaluate the outgassing and mass loss of thermal control coatings. Results indicated that the percentage of total mass loss for the different anodized coatings was less than 1%.

3.3 Combination with other techniques

Generally, the heat dissipation efficiency of the radiator depends not only on the effective radiation area and surface emissivity, but also on the temperature uniformity of the radiator surface as well as the efficiency of the thermal coupling between different devices in the thermal management system. Heat pipes are commonly used to achieve good temperature uniformity by spreading heat throughout the radiator. Moreover, the PCMs are usually embedded in the thermal management system to improve environmental adaptivity under fluctuated thermal environment. To meet the high power components operating intermittently with short duty, Kim et al. [168] developed a new thermal control

device for radiator which embedded the heat pipes and PCMs in two parallel channels inside the honeycomb structure radiator, as shown in Fig. 25 (a). The thermal energy storage capacity by PCM and the effect of heat pipe working on PCM were quantitatively studied via numerical simulations. Results demonstrated that this device could redistribute the temporal peak power around a whole orbit period through alternate melting and freezing of PCM, thus reducing the component operating temperature range by 28 °C. Velson et al. [169] developed a variable heat rejection system with high turndown ratios by using the multiple LHPs to release large heat loads from a single-phase MPFL, as shown in Fig. 25 (b). The evaporators of the LHPs were thermally coupled in series to the single-phase MPFL through heat exchangers. The heat dissipated by the LHPs was controlled by the modulation of the local single-phase fluid flow rate. The feasibility of the system was validated through numerical modeling and experimental test. A significant turndown ratio was theoretically demonstrated for a wide range of sink temperatures. To further improve the turndown ratio, complementary control technologies such as compensation chamber heating could be integrated in this system.

Based on currently mature thermal management system using for spacecrafts, it was expected to maintain the operating temperature of radiators between 400 to 550 K. However, the currently used space radiator system using aluminum heat pipes, aluminum face sheets and aluminum honeycomb core cannot operate in the upper part of this temperature region. Anderson et al. [170] engineered a radiator composed of graphite fiber-reinforced composite material. This was combined with a high-temperature titanium-water heat pipe to efficiently discharge the waste heat from Brayton cycle converters, a key component envisioned for future nuclear-electric propulsion systems. Test results indicated that the titanium-water heat pipe successfully operated at temperature up to 550 K. Through a careful material selection and composite laminate design, this sandwiched radiator panel could survive long term high-temperature exposure while maintaining structural integrity. In terms of the future high-power spacecrafts where large amount of waste heat has to be radiated into space via radiators, the radiator size will be further increased to enhance the heat rejection capacity. However, this is not applicable for future high-power spacecrafts. In this regard, the heat pump, also named two-phase refrigerator loop, is promising to be used to increase the heat rejection capacity without increasing the size of the radiators. A vapor compression heat pump is composed of a compressor, heat exchanger at the heat source (evaporator), heat exchanger at the heat sink (condenser) and expansion valve. When increasing the radiator temperature, the operating pressure over a heat pump compressor becomes significantly large. Due to the limitations of commercially accessible compressors — characterized by their considerable mass and design for maximal operating temperatures of 65 °C, which falls short of the 100 °C requisite for space heat pump deployments — specialized aerospace compressors have been crafted. Within a project backed by the European Space Agency, an electrically powered, high-velocity, centrifugal compressor was developed. This cutting-edge 3-stage compressor system boasts a

minimal mass of merely 2 kg, surpassing the efficiency of prior aerospace compressors. It was seamlessly integrated into a prototype heat pump, utilizing isopentane (R601a) as the refrigerant. [171]. However, the implementation of a heat pump can simultaneously increase the system size and total mass, cause excessive vibrations and consume more energy. Some fundamental and technical issues should be considered to further promote the practical application of the heat pump in spacecraft thermal management system, including the improvement of the system coefficient of performance, heat transfer under microgravity environment and compressor lubrication under the space environment.

4 Conclusion

This paper reviews the thermal management technologies for spacecraft electronics by following the sequential heat transfer processes, including heat acquisition, heat transport and heat dissipation. Researches on the efficient heat acquisition methods including the utilization of advanced materials with high thermal conductance, development of novel package structure based on MEMS/NEMS technologies and advanced microfluidic cooling techniques. When focusing on the heat transport process, a diverse array of heat pipes, along with MPFLs, are acknowledged for their pivotal roles in channeling heat away from its sources to designated heat sinks. Considering the structure layout, the separated heat pipes and unseparated heat pipes are respectively reviewed. The merits and demerits of various heat pipes and MPFLs (including single-phase MPFL and two-phase MPFL) are also discussed and summarized. The final heat dissipation stage for spacecraft, constrained by the unique challenges of the space environment, pivots mainly on thermal radiators. Major efforts on the radiator development focused on the development of deployable radiators, variable emissivity radiators, and the combination with other techniques to satisfy the large heat dissipation power and fluctuated thermal environment. Due to the fluctuated heat power of internal electronics, the PCMs exhibit great advantages and attract a lot of research attention. Based on the reviewed literatures, some major conclusions can be drawn as follows:

- (1) Innovations in materials with high thermal conductivity are indeed crucial for TIMs or heat spreaders within spacecraft applications. These thermal conductive materials include the carbon-polymer composites, carbon-carbon composites, APG and diamond films, exhibiting low coefficient of thermal expansion, outstanding thermal conductivity, and low density. Meanwhile, novel package structures and manufacture processes of electronics are also developed based on micro/nano manufacture technology, aiming to achieve effective near-junction thermal transport.
- (2) Heat pipes are widely implemented in the spacecraft thermal management system due to the good thermal performance, low weight penalty, maintenance-free operation, and high reliability. Usually, the heat pipes can be

embedded in the devices such as thermal conductive chassis or radiator panels to promote heat transfer and achieve surface temperature isothermality. On the other hand, they can also serve as the essential heat transport devices to passively transport heat from the heat sources to the radiators. Generally, they are more suitable to serve as heat transport devices for small satellites, facing the fact of their limited heat transfer capacity and valid thermal transport distance.

- (3) With the fast-growing demand for multiple capabilities of spacecrafts with high-density electronic devices, the cooling requirements for future spacecrafts are steadily increasing. The active MPFL technology is regarded as the superior solution for scenarios where the payloads are multiple, distributed and of high heat flux. Although the single-phase MPFL has been successfully applied in various spacecrafts, it suffers limited cooling capacity and relatively poor temperature stability as the working fluid temperature varies greatly within the single-phase MPFL. In contrast, the two-phase MPFL system exhibits advantages of lightweight, low power consumption, good temperature uniformity and large cooling capability with small mass flow rate. Thus, the two-phase MPFL system is regarded as the most promising thermal management solution for next-generation high-power spacecrafts. Nonetheless, a deeper understanding of the underlying theoretical mechanism of the flow boiling under microgravity conditions is essential to realize and enhance the technical maturity of two-phase MPFL systems.
- (4) The PCMs is involved in the whole heat transfer processes to improve the thermal performance of the spacecraft thermal management system, acting as heat storage unit and the thermal buffer integrated in the thermal management system. The temperature stability of target components and the magnitude of temperature cycles can be improved, and the accumulated solder/bond line stresses resulting in fatigue damage during cyclic operation can be effectively reduced. On the other hand, PCMs are usually encapsulated in a chamber, displaying a heat storage module to accommodate temporary mismatches between heat generation and heat rejection capacity by absorbing or releasing heat while stabilizing the temperatures of the heat source and radiator. As the result, the design of the heat transport devices and the radiator can be determined based on the average thermal power rather than the peak power, thus greatly reducing the weight and size of the thermal management system.
- (5) The radiator serves as the final heat release component in spacecraft thermal management, where heat is ultimately dissipated through radiation. To satisfy the large heat dissipation power of future spacecrafts and the fluctuating thermal environment, various approaches for radiators performance improvement including the development of the deployable radiators, novel variable emissivity devices and the combination with other thermal control technologies such as heat pipes, PCMs and heat pumps, should be further explored.

5 Future prospects

In the foreseeable trajectory of aerospace industry development, countries worldwide will continue to launch various types of spacecrafts, including satellites with differing functionalities, space probes, space stations, and more. Primarily, the heat dissipation power and size of a spacecraft play a decisive role in the architecture of the thermal management system. Detailly, the size of the spacecraft typically determines the available electrical power and the distance over which the generated heat is rejected. In this regard, a payload-matched hybrid thermal management system architecture is proposed to guide the design of thermal management system for various spacecrafts, as illustrated in Fig. 26. To develop thermal management systems with superior overall performance, considerable further research is urgently needed.

- (1) With the aforementioned progression, the normal electronic devices and high heat-flux devices usually coexist within the spacecraft. Thus, a hybrid thermal management system is proposed via the integration of various thermal management techniques, such as the active and passive cooling techniques, and the single-phase and two-phase solutions, etc. Such kind of system can not only meet the thermal control requirements of distinct devices, but also ensure better efficiency and performance. However, any modifications within the heat acquisition, heat transport, and heat rejection phases could significantly affect the entire system's effectiveness. Moreover, the reciprocal effect of the electrical, magnetic, thermal, fluidic, and mechanical properties of the spaceborne components necessitate the codesign via multidiscipline coupling. Thus, how to eliminate the incompatibility of the thermal and hydraulic characteristics of different components and the performance inhibition of the electronic equipment through rational co-design, so as to achieve the efficient integration of the thermal management system will be a critical issue that engineers need to consider carefully.
- (2) Due to the unique microgravity environment, the mechanisms of the heat transfer processes involved in different forms of flow (both single-phase and two-phase) in thermal control systems are significantly different from those in their terrestrial applications. However, there is a lack of knowledge on the characteristics of single-phase and two-phase flow heat transfer (e.g., flow boiling, solid-liquid phase change, spray cooling, etc.) within different components (e.g., tubes, microchannels, and porous media, etc.) under microgravity. Moreover, there is also a lack of in-depth understanding on the mechanism of the flow instability and its impact on the system performance under various operating conditions, as well as researches on corresponding countermeasures. Consequently, further experimental researches on these basic physical process under microgravity conditions and the on-orbit verification of important components are needed to pave the way for the deployment of these thermal control system in the future spacecrafts. Meanwhile, the effects of vibration, shock, radiation ageing on the operation of

the key components (such as the evaporator, accumulator, heat pipes, etc.) of the thermal management system during the whole operating cycle should also be systematically investigated.

- (3) Though the principle of the MPFL technology is simple, its application in the thermal control system of spacecrafts is still challengeable. One of the important reasons is that the application of MPFL technology relies heavily on the design and manufacturing of key components such as micro-pumps, micro-valves, reservoirs, micro-heat exchangers, etc. However, the cost-effective deployment of these technologies is dependent on the development of advanced functional materials and the advancement of micro/nano-scale manufacturing processes and 3D printing technology. In addition, the on-orbit service life and reliability of these key components have also seriously limited the deployment of the thermal management system. Therefore, efforts should be made to improve the design ability and manufacturing level of these key components (such as micro-pumps featured lightweight, compact, long-life and low-power), so as to make the innovation of the thermal control technology and the development of the advanced materials, as well as the advancement of the manufacturing level of the components mutually promote each other and form a benign cycle.

Acknowledgements

The work is financially supported by the National Science Foundation of China No. 52206113, and the Science Fund Program for Distinguished Young Scholars (Overseas), No. GYKP020.

References

- [1] S.H. Yeo, H. Ogawa, D. Kahnfeld, et al., Miniaturization perspectives of electrostatic propulsion for small spacecraft platforms, *Progress in Aerospace Sciences*, 126 (2021) 100742.
- [2] E. Turan, S. Speretta, E. Gill, Autonomous navigation for deep space small satellites: Scientific and technological advances, *Acta Astronautica*, 193 (2022) 56-74.
- [3] X.Y. Ji, Y.Z. Li, G.Q. Liu, et al., A brief review of ground and flight failures of Chinese spacecraft, *Progress in Aerospace Sciences*, 107 (2019) 19-29.
- [4] D. Hengeveld, M. Mathison, J. Braun, et al., A. Williams, Review of Modern Spacecraft Thermal Control Technologies, *HVAC&R Research*, 16(2) (2010) 189-220.
- [5] V.A. Rohachev, O.M. Terekh, A.V. Baranyuk, et al., Heataerodynamic efficiency of small size heat transfer surfaces for cooling thermally loaded electronic components, *Thermal Science and Engineering Progress*, 20 (2020) 100726.
- [6] D.G. Yang, F.F. Wan, Z.Y. Shou, et al., Effect of high temperature aging on reliability of automotive electronics, *Microelectronics Reliability*, 51(9-11) (2011) 1938-1942.
- [7] A. Hees, M. Stangl, G. Adamiuk, et al., Status and Future Trends of Active Phased Array Antennas for AIRBUS Space-Borne SAR Systems, in: 2019 IEEE International Symposium on Phased Array System & Technology (PAST), Waltham, MA, USA, 2019.
- [8] R. Ponnappan, B. Donovan, L. Chow, High-power thermal management issues in space-based systems, in: *AIP Conf Proc*, 2002, pp. 65-72.

- [9] G. Upadhyaya, C. Pullins, K. Freitag, et al., State of the art of electronics cooling for radar antenna, in: ASME 2017 International Technical Conference and Exhibition on Packaging and Integration of Electronic and Photonic Microsystems (InterPACK2017), San Francisco, California, USA, 2017.
- [10] S. Weston, State of the Art of Small Spacecraft Technology, NASA, 2018. <https://ntrs.nasa.gov/api/citations/20200001421/downloads/20200001421.pdf>. (Accessed 4 March, 2024).
- [11] Y. Wang, C. Wang, P. Lian, et al., Effect of Temperature on Electromagnetic Performance of Active Phased Array Antenna, *Electronics*, 9(8) (2020) 1211.
- [12] C. Wang, Y. Wang, P. Lian, et al., Space Phased Array Antenna Developments: A Perspective on Structural Design, *IEEE Aerospace and Electronic Systems Magazine*, 35(7) (2020) 44-63.
- [13] K.E. Boushon, Thermal Analysis and Control of Small Satellites in Low Earth Orbit, Missouri University of Science and Technology, 2018.
- [14] J. Wang, Y. Li, X. Liu, et al., Recent active thermal management technologies for the development of energy-optimized aerospace vehicles in China, *Chinese Journal of Aeronautics*, 34(2) (2021) 1-27.
- [15] ACT Inc., Super Cool Small Satellite Thermal Control System, 2021. <https://www.1-act.com/resources/learning-center/case-studies/super-cool-satellite-thermal-control-system/>. (Accessed 4 March, 2024).
- [16] J. Young, Advanced Concepts for Small Satellite Thermal Control, in: 35th Annual Small Satellite Conference, 2021.
- [17] E.M. Silverman, Product development of engineered thermal composites for cooling spacecraft electronics, *Technology Review Journal*, (2005) 1-19.
- [18] H.S. Lee, Advanced Conductive Composite Materials for Spacecraft Application, *Advanced Materials Research*, 123-125 (2010) 7-10.
- [19] M.J. Montesano, Spacecraft Thermal Management Solutions Using Annealed Pyrolytic Graphite, in: 49th AIAA/ASME/ASCE/AHS/ASC Structures, Structural Dynamics, and Materials Conference, Schaumburg, IL, 2008.
- [20] X. Guo, S. Cheng, W. Cai, Advanced Materials Research, A review of carbon-based thermal interface materials: Mechanism, thermal measurements and thermal properties, *Materials & Design*, 209 (2021) 109936.
- [21] R. Suresh, K.P. Bloschock, A. Bar-Cohen, Advanced thermal management technologies for defense electronics, in: Defense Transformation and Net-Centric Systems 2012, 2012.
- [22] Y. Zhao, T. Semenic, A. Bhunia, Advanced Packaging and Thermal Management for High Power Density GaN Devices, in: 2013 IEEE Compound Semiconductor Integrated Circuit Symposium (CSICS), IEEE, Monterey, CA, USA, 2013, pp. 1-4.
- [23] R.A. Sayer, T.P. Koehler, S.M. Dalton, et al., Thermal Contact Conductance of Radiation-Aged Thermal Interface Materials for Space Applications, in: ASME 2013 Heat Transfer Summer Conference (HT2013), Minneapolis, MN, USA, 2013.
- [24] A.J. McNamara, Y. Joshi, Z. Zhang, Characterization of Nanostructured Thermal Interface Materials - A Review, in: the International Symposium on Thermal and Materials Nanoscience and Nanotechnology, Antalya, Turkey, 2011.
- [25] P. Puneet, A.M. Rao, R. Podila, Shape-controlled carbon nanotube architectures for thermal management in aerospace applications, *MRS Bulletin*, 40(10) (2015) 850-855.
- [26] M.T. Barako, V. Gambin, J. Tice, Integrated nanomaterials for extreme thermal management: a perspective for aerospace applications, *Nanotechnology*, 29(15) (2018) 154003.
- [27] F. Zhou, S.N. Joshi, Y. Liu, et al., Near-junction cooling for next-generation power electronics, *International Communications in Heat and Mass Transfer*, 108 (2019) 104300.
- [28] P.C. Chao, K. Chu, C. Creamer, et al., Low-Temperature Bonded GaN-on-Diamond HEMTs With 11 W/mm Output Power at 10 GHz, *IEEE Transactions on Electron Devices*, 62(11) (2015) 3658-3664.
- [29] R.M. Radway, Near junction thermal management of GaN HEMTs via wafer bonding, Massachusetts Institute of

Technology, 2017.

- [30] A. Bar-Cohen, J.J. Maurer, A. Sivananthan, Near-Junction Microfluidic Cooling for Wide Bandgap Devices, *MRS Advances*, 1(2) (2016) 181-195.
- [31] A. Bar-Cohen, J.J. Maurer, D.H. Altman, Embedded Cooling for Wide Bandgap Power Amplifiers: A Review, *Journal of Electronic Packaging*, 141(4) (2019) 040803.
- [32] J. Cho, Z. Li, E. Bozorg-Grayeli, et al., Thermal Characterization of Composite GaN Substrates for HEMT Applications, in: 13th InterSociety Conference on Thermal and Thermomechanical Phenomena in Electronic Systems, San Diego, CA, USA, 2012.
- [33] D.M. Tanner, H.R. Shea, R. Ramesham, Reliability of MEMS for space applications, in: *MOEMS-MEMS 2006 Micro and Nanofabrication*, 2006.
- [34] W. Yoonjin, C. Jungwan, D. Agonafer, et al., Fundamental Cooling Limits for High Power Density Gallium Nitride Electronics, *IEEE Transactions on Components, Packaging and Manufacturing Technology*, 5(6) (2015) 737-744.
- [35] K.N. Shukla, Heat Pipe for Aerospace Applications - An Overview, *Journal of Electronics Cooling and Thermal Control*, 05(01) (2015) 1-14.
- [36] M.T. Ababneh, C. Tarau, W.G. Anderson, et al., Advanced Passive Thermal Experiment for Hybrid Variable Conductance Heat Pipes and High Conductivity Plates on the International Space Station, in: 47th International Conference on Environmental Systems, Charleston, South Carolina, 2017.
- [37] P.R. Mock, D.B. Marcus, E.A. Edelman, Communications Technology Satellite: A Variable Conductance Heat Pipe Application, *Journal of Spacecraft and Rockets*, 12(12) (1975) 750-753.
- [38] M. Cleary, M.T. North, M. Van Lieshout, et al., Reduced Power Precision Temperature Control Using Variable Conductance Heat Pipes, *IEEE Transactions on Components, Packaging and Manufacturing Technology*, 3(12) (2013) 2048-2058.
- [39] K.L. Lee, C. Tarau, A. Lutz, et al., Advanced Hot Reservoir Variable Conductance Heat Pipes, in: International Conference on Environmental Systems, 2020.
- [40] K.L. Lee, C. Tarau, S. Adhikari, et al., Hot Reservoir Variable Conductance Heat Pipe with Advanced Fluid Management, in: 50th International Conference on Environmental Systems, 2021.
- [41] M.T. Ababneh, C. Tarau, W.G. Anderson, High Temperature Lightweight Heat Pipes for Solid-State Power Amplifier (SSPA) Thermal Management, in: The 18th IEEE Intersociety Conference on Thermal and Thermomechanical Phenomena in Electronic Systems (ITherm), Las Vegas, NV, USA, 2019.
- [42] H. Tang, Y. Tang, J. Li, et al., Experimental investigation of the thermal performance of heat pipe with multi-heat source and double-end cooling, *Applied Thermal Engineering*, 131 (2018) 159-166.
- [43] P.R. Mashaei, M. Shahryari, S. Madani, Analytical study of multiple evaporator heat pipe with nanofluid; A smart material for satellite equipment cooling application, *Aerospace Science and Technology*, 59 (2016) 112-121.
- [44] H.S.B. Brouwer, Performance Characterization of Water Heat Pipes and their Application in CubeSats, Delft University of Technology, 2016.
- [45] P. Dussinger, J. Weyant, R. Spangler, Cooling High Power Processing Devices Onboard Satellites: Testing Considerations for Space Copper-Water Heat Pipes (SCWHPs), 2021.
- [46] S.Y. Semenov, K.A. Burke, M.S. El-Genk, Titanium Heat Pipe Thermal Plane, in: *AIP Conf Proc*, 2008, pp. 131-137.
- [47] C. Oshman, B. Shi, C. Li, R. Yang, et al., The Development of Polymer-Based Flat Heat Pipes, *Journal of Microelectromechanical Systems*, 20(2) (2011) 410-417.
- [48] S. Isaacs, D. Arias, M. Hulse, et al., Enhancing CubeSat and Small Satellite Reliability through Improved Thermal Management, 2016. <https://digitalcommons.usu.edu/cgi/viewcontent.cgi?article=3511&context=smallsat>. (Accessed 4 March, 2024).
- [49] S.A. Isaacs, D.A. Arias, D. Hengeveld, et al., Experimental Development and Computational Optimization of Flat

Heat Pipes for CubeSat Applications, *Journal of Electronic Packaging*, 139(2) (2017) 020910.

[50] BOYD Corporation, Two Phase Thermal Solution Guide - A Quick & Easy Reference to Two Phase Cooling Technologies, 2021.

<https://info.boydcorp.com/hubfs/Thermal/Two-Phase-Cooling/Boyd-Two-Phase-Cooling-Guide-v2.pdf>. (Accessed 4 March, 2024).

[51] D.A. Nesterov, V.A. Derevyanko, S.B. Suntsov, Experimental investigations of flat T-shaped copper and titanium heat pipes, *Applied Thermal Engineering*, 198 (2021) 117454.

[52] M. Slobodeniuk, V. Ayel, R. Bertossi, et al., Experimental Analysis of The Fluid Flow in the Flat Plate Pulsating Heat Pipe under Microgravity Conditions, in: *International Symposium on Oscillating/Pulsating Heat Pipes (ISOPHP 2019)*, Daejeon, Korea, 2019.

[53] L.L. Vasiliev, L.L.V. Jr, The sorption heat pipe - a new device for thermal control and active cooling, *Superlattices and Microstructures*, 35(3-6) (2004) 485-495.

[54] Y.C Xiang, J.X. Chen, B.Q. Zhang, Thermal Control for Jade Rabbit Rover of Chang'E-3, *Journal of Astronautics*, 36(10) (2015) 1203-1209 (in Chinese).

[55] D.C. Bugby, Development and Testing of a Miniaturized Multi-Evaporator Hybrid Loop Heat Pipe, in: *AIP Conf Proc*, 2005, pp. 69-81.

[56] T.D. Swanson, G.C. Birur, NASA thermal control technologies for robotic spacecraft, *Applied Thermal Engineering*, 23(9) (2003) 1055-1065.

[57] D. Mishkinis, G. Wang, D. Nikanpour, et al., Advances in Two-Phase Loop with Capillary Pump Technology and Space Applications, in: *35th International Conference on Environmental Systems (ICES)*, Rome, Italy, 2005.

[58] G. Wang, D. Mishkinis, D. Nikanpour, Capillary heat loop technology: Space applications and recent Canadian activities, *Applied Thermal Engineering*, 28(4) (2008) 284-303.

[59] D.K. Mishra, T.T. Saravanan, G.P. Khanra, et al., Studies on the processing of nickel base porous wicks for capillary pumped loop for thermal management of spacecrafts, *Advanced Powder Technology*, 21(6) (2010) 658-662.

[60] Y.F. Maydanik, Development and Test Results of a Multi-Evaporator-Condenser Loop Heat Pipe, in: *AIP Conf Proc*, 2003, pp. 42-48.

[61] H. Nagano, J. Ku, Gravity Effect on Capillary Limit in a Miniature Loop Heat Pipe with Multiple Evaporators and Multiple Condensers, in: *AIP Conf Proc*, 2007, pp. 3-10.

[62] D. Cytrynowicz, M. Hamdan, P. Medis, et al., MEMS loop heat pipe based on coherent porous silicon technology, *AIP Conference Proceedings*, 608(1) (2002) 220.

[63] Y. Guo, Q. Zhou, X. Liu, et al., Co-designing cryogenic system with pulse tube cryocooler and loop heat pipe for infrared energy management, *Applied Thermal Engineering*, 195 (2021) 117228.

[64] T. Yang, S.L. Zhao, T. Gao, et al., Design and In-orbit Application of Temperature Controlled Loop Heat Pipe for Aerospace Distributed Heat Sources, *Journal of Astronautics*, 42(6) (2021) 798-806 (in Chinese).

[65] B. Richard, B. Anderson, C.H. Chen, et al., Development of a 3D Printed Loop Heat Pipe, in: *49th International Conference on Environmental Systems*, Boston, Massachusetts, 2019.

[66] B. Richard, D. Pellicone, W.G. Anderson, Loop Heat Pipe Wick Fabrication via Additive Manufacturing, in: *Joint 19th IHPC and 13th IHPS*, Pisa, Italy, 2018.

[67] T. Dutra, Loop Heat Pipe: Design and Performance During Operation, in: *AIP Conf Proc*, 2004, pp. 51-58.

[68] R.R. Riehl, T. Dutra, Development of an experimental loop heat pipe for application in future space missions, *Applied Thermal Engineering*, 25(1) (2005) 101-112.

[69] A. AlShehhi, A. AlMarar, Y. AlShehhi, et al., Thermal design evaluation of Loop Heat Pipe for small satellite applications using graphene Nano- Particles, in: *70th International Astronautical Congress (IAC)*, Washington D.C., United States, 2019.

[70] J. Ku, Temperature oscillations in loop heat pipe operation, in: *AIP Conf Proc*, 2001, pp. 255-262.

- [71] J. Ku, S.I. Jeong, D. Butler, Testing of a Miniature Loop Heat Pipe Using a Thermal Electrical Cooler for Temperature Control, in: 34th International Conference on Environmental Systems (ICES), Colorado Springs, Colorado, 2004.
- [72] J.Y. Huang, F.M. Pan, W.C. Fu, et al., Thermal design and verification of laser altimeter for GF-7 satellite, *Spacecraft Engineering*, 29(3) (2020) 138-143 (in Chinese).
- [73] T. Hoang, Development of a Two-Phase Capillary Pumped Heat Transport for Spacecraft Central Thermal Bus, in: *AIP Conf Proc*, 2003, pp. 49-54.
- [74] J. Yun, D. Bugby, Thermal Performance of Multi-Evaporator Hybrid Loop Heat Pipe (ME-HLHP) with a Liquid Cooled Shield (LCS), in: 5th International Energy Conversion Engineering Conference and Exhibit (IECEC), 2007.
- [75] L.L. Vasiliev, L.L.V. Jr., Sorption heat pipe - a new thermal control device for space and ground application, *Int J Heat Mass Transfer*, 48(12) (2005) 2464-2472.
- [76] C. Camañes, B. Champel, M. Mariotto, et al., Study of the state of the art of Space Thermal Control Systems, 2019.
- [77] W. Guo, Y. Li, Y.Z. Li, et al., An integrated hardware-in-the-loop verification approach for dual heat sink systems of aerospace single phase mechanically pumped fluid loop, *Applied Thermal Engineering*, 106 (2016) 1403-1414.
- [78] R.C.v. Benthem, W.d. Grave, J.v.E.J. Elst, et al., Development of a Mechanically Pumped Fluid Loop for 3 to 6 kW Payload Cooling, 2010.
- [79] R.C.v. Benthem, H.J.v. Gerner, J.v. Es, et al., Valve-less Mechanically Pumped Fluid Loop (MPFL) using East and West Panels of a Large Telecommunication Satellite as Radiator, in: 45th International Conference on Environmental Systems, Bellevue, Washington, 2015.
- [80] L. Anderson, C. Swenson, A.J. Mastropietro, et al., The Active CroCubeSat Project: Design and Status, in: 31st Annual AIAA/USU Conference on Small Satellites, 2017.
- [81] L. Anderson, C. Swenson, A.J. Mastropietro, et al., Active Thermal Architecture: Design and Status, in: 34th Annual Small Satellite Conference, 2020.
- [82] J.v. Es, T.H.v.d. Berg., A.v. Vliet, et al., The mini Mechanically Pumped Loop for CubeSat thermal control, in: 50th International Conference on Environmental Systems, Lisbon, Portugal, 2020.
- [83] S. Mohith, P.N. Karanth, S.M. Kulkarni, Recent trends in mechanical micropumps and their applications: A review, *Mechatronics*, 60 (2019) 34-55.
- [84] E. Kotlyarov, R. Reuvers, P.v. Put, et al., Modeling and Correlation of an Actively-Controlled Single Phase Mechanically-Pumped Fluid Loop, in: 37th International Conference on Environmental Systems (ICES), Chicago, Illinois, 2007.
- [85] J. Wang, Y.Z. Li, X.W. Ning, et al., Influences of Thermostatic Valve with Sensitive Wax on Dynamic Performance of Spacecraft Thermal Control System, *Journal of Astronautics*, 34(5) (2013) 734-740 (in Chinese).
- [86] J.X. Wang, Y.Z. Li, H.S. Zhang, et al., A highly self-adaptive cold plate for the single-phase mechanically pumped fluid loop for spacecraft thermal management, *Energy Conversion and Management*, 111 (2016) 57-66.
- [87] H. Lei, W. Fujun, Y. Xingang, et al., Simulation analysis on water hammer effect of single phase fluid loop used in thermal control of spacecraft, *Spacecraft Engineering*, 27(2) (2018) 68-73.
- [88] R. Turna, A. Hodunov, Development Status of Satellite Two-Phase Thermal Control Systems, *Aerospace technic and technology*, (2) (2021) 36-51.
- [89] P. Zhang, X. Wei, L. Yan, et al., Review of recent developments on pump-assisted two-phase flow cooling technology, *Applied Thermal Engineering*, 150 (2019) 811-823.
- [90] Z. Zhang, X.H. Sun, G.N. Tong, et al., Stable and self-adaptive performance of mechanically pumped CO₂ two-phase loops for AMS-02 tracker thermal control in vacuum, *Applied Thermal Engineering*, 31(17-18) (2011) 3783-3791.
- [91] A.S. Merino, J. Hugon, Y. Cailloce, et al., Development of a two-phase mechanically pumped loop(2MPDL) for the thermal dissipation management of an active antenna, in: 40th International Conference on Environmental Systems,

2010.

- [92] A.S. Merino, H. Julien, R. Nicolas, et al., Mock up definition and test plan for a two-phase mechanically pumped loop (2FMPDL) to manage the thermal dissipation of an active antenna, in: 41st International Conference on Environmental Systems, Portland, Oregon, 2011.
- [93] M.C. Ellis, R.C. Kurwitz, Development of a Pumped Two-phase System for Spacecraft Thermal Control, in: 46th International Conference on Environmental Systems, Vienna, Austria, 2016.
- [94] H.J.v. Gerner, T.H.v.d. Berg, J.v. Es, et al., Preliminary design of a mechanically pumped cooling system for active antennae, in: 50th International Conference on Environmental Systems, 2021.
- [95] J. Zuo, Robust Cooling of High Heat Fluxes Using Hybrid Loop Technology, in: AIP Conf Proc, 2005, pp. 64-68.
- [96] C. Park, A. Vallury, J. Zuo, et al., Spacecraft Thermal Management Using Advanced Hybrid Two-Phase Loop Technology, in: AIP Conf Proc, 2007, pp. 11-18.
- [97] B. Furst, S. Cappucci, T. Daimaru, et al., A Mechanically Pumped Two-Phase Fluid Loop for Thermal Control Based on the Capillary Pumped Loop, in: 49th International Conference on Environmental Systems, Boston, Massachusetts, 2019.
- [98] E. Sunada, B. Furst, P. Bhandari, et al., A two-phase mechanically pumped fluid loop for thermal control of deep space science missions, in: 46th International Conference on Environmental Systems, Vienna, Austria, 2016.
- [99] S. Jeong, J. Didion, Thermal Control Utilizing an Electrohydrodynamic Conduction Pump in a Two-Phase Loop With High Heat Flux Source, *Journal of Heat Transfer*, 129(11) (2007) 1576-1583.
- [100] W.W. Wits, S.J. Weitkamp, J. van Es, Metal Additive Manufacturing of a High-pressure Micro-pump, *Procedia CIRP*, 7 (2013) 252-257.
- [101] J.v. Es, A. Pauw, R.v.d. Berg, et al., Micro-pumped cooling loop to standardize micro-sat thermal control, in: 69th International Astronautical Congress (IAC), Bremen, Germany, 2018.
- [102] Q. Meng, Z. Zhao, H. Zhang, et al., Test study of the operating performance of a mechanically pumped two-phase loop for a space remote sensor, *Science China: Technological Sciences*, 50(11) (2020) 1474-1486.
- [103] Q. Meng, Z. Zhao, T. Zhang, et al., Experimental study on the transient behaviors of mechanically pumped two-phase loop with a novel accumulator for thermal control of space camera payload, *Applied Thermal Engineering*, 179 (2020) 115714.
- [104] Q. Meng, T. Zhang, F. Yu, et al., Experimental study on dynamic behavior of mechanically pumped two-phase loop with a novel accumulator in simulated space environment, *Chinese Journal of Aeronautics*, 35 (12) (2022) 102-116.
- [105] R.V. Bejarano, C. Park, Active flow control for cold-start performance enhancement of a pump-assisted, capillary-driven, two-phase cooling loop, *Int J Heat Mass Transfer*, 78 (2014) 408-415.
- [106] G.C. Birur, T.W. Sur, A.D. Paris, et al., Micro-nano spacecraft thermal control using a MEMS-based pumped liquid cooling system, in: *Micromachining and Microfabrication-2001*, San Francisco, CA, United States, 2001.
- [107] A. Bar-Cohen, J.J. Maurer, A. Sivanathan, Near-junction microfluidic thermal management of RF power amplifiers, in: *IEEE International Conference on Microwaves, Communications, Antennas and Electronic Systems (COMCAS 2015)*, Tel Aviv, Israel, 2015.
- [108] K. Matin, A. Bar-Cohen, J.J. Maurer, Modeling and Simulation Challenges in Embedded Two Phase Cooling DARPA's ICECool Program, in: *ASME 2015 International Technical Conference and Exhibition on Packaging and Integration of Electronic and Photonic Microsystems*, San Francisco, California, USA, 2015.
- [109] D.H. Altman, A. Gupta, M. Tyhach, Development of a Diamond Microfluidics-Based Intra-Chip Cooling Technology for GaN, in: *ASME 2015 International Technical Conference and Exhibition on Packaging and Integration of Electronic and Photonic Microsystems*, San Francisco, California, USA, 2015.
- [110] X.G. Yu, K. Xu, J.Y. Miao, et al., Design and On-Board Validation of Pumped Two-Phase Fluid Loop for High Heat Flux Removal, *Journal of Astronautics*, 38(2) (2017) 192-197.

- [111] Y. Huang, Q. Yang, J. Zhao, et al., Experimental Study on Flow Boiling Heat Transfer Characteristics of Ammonia in Microchannels, *Microgravity Science and Technology*, 32(3) (2020) 477-492.
- [112] T. Alam, W. Li, W. Chang, et al., Favourably regulating two-phase flow regime of flow boiling HFE-7100 in microchannels using silicon nanowires, *Sci Rep*, 11(1) (2021) 11131.
- [113] W.X. Chu, K.C. Huang, M. Amer, et al., Experimental and Numerical Investigations on Jet Impingement Cooling for Electronic Modules, *Journal of Heat Transfer*, 141(10) (2019) 102201.
- [114] R.D. Plant, J. Friedman, M.Z. Saghir, A review of jet impingement cooling, *International Journal of Thermofluids*, 17 (2023) 100312.
- [115] S.V. Ekkad, P. Singh, A Modern Review on Jet Impingement Heat Transfer Methods, *Journal of Heat Transfer*, 143(6) (2021) 064001.
- [116] Z. Lin, X. Wang, S. Liu, A microjet array cooling for the thermal management of active radar systems, in: 56th Electronic Components and Technology Conference San Diego, CA, USA, 2006.
- [117] J. Ditri, M.K. McNulty, S. Igoe, Embedded microfluidic cooling of high heat flux electronic components, in: 2014 Lester Eastman Conference on High Performance Devices (LEC), Ithaca, NY, USA, 2014.
- [118] J. Ditri, J. Hahn, R. Cadotte, et al., Embedded cooling of high heat flux electronics utilizing distributed microfluidic impingement jets, in: ASME 2015 International Technical Conference and Exhibition on Packaging and Integration of Electronic and Photonic Microsystems (InterPACK2015), San Francisco, California, USA, 2015.
- [119] V. Gambin, B. Poust, D. Ferizovic, et al., Impingement cooled embedded diamond multiphysics co-design, in: 15th IEEE Intersociety Conference on Thermal and Thermomechanical Phenomena in Electronic Systems (ITherm), Las Vegas, NV, USA, 2016.
- [120] S.M. Walsh, *Microjet Impingement Cooling of High PowerDensity Electronics*, Massachusetts Institute of Technology, 2018.
- [121] R. Xu, G. Wang, P. Jiang, Spray Cooling on Enhanced Surfaces: A Review of the Progress and Mechanisms, *Journal of Electronic Packaging*, 144(1) (2022) 010802.
- [122] J.D. Benter, J.D. Pelaez-Restrepo, C. Stanley, et al., Heat transfer during multiple droplet impingement and spray cooling: Review and prospects for enhanced surfaces, *Int J Heat Mass Transfer*, 178 (2021) 121587.
- [123] G. Liang, I. Mudawar, Review of spray cooling – Part 1: Single-phase and nucleate boiling regimes, and critical heat flux, *Int J Heat Mass Transfer*, 115 (2017) 1174-1205.
- [124] Q. Dang, M. Song, X. Luo, et al., A modeling study of different kinds of sessile droplets on the horizontal surface with surface wettability and gravity effects considered, *Energy Storage and Saving*, 1(1) (2022) 22-32.
- [125] E. Silk, Spray cooling and the next generation of NASA space flight, in: *Space Technology and Applications International Forum (ATAIF-2005)*, Albuquerque, New Mexico USA, 2005.
- [126] B.L. Rowden, Spray Cooling Development Effort for Microgravity Environments, in: *AIP Conf Proc*, 2006, pp. 134-144.
- [127] E.A. Silk, E.L. Gollither, R. Paneer Selvam, Spray cooling heat transfer: Technology overview and assessment of future challenges for micro-gravity application, *Energy Conversion and Management*, 49(3) (2008) 453-468.
- [128] J.X. Wang, Y.Z. Li, Y. Zhang, et al., A hybrid cooling system combining self-adaptive single-phase mechanically pumped fluid loop and gravity-immune two-phase spray module, *Energy Conversion and Management*, 176 (2018) 194-208.
- [129] Y. Zhang, L.P. Pang, Y.Q. Xie, et al., Experimental Investigation Of Spray Cooling Heat Transfer On Straight Fin Surface Under Acceleration Conditions, *Experimental Heat Transfer*, 28(6) (2014) 564-579.
- [130] T.E. Michalak, K.L. Yerkes, S.K. Thomas, et al., Acceleration Effects on the Cooling Performance of a Partially Confined FC-72 Spray, *Journal of Thermophysics and Heat Transfer*, 24(3) (2010) 463-479.
- [131] L. Lin, R. Ponnappan, K. Yerkes, Actively Pumped Two-Phase Loop for Spray Cooling, *Journal of Thermophysics and Heat Transfer*, 20(1) (2006) 107-110.

- [132] J.X. Wang, Y.Z. Li, G.C. Li, et al., Investigation of a gravity-immune chip-level spray accooling for thermal protection of laser-based wireless power transmission system, *International Journal of Heat and Mass Transfer*, 114 (2017) 715-726.
- [133] J.X. Wang, W. Guo, K. Xiong, et al., Review of aerospace-oriented spray cooling technology, *Progress in Aerospace Sciences*, 116 (2020) 100635.
- [134] J. Smay, C. Hose, R. Spangler, Passive Thermal Storage of Small Satellites for SWaP Improvements Over Thousands of Operational Cycles, in: 35th Annual Small Satellite Conference, 2021.
- [135] X.D. Zhang, J. Liu, Perspective on liquid metal enabled space science and technology, *Science China Technological Sciences*, 63(7) (2020) 1127-1140.
- [136] C. Zhao, M. Opolot, P. Keane, et al., Thermal characteristics of melting of a phase change material enhanced by a stainless-steel 304 periodic structure, *Energy Storage and Saving*, 2(2) (2023) 442-448.
- [137] S. Zhang, Z. Li, Y. Yan, et al., Comparative study on heat transfer enhancement of metal foam and fins in a shell-and-tube latent heat thermal energy storage unit, *Energy Storage and Saving*, 2(3) (2023) 487-494.
- [138] A. Chibani, A. Dehane, S. Merouani, et al., Melting/solidification of phase change material in a multi-tube heat exchanger in the presence of metal foam: effect of the geometrical configuration of tubes, *Energy Storage and Saving*, 1(4) (2022) 241-258.
- [139] D.L. Vrable, M.D. Vrable, Space-based radar antenna thermal control, in: *Space Technology and Applications International Forum*, AIP, 2001, pp. 277-282.
- [140] K. Yamada, H. Nagano, Y. Kobayashi, et al., Heat Storage Panel Using a Phase-change Material Encapsulated in a High-thermal conductivity CFRP for Micro Satellites, in: 44th International Conference on Environmental Systems, Tucson, Arizona, 2014.
- [141] M.K. Choi, Paraffin Phase Change Material for Maintaining Temperature Stability of IceCube Type of CubeSats in LEO, in: 13th International Energy Conversion Engineering Conference, Orlando, FL, 2015.
- [142] S. Isaacs, D.A. Arias, G. Shoukas, Development of a lightweight and low-cost 3D printed aluminum and PCM panel for thermal, in: 47th International Conference on Environmental Systems, Charleston, South Carolina, 2017.
- [143] T.G. Desai, D. Piedra, R. Bonner, T. Palacios, Novel junction level cooling in pulsed GaN devices, in: 13th InterSociety Conference on Thermal and Thermomechanical Phenomena in Electronic Systems, San Diego, CA, USA, 2012.
- [144] M.G. Izenon, D.A. Knaus, L. O'Neill, Thermal Storage for High-Power Small Satellites, in: 34th Annual Small Satellite Conference, 2020.
- [145] H. Madhav, V. Raghavendra, P. Kumar, et al., Development of a Canister Module For PCM Coupled Heat Pipe in Spacecraft Thermal Management, *IEEE Transactions on Components, Packaging and Manufacturing Technology*, 11(11) (2021) 1804 - 1815.
- [146] ACT Inc., *Smallsat Thermal Management*, 2021. <https://info.1-act.com/ebook-smallsat-thermal-management>. (Accessed 4 March, 2024)
- [147] K.L. Lee, C. Tarau, N.V. Velson, Development of a Heat Exchanger with Integrated Thermal Storage for Spacecraft Thermal Management Applications, in: 47th International Conference on Environmental Systems, Charleston, South Carolina, 2017.
- [148] M. Kabir, T. Gameda, E. Preller, et al., Design and Development of a PCM-Based Two-Phase Heat Exchanger Manufactured Additively for Spacecraft Thermal Management Systems, *Int J Heat Mass Transfer*, 180 (2021).
- [149] J. Yun, C. Tarau, N.V. Velson, Status of the Development of a Vapor Chamber with Phase Change Material-Based Wick Structure, in: 46th International Conference on Environmental Systems, Vienna, Austria, 2016.
- [150] C.R. Hartsfield, T.E. Shelton, B.O. Palmer, et al., All-Metallic Phase Change Thermal Management Systems for Transient Spacecraft Loads, *Journal of Aerospace Engineering*, 33(4) (2020) 04020039.
- [151] C.R. Raj, S. Suresh, R.R. Bhavsar, et al., Influence of fin configurations in the heat transfer effectiveness of Solid

- solid PCM based thermal control module for satellite avionics: Numerical simulations, *Journal of Energy Storage*, 29 (2020) 101332.
- [152] A.S. Galouye, T. Tjiptahardja, S.V. Oost, et al., DELPHRAD - Lightweight & High Performance Deployable Radiator Development Program, in: 34th International Conference on Environmental Systems (ICES), Colorado Springs, Colorado, 2004.
- [153] D.W. Hengeveld, M.R. Wilson, J.A. Moulton, et al., Thermal design considerations for future high-power small satellites, in: 48th International Conference on Environmental Systems, Albuquerque, New Mexico, 2018.
- [154] B. Yendler, A. Meginnis, A. Reif, Thermal Management for High Power Cubesats, in: 34th Annual AIAA/USU Small Satellite Conference, 2020.
- [155] J. Chen, L. Lei, G. Fang, Elastocaloric cooling of shape memory alloys: A review, *Materials Today Communications*, 28 (2021) 102706.
- [156] C.L. Bertagne, T.J. Cognata, R.B. Sheth, et al., Testing and analysis of a morphing radiator concept for thermal control of crewed space vehicles, *Applied Thermal Engineering*, 124 (2017) 986-1002.
- [157] A. Ueno, K. Yamada, K. Miyata, et al., Proposal of Functional Thermal Control Systems for High-Power Micro-Satellite and Its Demonstration under Thermal Vacuum Condition, *Journal of Electronics Cooling and Thermal Control*, 08(01) (2018) 1-17.
- [158] M. Bsibsi, G.v. Donk, A. Pauw, et al., The Variable Effective Surface Radiator, Novel Heat Switch Technology Based on the Oscillating Heat Pipe Principle, in: 36th International Conference on Environmental Systems (ICES), Norfolk, Virginia, 2006.
- [159] S. Cao, X. Chen, G. Wu, et al., Variable Emissivity Surfaces for Micro and Nano-satellites, *Physics Procedia*, 18 (2011) 91-94.
- [160] J. Currano, S. Moghaddam, J. Lawler, et al., Performance Analysis of an Electrostatic Switched Radiator Using Heat-Flux-Based Emissivity Measurement, *Journal of Thermophysics and Heat Transfer*, 22(3) (2008) 360-365.
- [161] D. Zhou, D. Xie, X. Xia, et al., All-solid-state electrochromic devices based on WO₃/NiO films: material developments and future applications, *Science China Chemistry*, 60(1) (2016) 3-12.
- [162] R. Osiander, S.L. Firebaugh, J.L. Champion, et al., Microelectromechanical Devices for Satellite Thermal Control, *IEEE Sensors Journal*, 4(4) (2004) 525-531.
- [163] Y.Z. Li, Y.Y. Wang, K.M. Lee, Dynamic Modeling and Transient Performance Analysis of a LHP-MEMS Thermal Management System for Spacecraft Electronics, *IEEE Transactions on Components and Packaging Technologies*, 33(3) (2010) 597-606.
- [164] A. Ueno, Y. Suzuki, Parylene-based active micro space radiator with thermal contact switch, *Applied Physics Letters*, 104(9) (2014).
- [165] H. Demiryont, K.C. Shannon, Variable Emittance Electrochromic Devices for Satellite Thermal Control, in: AIP Conf Proc, 2007, pp. 51-58.
- [166] S. Taylor, N. Boman, J. Chao, et al., Cryothermal vacuum measurement of thermochromic variable-emittance coatings with heating/cooling hysteresis for spacecraft thermal management, *Applied Thermal Engineering*, 199 (2021) 117561.
- [167] S.C. Joshi, Outgassing studies on thermal control coatings for micro - satellites, *Aircraft Engineering and Aerospace Technology*, 83(2) (2011) 69-74.
- [168] T.Y. Kim, B.S. Hyun, J.J. Lee, et al., Numerical study of the spacecraft thermal control hardware combining solid-liquid phase change material and a heat pipe, *Aerospace Science and Technology*, 27(1) (2013) 10-16.
- [169] N.V. Velson, C. Tarau, M. DeChristopher, et al., Multiple Loop Heat Pipe Radiator for Variable Heat Rejection in Future Spacecraft, in: 45th International Conference on Environmental Systems, Bellevue, Washington, 2015.
- [170] W. Anderson, D. Sarraf, P. Dussinger, et al., Development of a High-Temperature Water Heat Pipe Radiator, in: 3rd International Energy Conversion Engineering Conference, 2005.

- [171] H.J.v. Gerner, G.v. Donk, A. Pauw, et al., A Heat Pump for Space Applications, in: 45th International Conference on Environmental Systems, Bellevue, Washington, 2015.
- [172] W. Kowbel, W. Champion, P. Oliver, et al., Novel composites for space microelectronics and optics, in: 2001 IEEE Aerospace Conference Proceedings, IEEE, Big Sky, MT, USA, 2001, pp. 2549-2554.
- [173] J.J. Banisaukas, Carbon Fiber Composites for Spacecraft Thermal Management Opportunities, in: AIP Conf Proc, 2005, pp. 10-21.
- [174] D. Shaddock, S. Weaver, I. Chasiotis, et al., Development of a Compliant NanoThermal Interface Material, in: ASME 2011 Pacific Rim Technical Conference & Exposition on Packaging and Integration of Electronic and Photonic Systems, Portland, Oregon, USA, 2011.
- [175] Y. Zhao, D. Strauss, T. Liao, et al., Development of a High Performance Thermal Interface Material With Vertically Aligned Graphite Platelets, in: ASME/JSME 2011 8th Thermal Engineering Joint Conference, Honolulu, Hawaii, USA, 2011.
- [176] J.R. Wasniewski, D.H. Altman, S.L. Hodson, et al., Characterization of Metallically Bonded Carbon Nanotube-Based Thermal Interface Materials Using a High Accuracy 1D Steady-State Technique, *Journal of Electronic Packaging*, 134(2) (2012) 020901.
- [177] C.H. Walker, E.T. Winlow, Application of amorphous diamond materials to provide a reliable, electrically insulating, thermal interface for IC devices for electronics applications in harsh environments, in: 23rd International Workshop on thermal Investigations of ICs and systems, Amsterdam/NL, 2017.
- [178] M.T. Ababneh, C. Tarau, W.G. Anderson, et al., Copper-Water and Hybrid Aluminum-Ammonia Heat Pipes for Spacecraft Thermal, in: Joint 19th IHPC and 13th IHPS, Pisa, Italy, 2018.
- [179] Z. Qiang, W. Lu, L. Chang, et al., Design and Verification of 3D Printing Titanium-water Heat Pipe Used in High-power Spacecraft, *Spacecraft Engineering*, 29(4) (2020) 86-92 (in Chinese).
- [180] J. Kirshberg, K.L. Yerkes, D. Liepmann, Demonstration of a micro-CPL based on MEMS fabrication technologies, in: 35th Intersociety Energy Conversion Engineering Conference and Exhibit (IECEC), Las Vegas, NV, USA, 2000.
- [181] K. Goncharov, A. Orlov, A. Tarabrin, et al., 1500 W deployable radiator with loop heat pipe, in: 31st International Conference on Environmental Systems, Orlando, Florida, 2001.
- [182] Y.F. Maydanik, S.V. Vershinin, M.A. Korukov, et al., Miniature loop heat pipes-a promising means for cooling electronics, *IEEE Transactions on Components and Packaging Technologies*, 28(2) (2005) 290-296.
- [183] J. Lee, D. Kim, J. Mun, et al., Heat-Transfer Characteristics of a Cryogenic Loop Heat Pipe for Space Applications, *Energies*, 13(7) (2020) 1616.
- [184] J.v. Es, H.J.v. Gerner, R.C.v. Benthem, et al., Component development in Europe for Mechanically Pumped Loop Systems (MPLs) for cooling applications in space, in: 46th International Conference on Environmental Systems, Vienna, Austria, 2016.
- [185] J.C. Mulligan, D.P. Colvin, Y.G. Bryant, Microencapsulated phase-change material suspensions for heat transfer in spacecraft thermal systems, *Journal of Spacecraft and Rockets*, 33(2) (1996) 278-284.
- [186] G.C. Birur, K.R. Johnson, Keith S. Novak, et al., Thermal control of mars lander and rover batteries and electronics using loop heat pipe and phase change material thermal storage technologies, in: International Conference On Environmental Systems, 2000.
- [187] X. Shao, Y. Xiang, C. Tan, Heat pipe applications and test in Chang'E-1 satellite, *Spacecraft Engineering*, 17(1) (2008) 63-67 (in Chinese).
- [188] M.K. Choi, Using Paraffin PCM to Make Optical Communication Type of Payloads Thermally Self-Sufficient for Operation in Orion Crew Module, in: 14th International Energy Conversion Engineering Conference, 2016.
- [189] J. Xu, C. Tarau, M. Ellis, et al., Design of an Additively Manufactured Vapor Chamber Heat Exchanger for Space Applications, in: 2021 20th IEEE Intersociety Conference on Thermal and Thermomechanical Phenomena in Electronic Systems (iTherm), 2021, pp. 1091-1097.

[190] C.R. Raj, S. Suresh, V.K. Singh, et al., Experimental investigation on nanoalloy enhanced layered perovskite PCM tamped in a tapered triangular heat sink for satellite avionics thermal management, *International Journal of Thermal Sciences*, 167 (2021) 107007.

[191] P. Kumar Rai, S. Rao Chikkala, A.A. Adoni, et al., Space Radiator Optimization for Single-Phase Mechanical Pumped Fluid Loop, *Journal of Thermal Science and Engineering Applications*, 7(4) (2015) 041021.

Journal Pre-proof

Table captions

Table 1	Summary of advanced thermal conductive materials applicable for spacecrafts.
Table 2	Summary of unseparated heat pipes applicable for spacecrafts.
Table 3	Comparison of various capillary pumped two-phase loops.
Table 4	Summary of separated heat pipes in spacecraft applications.
Table 5	Comparison of single-phase and two-phase MPFL.
Table 6	Implementation of PCMs for thermal management of spacecraft electronics.
Table 7	Summary of thermal radiator techniques developed for spacecrafts thermal management.

Table 1

Summary of advanced thermal conductive materials applicable for spacecrafts.

Developer/organization	Application	Material	Thermal conduction performance	Major characteristics
ACT, Inc [16]	TIM	Annealed pyrolytic graphite (APG)	$k_{xy} = 1700 \text{ W}\cdot\text{m}^{-1}\cdot\text{K}^{-1}$; $k_z = 10 \text{ W}\cdot\text{m}^{-1}\cdot\text{K}^{-1}$	APG alone is brittle and low strength, and requires encapsulation by a stronger material.
Boyd Corp. [16]	TIM	Carbon nanotube embedded film	N/A	Combine through-plane with high in-plane thermal conduction by aligning the carbon nanotubes. It enhances heat transfer and decrease mass by layering sheets of graphene like a traditional layered heat strap. It provides orders of magnitude higher flexibility with twice the thermal conductance to mass ratio than pyrolytic graphene sheet or graphene composite sheets.
Thermal Space Ltd. [16]	HS	Layered Nanostructured Cross(X)-Linked (LyNX) Graphene	N/A	
Thermotive Technology [16]	HS	Pyrovo™ Pyrolytic Graphite Film	$k \approx 1500 \text{ W}\cdot\text{m}^{-1}\cdot\text{K}^{-1}$	N/A
Boyd k-Core [16]	HS	Encapsulated APG core in a flexible strap	$k = 1200 \text{ W}\cdot\text{m}^{-1}\cdot\text{K}^{-1}$	It provides increased conductivity at cryogenic temperatures.
Northrop Grumman Space Technology [17]	HS	Carbon polymer composite encapsulated APG	$k \approx 800 \text{ W}\cdot\text{m}^{-1}\cdot\text{K}^{-1}$	It is developed for spacecraft thermal radiator subsystem with significant cost, weight, and risk savings.
MER Corporation [172]	HS	C-SiC composite	$k_{xy} = 340 \text{ W}\cdot\text{m}^{-1}\cdot\text{K}^{-1}$; $k_z = 38 \text{ W}\cdot\text{m}^{-1}\cdot\text{K}^{-1}$	It features low-cost, matching the coefficient of thermal expansion of Si and excellent performance in cyclic testing.
MER Corporation [172]	HS	C-C and Al-infiltrated graphite and diamond composite	$k = 580 \text{ W}\cdot\text{m}^{-1}\cdot\text{K}^{-1}$	It features low-cost, matching the coefficient of thermal expansion of GaAs.
Northrop Grumman Space Technology [173]	HS	Al-clad carbon fiber reinforced composite	$k_{xy} = 503\sim 509 \text{ W}\cdot\text{m}^{-1}\cdot\text{K}^{-1}$	It is developed for efficient, light weight satellite radiator panels. It features high specific modulus capability and can be attached to aluminum face sheet honeycomb panels.
k Technology Corporation [19]	HS	Encapsulated APG within a structural shell	$k_{xy} = 1400 \text{ W}\cdot\text{m}^{-1}\cdot\text{K}^{-1}$; $k_z \approx 5 \text{ W}\cdot\text{m}^{-1}\cdot\text{K}^{-1}$	It features low mass density (as low as $1.9 \text{ g}\cdot\text{cm}^{-3}$), high stiffness (up to 50 Msi), and engineered coefficient of thermal expansion.

General Electric Research [174]	TIM	Copper nanosprings	$R < 0.01 \text{ cm}^2 \cdot \text{K} \cdot \text{W}^{-1}$.	It allows for thin solder bond lines using a compliant structure within the bond line.
Georgia Institute of Technology [24]	TIM	Multi-walled vertically oriented carbon nanotube	$R \approx 0.02 \text{ cm}^2 \cdot \text{K} \cdot \text{W}^{-1}$	N/A
Teledyne Scientific and Imaging Company [175]	TIM	Vertically aligned graphite platelet	$R = 0.03 \text{ cm}^2 \cdot \text{K} \cdot \text{W}^{-1}$	It features vertically laminated structure, in which thin solder layers are laminated with aligned graphite layers. It provides extraordinarily high z-axis thermal conductivity and controllable stiffness by simply setting the thickness of each component layer to match different surfaces.
Raytheon Integrated Defense Systems [176]	TIM	Metallically bonded short, vertically aligned double-sided, multiwalled carbon nanotube	$R = 3.5 \text{ mm}^2 \cdot \text{K} \cdot \text{W}^{-1}$	Vertically aligned carbon nanotubes grown on both sides of a thin interposer foil and interfaced with substrate materials via metallic bonding.
Diamond Hard Surfaces Ltd [177]	HS	Diamond-like carbon coating	$k = 850 \sim 1050 \text{ W} \cdot \text{m}^{-1} \cdot \text{K}^{-1}$	It is of high thermal conductivity and electrical resistance. Its breakdown voltages in excess of 500 V, even with a coating thickness of only 21 μm .

Table 2

Summary of unseparated heat pipes applicable for spacecrafts.

Reference	Type	Wick material	Working fluid	Characteristics
Mock et al. [37]	VCHP	304 stainless steel metal felt	Methanol	A two-artery/slab wick system with menisci-coalescence priming foils to aid in venting the arteries of entrapped gas bubbles was utilized. The control gas consists of 90% nitrogen and 10% helium. The thermal plane is with the total mass of 26.3 grams, and tested at the maximum heat flux of $60 \text{ W}\cdot\text{cm}^{-2}$. The thermal resistance at $40 \text{ W}\cdot\text{cm}^{-2}$ heat flux input is $0.9 \text{ K}\cdot\text{W}^{-1}$. The operating temperature ranges from $5 \text{ }^\circ\text{C}$ to $90 \text{ }^\circ\text{C}$.
Semenov et al. [46]	VC	Titanium	Water	The thermal resistance at $40 \text{ W}\cdot\text{cm}^{-2}$ heat flux input is $0.9 \text{ K}\cdot\text{W}^{-1}$. The operating temperature ranges from $5 \text{ }^\circ\text{C}$ to $90 \text{ }^\circ\text{C}$.
Oshman et al. [47]	VC	Copper micropillar and woven mesh hybrid wick	Water	Flexible liquid-crystal polymer films with copper-filled thermal vias were employed as the case material. The effective thermal conductivity ranges between 650 to $830 \text{ W}\cdot\text{m}^{-1}\cdot\text{K}^{-1}$ at the heat flux of $11.94 \text{ W}\cdot\text{cm}^{-2}$
Cleary et al. [38]	VCHP	Sintered copper	Methanol	The TEC-VCHP assembly is developed for reduced-power precision temperature control of photonics components. Argon is used as the control gas.
Brouwer [44]	Cylindrical heat pipe	Axial grooved copper wick	Water	It explores the possibility of employing water heat pipes in CubeSats. The heat pipe can passively transport the heat loads expected (up to 10 W) in the next-generation CubeSats.
Mashaie et al. [43]	Cylindrical heat pipe	Copper	Al_2O_3 -water nanofluid	It consists of three evaporators. A significant reduction in the thermal resistance and size of heat pipe can be achieved via the use of nanofluid.
Ababneh et al. [36]	VCHP	Copper hybrid wick	Ammonia or water	It is of a hybrid wick that contains screen mesh or sintered evaporator wicks for the evaporator region was developed to sustain high heat fluxes. The axial grooves in the adiabatic and condenser sections can transfer large amounts of power over long distances due to the high wick permeability and low liquid pressure drop.
Ababneh et al. [36]	Al plate with embedded copper/water heat pipe (HiK™ plate)	Copper	Water	Heat pipes is embedded in a plate to transfer heat from one location to another. The effective thermal conductivity ranges from 500 to $1200 \text{ W}\cdot\text{m}^{-1}\cdot\text{K}^{-1}$. In some spacecraft applications, the effective thermal conductivity can be as high as $2500 \text{ W}\cdot\text{m}^{-1}\cdot\text{K}^{-1}$, which is equivalent to diamond.
Isaacs et al. [49]	VC (FlexCool strap)	Copper	Acetone	The FlexCool strap is based on an assembly of $50.8 \text{ }\mu\text{m}$ thick copper foils (casing layers), fine copper woven meshes (wicks) and coarse copper woven meshes (vapor cores). The average effective thermal conductivity

Ababneh et al.[178]	CCHP	Aluminum	Ammonia	reached $2149 \text{ W}\cdot\text{m}^{-1}\cdot\text{K}^{-1}$ with the thickness of 0.86 mm, withstanding internal vapor pressures as high as 930 kPa. The hybrid wick contains screen mesh, metal foam, or sintered evaporator wicks, which can sustain high heat flux ($>50 \text{ W}\cdot\text{cm}^{-2}$), for the evaporator region. The thermal resistance is smaller than $0.012 \text{ K}\cdot\text{W}^{-1}$.
Tang et al. [42]	Cylindrical heat pipe	Grooved copper wick	Deionized water	The heat pipe with multi-heat source and double-end cooling is suitable for multi-heat source spacecraft. The multiple heat sources are placed at the middle section of an ordinary heat pipe while two heat sinks are installed at both ends of the pipe.
Ababneh et al. [41]	CCHP	Grooved titanium wick	Water	The 3D-printed, grooved titanium-water heat pipe allows the radiator size and mass to be significantly reduced. An internal buffer is adopted to improve freeze/thaw tolerance of the heat pipe and enable multiple freeze/thaw cycles without bursting the pipe.
Zhou et al. [179]	Cylindrical heat pipe	Grooved titanium wick	Water	The shell and capillary structure of the heat pipe are manufactured via 3D printing technology. The operating temperature range is $100\sim 300 \text{ }^\circ\text{C}$ and the heat transfer ability reaches the peak when working between $180\sim 250 \text{ }^\circ\text{C}$.
Lee et al. [39, 40]	VCHP	Grooved titanium wick	Acetone	Helium is selected as control gas. A hot reservoir VCHP loop concept with a loop configuration is developed to improve fluid management. The fluid management of a hot reservoir VCHP needs to be improved to ensure its long-term reliability
Nesterov et al. [51]	T-shaped flat heat pipe	Copper; Titanium	Water; acetonitrile	The novel T-shaped design of the heat pipes provides efficient heat transfer between perpendicular surfaces. Acetonitrile was used as the working fluid for the titanium heat pipes because of its restricted outgassing, work in sub-zero temperatures and relatively low pressure of saturated vapor compared to other conventional working fluids (acetone, methanol).

Table 3

Comparison of capillary pumped two-phase loops [55].

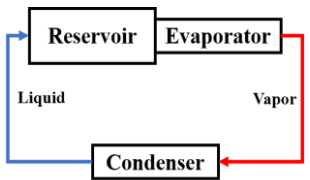
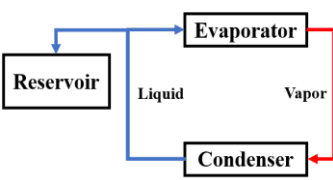
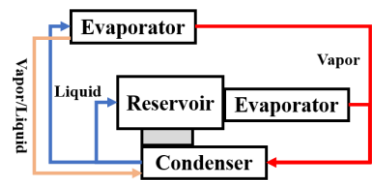
Type	LHP	CPL	HLHP
Configuration			
Advantages	Subcooling insensitivity; autonomous start-up	Remote reservoir easily "cold-biased"; multi-evaporator architectures are possible	Maximizes CPL and LHP advantages and mitigates their shortcomings
Disadvantages	Local reservoir harder to cold bias; practically limited to 1~2 evaporators	Subcooling sensitivity; loop preconditioning required for start-up	More complex configuration

Table 4

Summary of separated heat pipes in spacecraft applications.

Reference	Type	Materials	Working fluid	Characteristics
Kirshberg [180]	Micro-CPL	The wick structure is etched into a borofloat glass cover plate Evaporator: aluminum body;	Water	The three-port micro-CPL is developed via MEMS technology. The evaporator dimension is $1000 \mu\text{m} \times 2000 \mu\text{m}$ and the length of the liquid and vapor lines is 35 mm.
Goncharov [181]	LHP	condenser: embedded aluminum pipes Evaporator: aluminum;	N/A	Special design is performed over the LHP condenser to allow multiple freezing and melting cycles and provides high resistance to meteorite action.
Ku et al. [70]	Miniature LHP	compensation chamber: stainless steel; condenser: aluminum tubing	Ammonia	The miniature LHP has an envelope dimension of $178 \text{ mm} \times 127 \text{ mm} \times 51 \text{ mm}$ and a mass of about 160 g.
Cytrynowicz et al. [62]	Miniature LHP	Wick: coherent porous silicon	Deionized water	The breakthrough coherent porous silicon wick technology allows the MEMS-based planer LHP capable of handling high heat fluxes ($>300 \text{ W}\cdot\text{cm}^{-2}$).
Hoang et al. [73]	HLHP	Evaporator: axially grooved aluminum; wick: Sol-Gel; secondary wick: polyethylene	Ammonia	It combines a CPL and LHP into one loop. The objective is to manage the heat leak across the evaporator pump wick by an additional capillary pump.
Maydanik et al. [60]	Ramified LHP	Wick: nickel; other components: stainless steel	Ammonia	It consists of two cylindrical evaporators and two condensers developed for symmetrical and non-symmetrical heat load distributions between the evaporators.
Dutra et al. [67]	LHP	Evaporator: stainless steel; Wick: polyethylene; secondary wick: stainless steel screen mesh	Acetone	Heat transport capacity reaches up to 70 W. The selection of acetone was due to a tendency in substituting hazardous working fluids such as ammonia in two-phase capillary pumping systems, which present a high risk.
Ku et al. [71]	Miniature LHP	Evaporator: Aluminum; wick: stainless steel	Ammonia	A TEC is installed on the compensation chamber to cool or heat it. The LHP demonstrated very robust operation in all tests where the heat load varied between 0.5 W and 140 W, and the sink temperature varied between 243 K and 293 K.
Vasiliev et	SHP	Wick: titanium	Ammonia	The SHP can be considered as a combination

al. [53, 75]		sintered powder		of a LHP and an ammonia solid sorption cooler. The SHP has a sorbent bed at one end and a condenser and evaporator at the other end. It is insensitive to some hyper gravity. It consists of multiple evaporators. The heat transport capacity of the quad-evaporator HLHP ranges from 8 to 280 W while single-evaporator transport from 2 to 100 W. The maximum heat flux is 30 W/cm ² , and the temperature control is of ± 0.25 K with a variable set-point.
Bugby et al. [55]	HLHP	Wick: Teflon	Ammonia	The two miniature LHP possess mechanical flexibility and are adaptable to different conditions of location and operation. The mass ranges from 10 to 20 g. The diameter of the two cylindrical evaporators are 5 and 6 mm, respectively. They are capable of transferring heat loads of 100~200 W for distances up to 300 mm in the temperature range 50~100 °C at any orientation in 1 g conditions.
Maydanik et al. [182]	Miniature LHP	Body: stainless steel/copper; wick: titanium/copper	Ammonia/ water	The Miniature LHP consists of two parallel evaporators, two parallel condensers, a common vapor transport line and a common liquid return line. Titanium primary wicks with 6.35 mm outer diameter and 1.65 μ m pore size. A TEC is attached to each compensation chamber and copper thermal straps connect the rear side of the TEC to the evaporators.
Nagano et al. [61]	Miniature LHP	Wick: titanium, pipe lines: stainless steel; condenser: aluminum	Ammonia	The multi-evaporator HLHP includes a liquid cool shield. The liquid cool shield is specially designed to maximize loop robustness during transient variations in heat load via protecting the liquid return line from parasitic heat gains. Graphene-water nanofluid is adopted to enhance the thermal performance of the LHP.
Yun et al. [74]	Multi-Evaporator HLHP	Evaporator: aluminum; pipe lines: stainless steel; wick: titanium	Ammonia	The LHP incorporated with a deployable radiator provides a solution for high-power small satellites with payload power as high as 75W.
AlShehhi [69]	LHP	N/A	Graphene water nanofluid	
Richard et al. [65, 66]	LHP	Envelope: aluminum; all wetted parts: 316L stainless steel;	Ammonia	The primary and secondary wick in the evaporator is fabricated using a DMLS process to reduce the overall cost. DMLS parameters for producing wicks with a pore

		wick: nickel		radius of 5.6 μ m are developed to make LHPs with power levels of 100~200 W.
Huang et al. [72]	LHP	N/A	Ammonia.	Multiple evaporators are specially designed for different types of heat source. The temperature fluctuation is controlled within ± 0.3 °C, which better realized the precise temperature control of the key components on-board. An auxiliary operation heater is installed on the LHP capillary pump to ensure stable operation.
Lee et al. [183]	Cryogenic LHP	Evaporator and compensation chamber: copper and 304 stainless steel; condenser: copper	Liquid nitrogen	The cryogenic LHP with two evaporators included a subloop for initial start-up, and used a pressure reduction reservoir for the supercritical start-up from room to cryogenic temperature. The heat-transfer performance was verified for a heat-transfer distance of 500 mm at temperatures below -150 °C.
Guo et al.[63]	Cryogenic LHP	Copper	Neon	Two neon cryogenic LHPs are combined with two pulse tube cryocoolers to form a co-designing cryogenic system operating at temperature around 35 K. A novel integrated multifunctional heat exchanger is proposed to couple the heat exchange between the cold head of pulse tube cryocooler and the condenser of cryogenic LHP.
Yang et al.[64]	LHP	Evaporator: stainless steel; wick: silicon nitride; condenser: aluminum alloy	Ammonia	Multiple electric heaters are used to achieve precise temperature control of distributed heat sources, which are cooled by a cold plate assembly. The temperature stability of the cold plates is always maintained at ± 0.7 °C in a year.

Table 5

Comparison of single-phase and two-phase MPFL [184].

Loop type	Single-phase MPFL	Two-phase MPFL
Loop structure		
Advantages	Simple layout; high technical maturity and reliability	High heat removal capacity; high temperature control precision, stability and uniformity; small diameter of tubes; low pump power consumption
Disadvantages	Limited heat removal capacity; poor temperature control stability; the temperature control precision is dependent on the control algorithm	Large volume of accumulator; occurrence of flow instability; poor technical maturity

Table 6

Implementation of PCMs for thermal management of spacecraft electronics.

Reference	PCM	Density ($\text{kg}\cdot\text{m}^{-3}$)	Melting point ($^{\circ}\text{C}$)	Specific heat ($\text{kJ}\cdot\text{kg}^{-1}\cdot^{\circ}\text{C}^{-1}$)	Thermal conductivity ($\text{W}\cdot\text{m}^{-1}\cdot^{\circ}\text{C}^{-1}$)	Heat of Fusion ($\text{kJ}\cdot\text{kg}^{-1}$)	Application methods	Objective
Mulligan et al. [185]	n-heptadecane, n-octadecane, n-nonadecane, n-eicosane.	776, 775, 784, 787	23, 27, 32, 37	2.14, 2.09, 2.09, 2.09	0.15, 0.15, 0.15, 0.15	165, 237, 191, 239	Microencapsulated PCM suspensions that 10 to 30 μm particles of microencapsulated paraffins were slurried with either water or silicone oil as working fluid	Enhance both its heat transfer characteristics and its energy storage characteristics
Birur et al. [186]	dodecane	720 (at 65 $^{\circ}\text{C}$)	-9.6	N/A	N/A	217	In combination with a variable conductance miniature LHP	Store waste heat and reduce the electric heater power
Vrable et al. [139]	paraffin	800	37	N/A	N/A	240	Encapsulated in a lightweight open cell graphite foam material that provides both high thermal conductivity and high structural stiffness and a low coefficient of thermal expansion	Eliminate additional parasitic power for thermal control and reduce the large cyclic temperature variation to more tolerable values
Shao et al. [187]	n-dodecane	N/A	-10	N/A	N/A	N/A	Integrated in an Alumina-ammonia heat pipe	Reduce the temperature fluctuation and ensure survival under extreme cold conditions during lunar eclipse
Desai et al. [143]	erythritol	1480 (solid); 1300 (liquid)	118	1.383 (solid); 1.1 (liquid)	0.733 (solid); 0.326 (liquid)	340	Fill the PCM in the micro grooves that etched in the semiconductor substrate.	Reduce the peak junction temperature and the transient temperature fluctuations
Kim et al. [168]	octadecane	814	28	2.3	0.25	244	In combination with the heat pipe and	Redistribute the temporal peak

							embedded in the honeycomb structure radiator	heat around a whole orbit period and alleviate the maximum and minimum temperatures
Yamada et al. [140]	eicosane	N/A	36.6	N/A	N/A	232	Encapsulated in a carbon fiber reinforced polymer with high-thermal conductivity	Prevent the temperature of attached components from changing drastically
Choi [141]	n-hexadecane	739 (at 70 °C)	18.2	N/A	N/A	237	Encapsulated in a fine pore aluminum honeycomb core embedded with K1100 carbon fibers	Improve the temperature stability of CubeSats in LEO
Choi [188]	octadecane	768 (at 60 °C)	28	N/A	N/A	237	Encapsulated in a fine pore aluminum honeycomb core embedded with K1100 carbon fibers	Make optical communication type of payload thermally self-sufficient for operation in the Orion Crew Module
Yun et al. [149]	paraffin	775 (solid)	55	2.38	N/A	184	Encapsulated into micro particles and then arranged in a packed bed in a vapor chamber	Function as both thermal storage medium and wick structure for capillary pumping for effective liquid return
Isaacs et al. [142]	paraffin	818	39	2.95	0.15	266	Encapsulated in aluminum casing manufactured by using DMLS of aluminum powders	Achieve stable thermal control of CubeSats
Lee et al. [147], Kabir et al. [148]	PureTemp25®	950 (solid); 860 (liquid)	About 25	N/A	0.25(solid); 0.15(liquid)	187	The PCM is charged in the multiple ultra-thin rectangular drawers	Function as either a thermal capacitor or a two-phase heat

and Xu et al.[189]								and the exterior of each drawer is wrapped with screen mesh that serves as the wick structure.	exchanger with thermal storage capability depending on the sink temperature. Reduce the temperature drops across the device and improve the reliability of system with transient high-power loads. Improve the thermal stability during transient operation. Overcome the drawback such as volume expansion, leakage and gravitational effect faced by solid-liquid PCM.
Hartsfield et al.[150]	gallium	5910	29.65	0.37	29.4	80.1		Encapsulated in Inconel 718 and 316 stainless steel enclosure	Improve the thermal stability during transient operation. Overcome the drawback such as volume expansion, leakage and gravitational effect faced by solid-liquid PCM.
Izenson et al.[144]	pentadecane, octadecane	768, 777	10, 28	N/A	N/A	206, 240		Integrated with the evaporator of heat pipes as thermal storage unit	Improve the thermal stability during transient operation. Overcome the drawback such as volume expansion, leakage and gravitational effect faced by solid-liquid PCM.
Raj et al.[151]	layered perovskite (solid-solid PCM)	1050	17.78 (heating), 20.02 (cooling)	2.23	0.38	64.75 (heating), 65.49 (cooling)		Encapsulated in the aluminum chamber with optimized fin configuration	Improve the thermal stability during transient operation. Overcome the drawback such as volume expansion, leakage and gravitational effect faced by solid-liquid PCM.
Madhav et al.[145]	eicosane	770 (liquid), 790 (solid)	35-37	N/A	0.157 (liquid), 0.35 (solid)	247		Filled in a canister module which is thermally coupled to a dual-channel axially grooved aluminum-ammonia heat pipe	Increase the operating time and reduce the peak temperature and radiator size.
Raj et al.[190]	gallium-indium eutectic metal alloy and organometallic manganese layered perovskite (solid-solid)	1129	16.42 (heating), 20.37 (cooling)	2.14	0.374	74.56 (heating), 76.32 (cooling)		The nano-encapsulated liquid gallium-indium eutectic metal alloy homogenized with an organometallic manganese layered	Avoid temperature fluctuation and ensure smooth functioning of the system.

PCM)

perovskite is
tamped in a tapered
triangular heat sink

Journal Pre-proof

Table 7

Summary of thermal radiator techniques developed for spacecrafts thermal management.

Author	Radiator type	Heat transfer path	Characteristics
Galouye et al. [152]	Deployable Radiator	Two parallel aluminum LHPs with ammonia as working fluid	The LHP condensers are directly embedded in the double-sided aluminum honeycomb radiator panel. Motorized hinge deployment mechanism based on shape memory alloy and black-painted thermo-optical coatings are adopted.
Osiander et al. [162]	MEMS-based varying emissivity radiator via louver thermal controllers	N/A	Radiator panels are mechanically positioned to modulate the effective radiation surface area via louver thermal controllers. The miniature shutter arrays can operate independently to allow digital control of the effective emissivity.
Bsibsi et al. [158]	Variable effective surface radiator based on the heat switch technology via OHP	OHP	The radiator combines three functions: heat switch, heat transport and radiator.
Demiryont et al. [165]	Variable emissivity radiator using electrochromic devices	N/A	The device exhibits two emissivity modes: a non-absorbing, low-emissivity mode and a highly absorbing, low-reflectivity high-emissivity mode. The transition between the two modes is reversible and can be controlled by varying the applied voltage level and pulse duration.
Anderson et al. [170]	Graphite fiber reinforced composites radiator	HP	A high temperature titanium-water heat pipe is designed to meet the high operating temperature up to 550 K.
Lee et al. [18]	Radiator with multi-functional lightweight panel using advanced composite material	N/A	The advanced composite material is composed of a continuous high modulus pitch-based fiber with high thermal conductance and epoxy resin with low coefficient of thermal expansion. A considerable size and weight reduction can be obtained by replacing the aluminum alloy in the radiator facesheet.
Li et al. [163]	MEMS-based variable emissivity radiator	LHP	The MEMS louver array is mounted on the high emittance radiator surface. The cooling capacity can be adjusted by simply controlling the open number of louver cells in the MEMS array.
Joshi et al. [167]	Radiator using anodized coatings	N/A	Test and evaluate the outgassing and mass loss characteristics of a specimen surfaces treated with different types of anodized coatings, including chromic acid anodized, clear anodize with polytetrafluoroethylene polymer, and black- and brown-anodized coatings.

Kim et al. [168]	A honeycomb structure radiator embedded with heat pipes and PCMs	Heat pipe	The heat pipe-PCM device is embedded inside the core of the honeycomb structure radiator to redistribute temporal peak heat within a whole orbit period through the alternate melting and freezing of PCM.
Ueno et al. [164]	Parylene-based active micro space radiator using thermal contact switch	N/A	The active radiator is developed by using the contact resistance change. Unlike conventional bulky thermal louvers/shutters, higher fill factor can be accomplished with an array of electrostatically driven micro diaphragms suspended with polymer tethers.
Velson et al. [169]	A variable heat rejection system using multiple LHPs to reject large heat loads from a single-phase MPFL	Single-phase MPFL and multiple LHPs	The evaporators of the LHPs are thermally coupled in series to the single-phase MPFL through a heat exchanger. The heat dissipation power rejected by the LHPs is controlled by the modulation of the local single-phase fluid flow rate.
Rai et al. [191]	A radiator consists of a sandwich honeycomb panel embedded with parallel tubes	Single-phase MPFL	The tubes are mounted on the honeycomb panel surface or embedded inside the panel. A manifold is used to distribute the liquid flow in tubes.
Hengeveld et al. [153]	Deployable radiators	Heat pipe	The double sided deployable thermal radiator is deployed from the side of a bus to provide additional area. The strain energy in the stowed state is utilized to deploy the composite radiator.
Ueno et al. [157]	Flexible re-deployable radiator	Micro LHP	The flexible re-deployable radiator can change its deployment angle and the radiation area depending on its temperature by shape memory alloy.
Yendler et al. [154]	Rollout deployable radiator	Heat pipe	The radiator allows heat transfer from the main body to the radiator with very little or no thermal resistance. It has much higher mass and volume efficiency than a traditional heat pipe radiator.
Taylor et al. [166]	Radiator with VO ₂ -based nanophotonic variable-emittance coating	N/A	The heat rejection regulation is realized by using a VO ₂ -based nanophotonic thermochromic variable-emittance coating. The VO ₂ thin films and the variable emitter sample show good thermal stability and resistance to thermal cycling.
Bertagne et al. [156]	A passively adaptive radiator	Single-phase MPFL	The radiator combines the thermally induced mechanical response of the shape memory alloy with a highly thermally conductive and linearly elastic biasing structure to create a radiator

panel surface that reconfigures cyclically in
response to distributed temperature changes.

Journal Pre-proof

Figure captions

- Fig. 1 Schematic of the thermal environment for electronics in spacecraft.
- Fig. 2 Thermal management technologies for spacecraft electronics.
- Fig. 3 Trends in material performance for spacecraft.
- Fig. 4 Conceptual representation of a holistic integration of nanomaterials into a complete thermal architecture.
- Fig. 5 Double wafer bonding process for GaN-on-SiC HEMTs.
- Fig. 6 Schematic of the operation of VCHP.
- Fig. 7 Schematic of (a) the conventional hot reservoir VCHP and (b) the novel loop hot reservoir VCHP.
- Fig. 8 Schematic of a hybrid capillary wick.
- Fig. 9 LHP in combination with active temperature control methods.
- Fig. 10 Schematic of the SHP.
- Fig. 11 ACCS MPFL Thermal Accommodation of a Cryocooler.
- Fig. 12 Prototype of a Multi-parallel-micro-pump developed by the Netherlands Aerospace Centre.
- Fig. 13 Schematic of (a) the conventional MPFL and (b) the novel MPFL using paraffin-actuated thermal control valves.
- Fig. 14 Schematic of the hybrid cooling loop.
- Fig. 15 Schematic of (a) a CPL and (b) the novel two-phase MPFL.
- Fig. 16 Schematic of the three promising active cooling methods.
- Fig. 17 Schematic of diamond microfluidic intra-chip cooling structure and micro-channels fabricated in GaN-on-diamond substrates.
- Fig. 18 Schematic of (a) the bottom-side microjet array cooling structure, (b) the multilayer microfluidic manifold, (c) and (d) microchannel-microjet flow through diamond-lined die backside.
- Fig. 19 Schematic of (a) the space-oriented spray cooling system and (b) the mechanism of the ejector.
- Fig. 20 Encapsulated or embedded PCMs.
- Fig. 21 PCMs in combination with other thermal control techniques.
- Fig. 22 Schematic of (a) the rigid panel deployable radiator and (b) the rollout deployable radiator.
- Fig. 23 A conceptual illustration of the morphing design and (b) an array of radiator panels in a parallel flow configuration.
- Fig. 24 MEMS-based variable emissivity radiator.

Fig. 25 Radiators combining with other thermal control devices.

Fig. 26 Payload-matched hybrid thermal management system architecture.

Journal Pre-proof

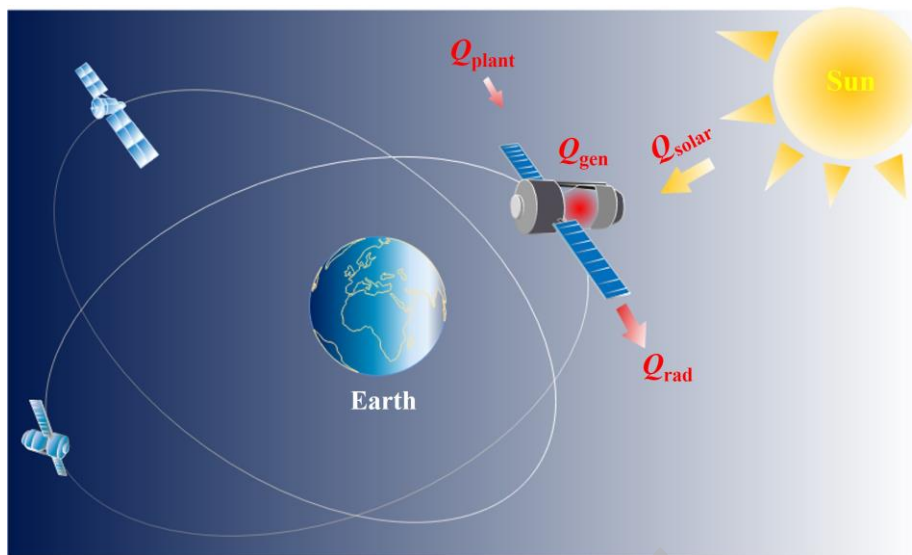


Fig.1 Schematic of the thermal environment for electronics in spacecraft.

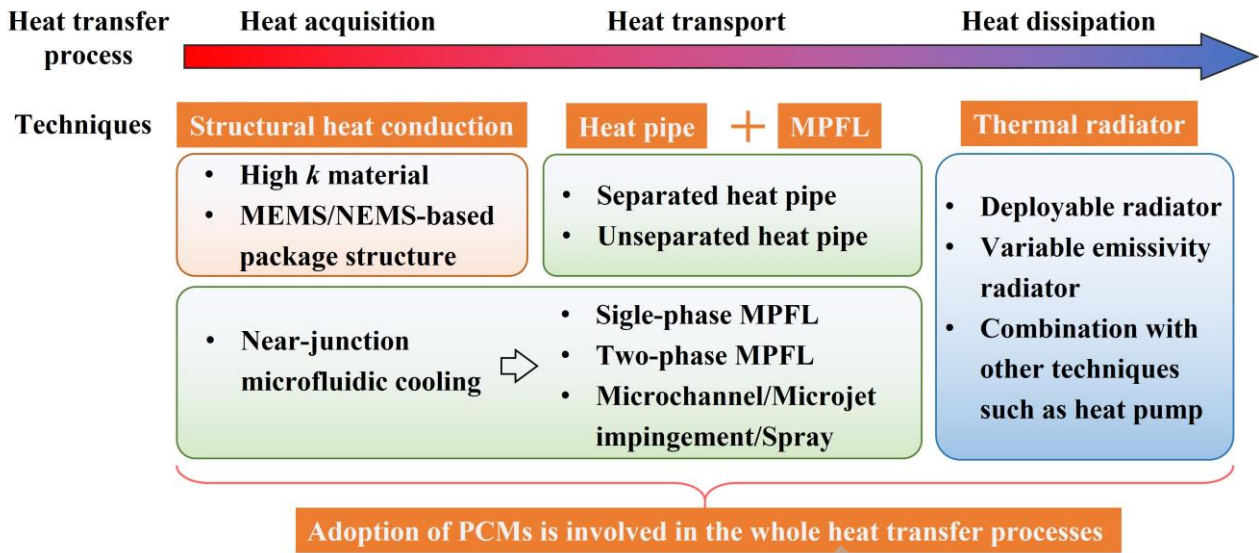


Fig. 2 Thermal management technologies for spacecraft electronics.

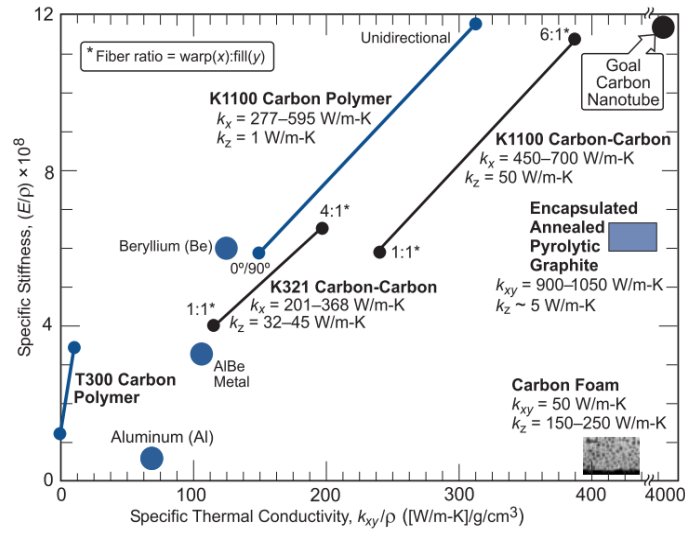


Fig. 3 Trends in material performance for spacecraft [17].

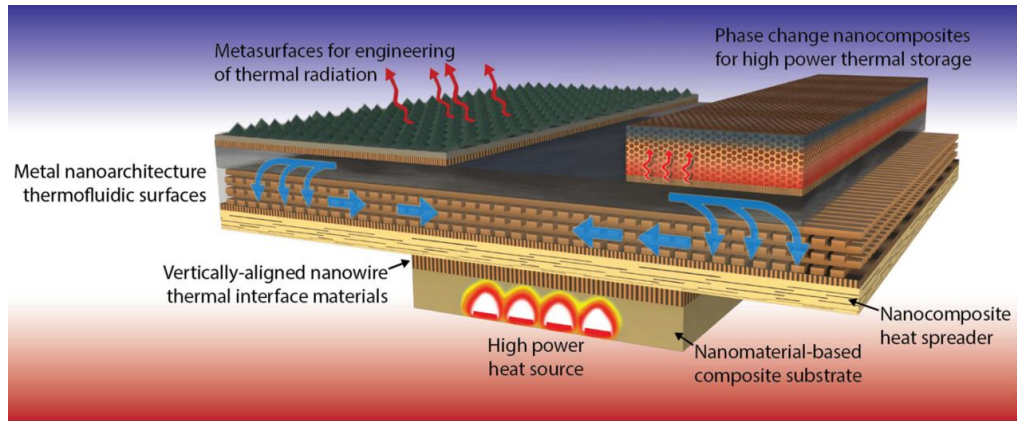


Fig. 4 Conceptual representation of a holistic integration of nanomaterials into a complete thermal architecture [26].

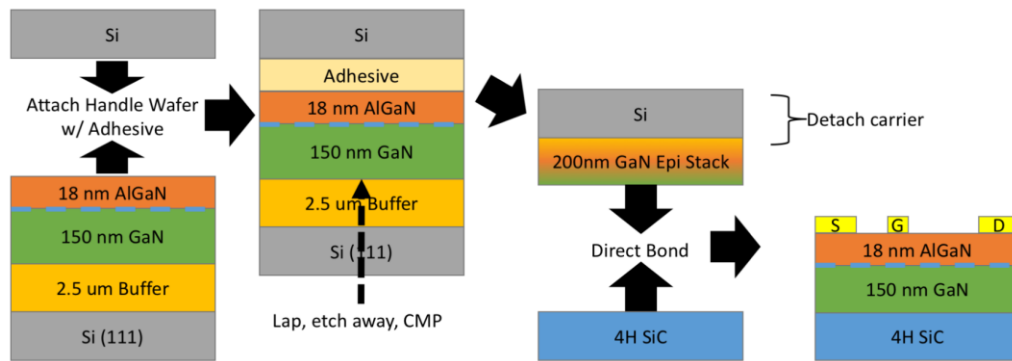


Fig. 5 Double wafer bonding process for GaN-on-SiC HEMTs [29].

Journal Pre-proof

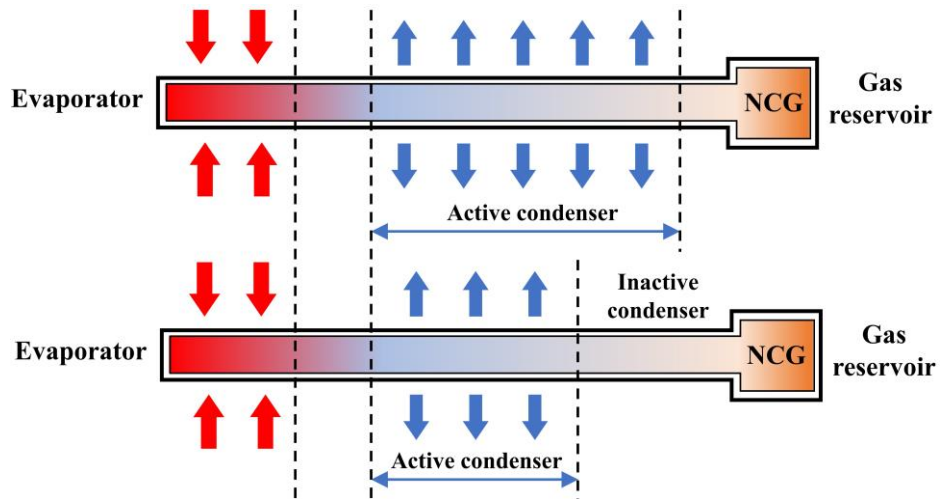


Fig. 6 Schematic of the operation of VCHP [36].

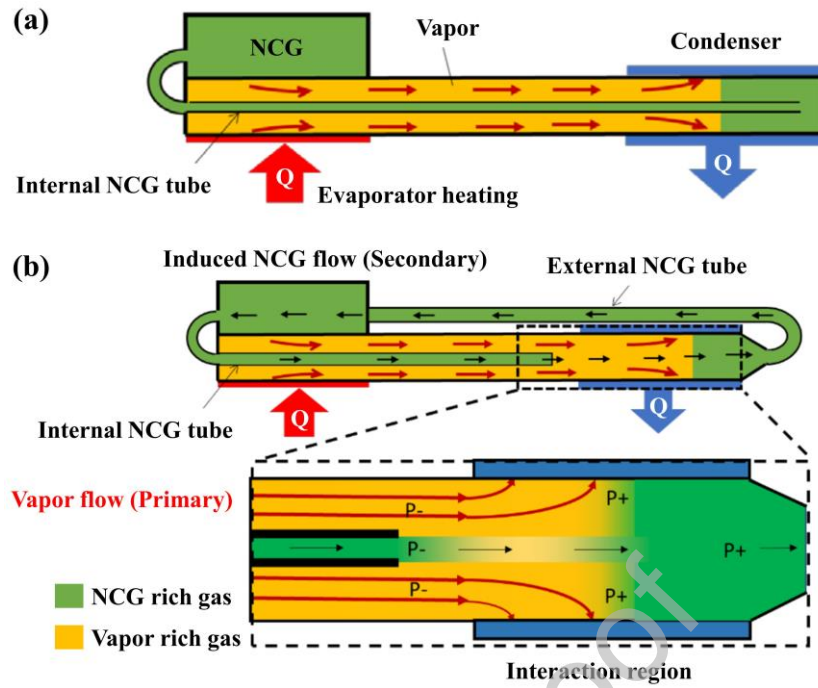


Fig. 7 Schematic of (a) the conventional hot reservoir VCHP and (b) the novel loop hot reservoir VCHP [39].

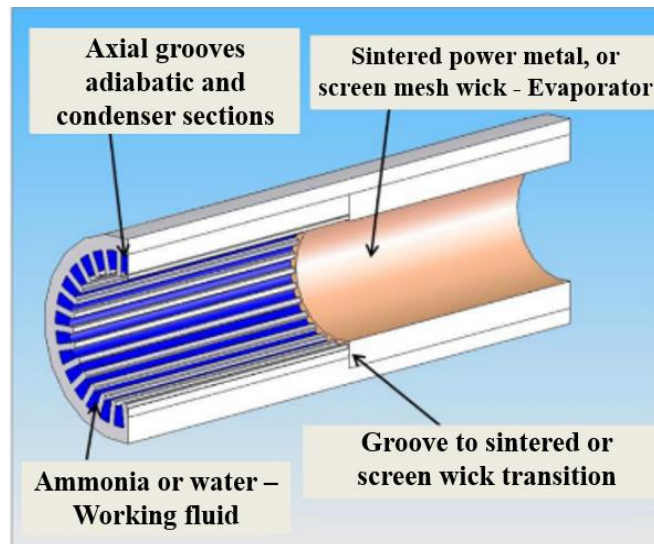


Fig. 8 Schematic of a hybrid capillary wick [36].

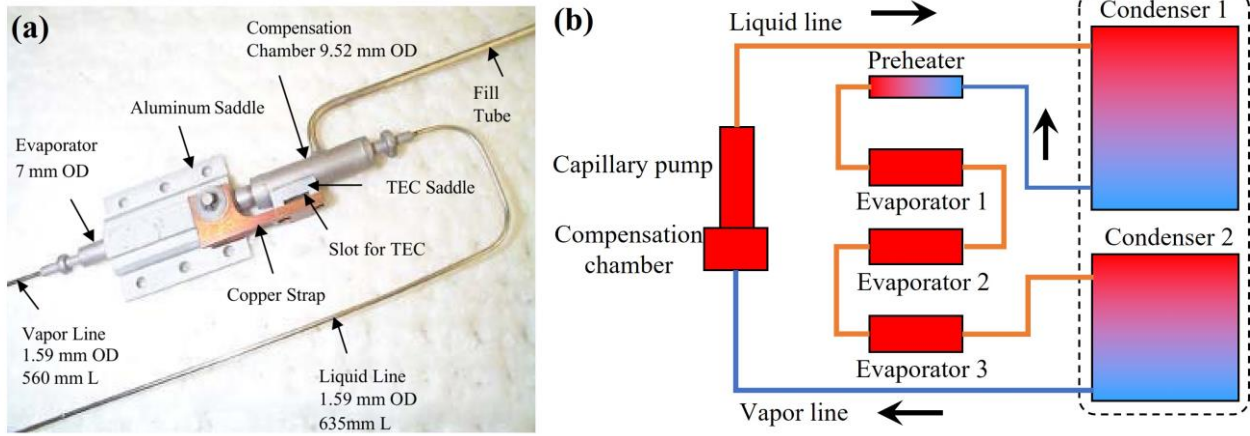


Fig. 9 LHP in combination with active temperature control methods [71, 72].

Journal Pre-proof

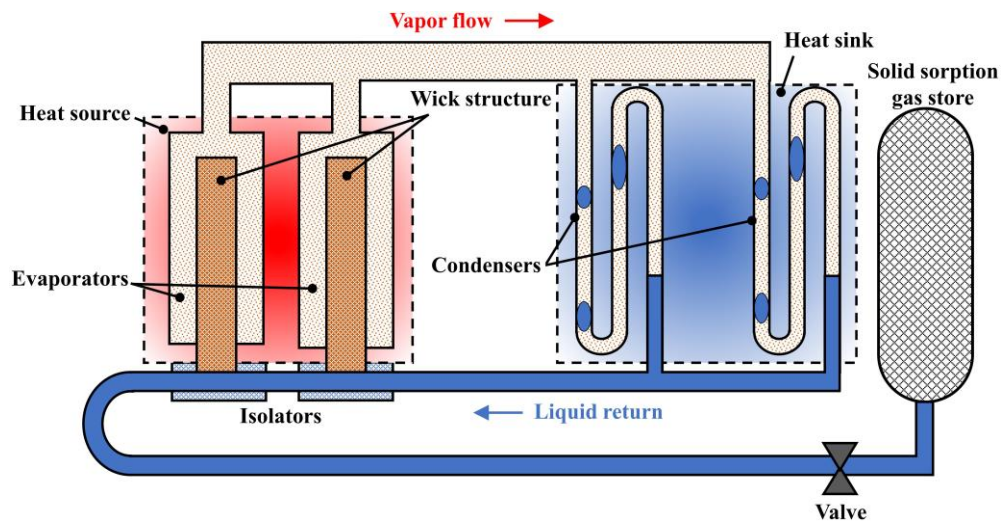
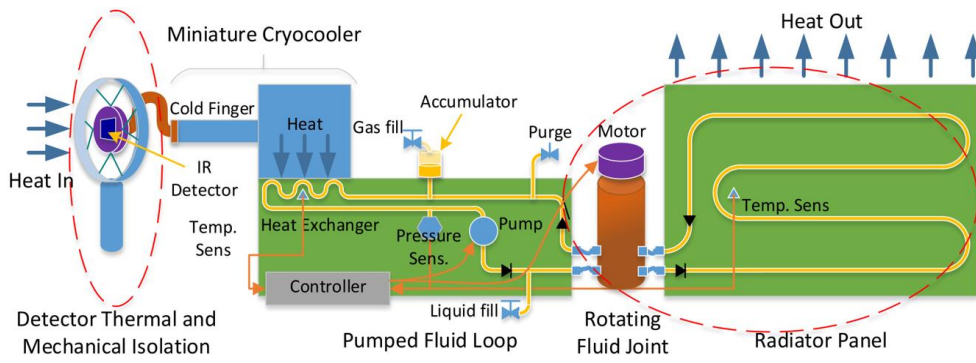


Fig. 10 Schematic of the SHP [53].



(a) ATA concepts of operations



(b) ATA Prototype

Fig. 11 ACCS MPFL Thermal Accommodation of a Cryocooler [81].

Journal Pre-proof

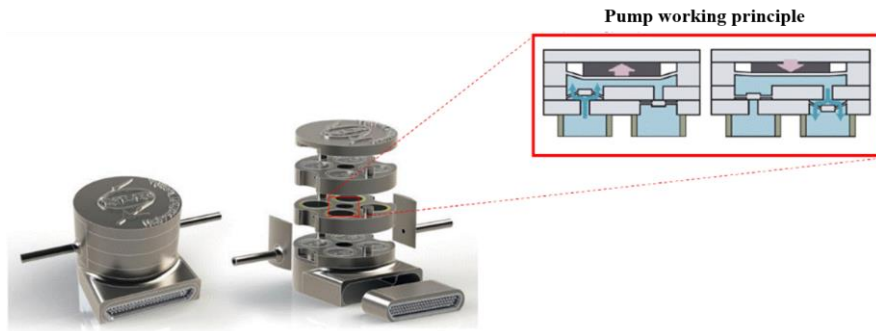
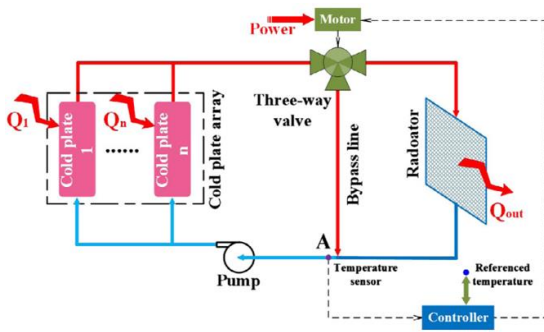
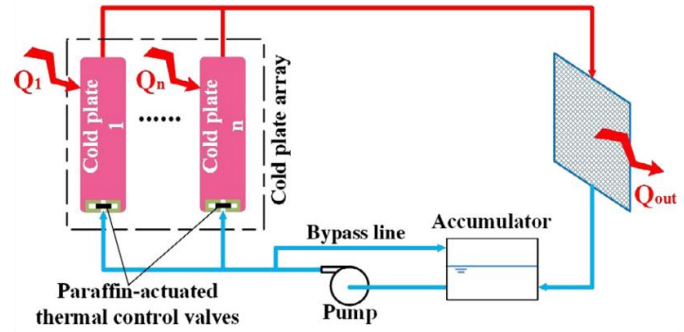


Fig. 12 Prototype of a Multi-parallel-micro-pump developed by the Netherlands Aerospace Centre [82].

Journal Pre-proof



(a) Conventional MPFL using splitting valve



(b) Novel MPFL using paraffin-actuated thermal control valves

Fig. 13 Schematic of (a) the conventional MPFL and (b) the novel MPFL using paraffin-actuated thermal control valves

[86].

Journal Pre-proof

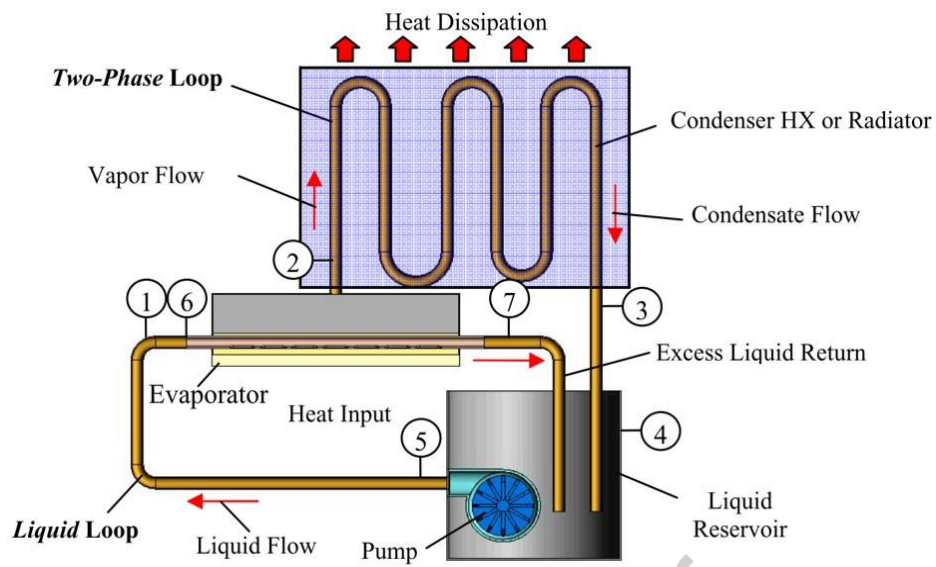


Fig. 14 Schematic of the hybrid cooling loop [96].

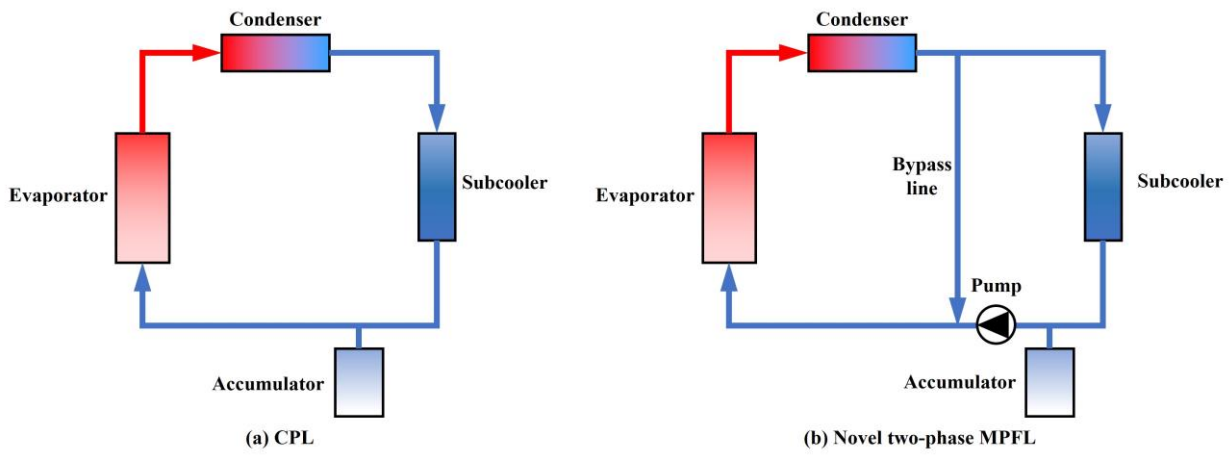


Fig. 15 Schematic of (a) a CPL and (b) the novel two-phase MPFL [97].

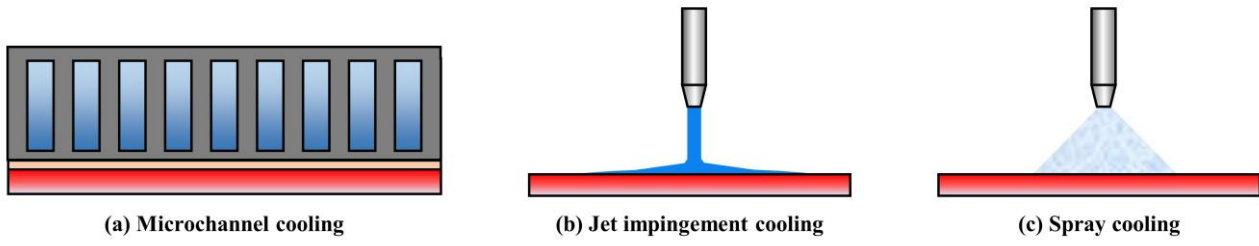


Fig. 16 Schematic of the three promising active cooling methods [14].

Journal Pre-proof

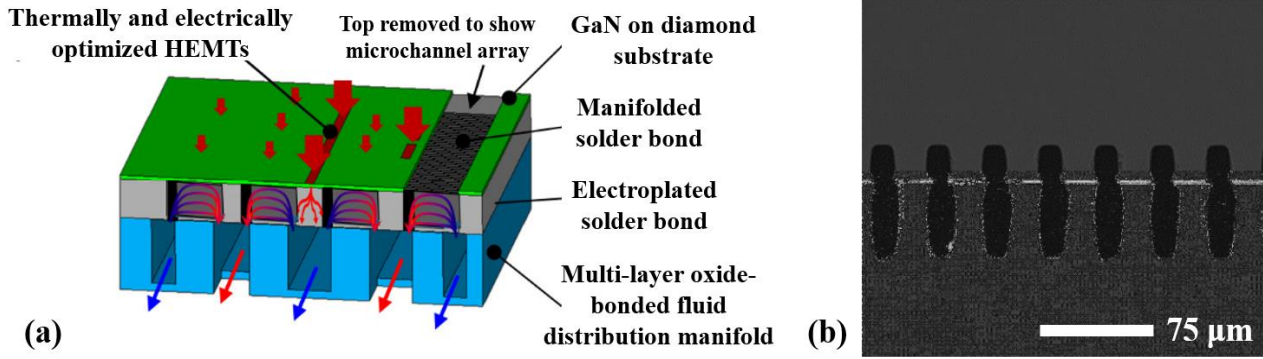


Fig. 17 Schematic of diamond microfluidic intra-chip cooling structure and micro-channels fabricated in GaN-on-diamond substrates [109].

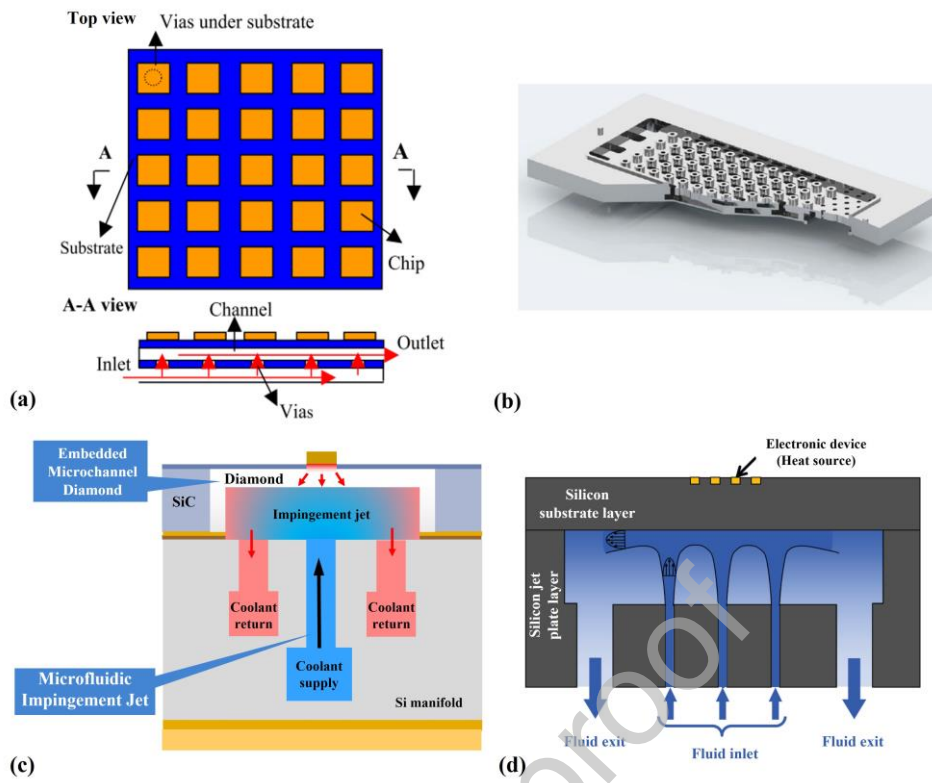


Fig. 18 Schematic of (a) the bottom-side microjet array cooling structure, (b) the multilayer microfluidic manifold, (c) and (d) microchannel-microjet flow through diamond-lined die backside [116, 117, 119, 120].

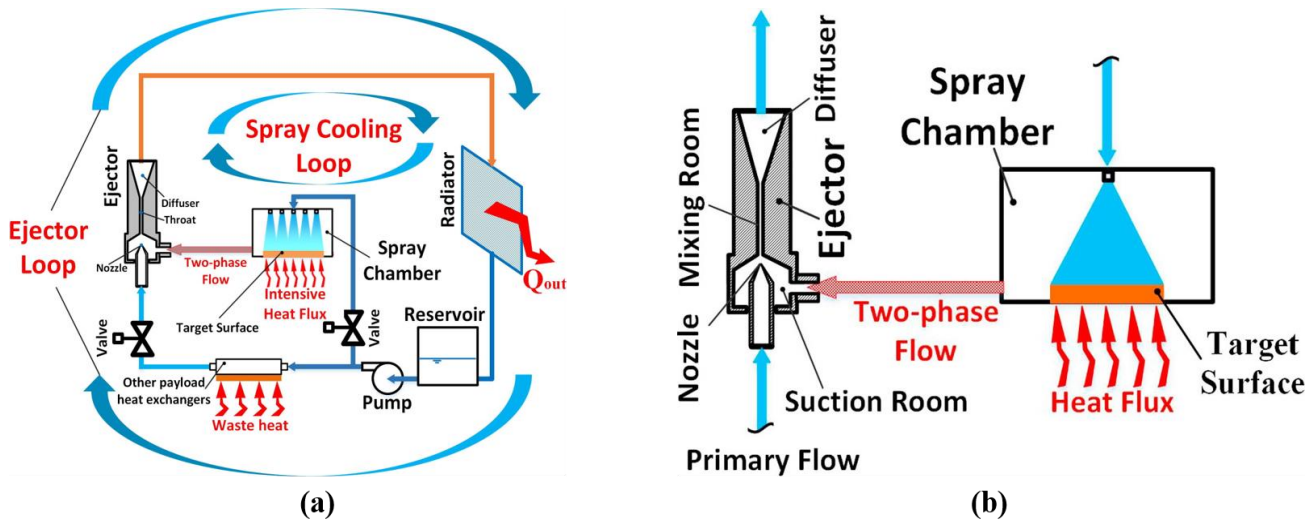


Fig. 19 Schematic of (a) the space-oriented spray cooling system and (b) the mechanism of the ejector [128, 132].

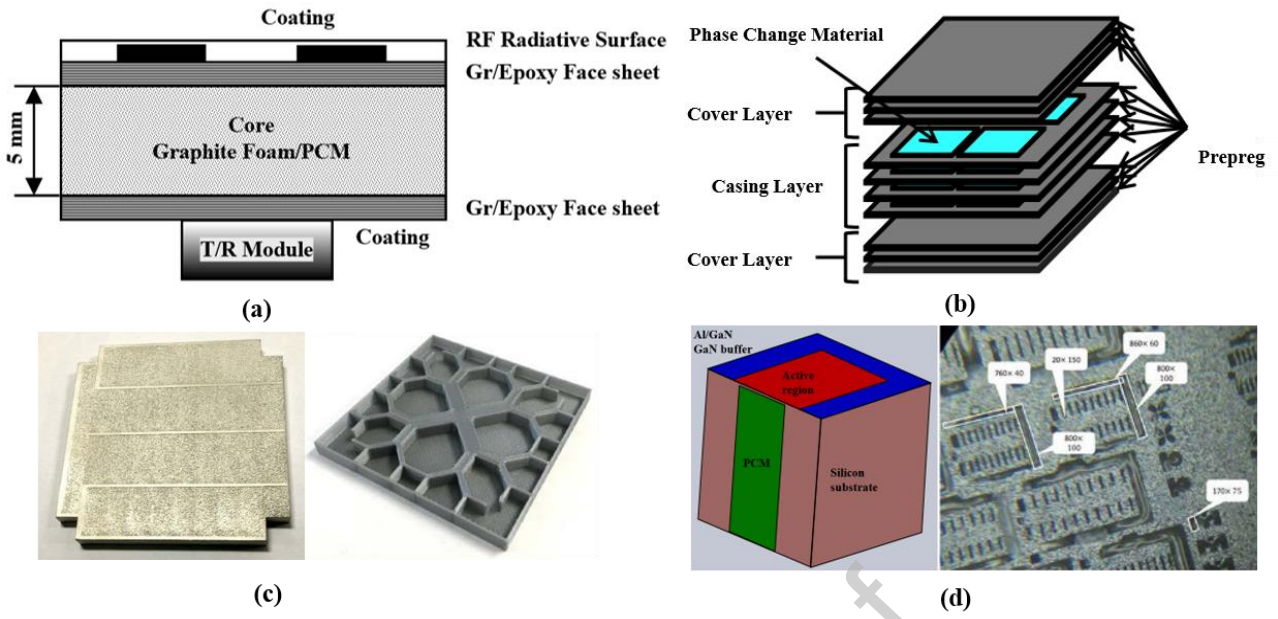


Fig. 20 Encapsulated or embedded PCMs [139, 140, 142, 143]

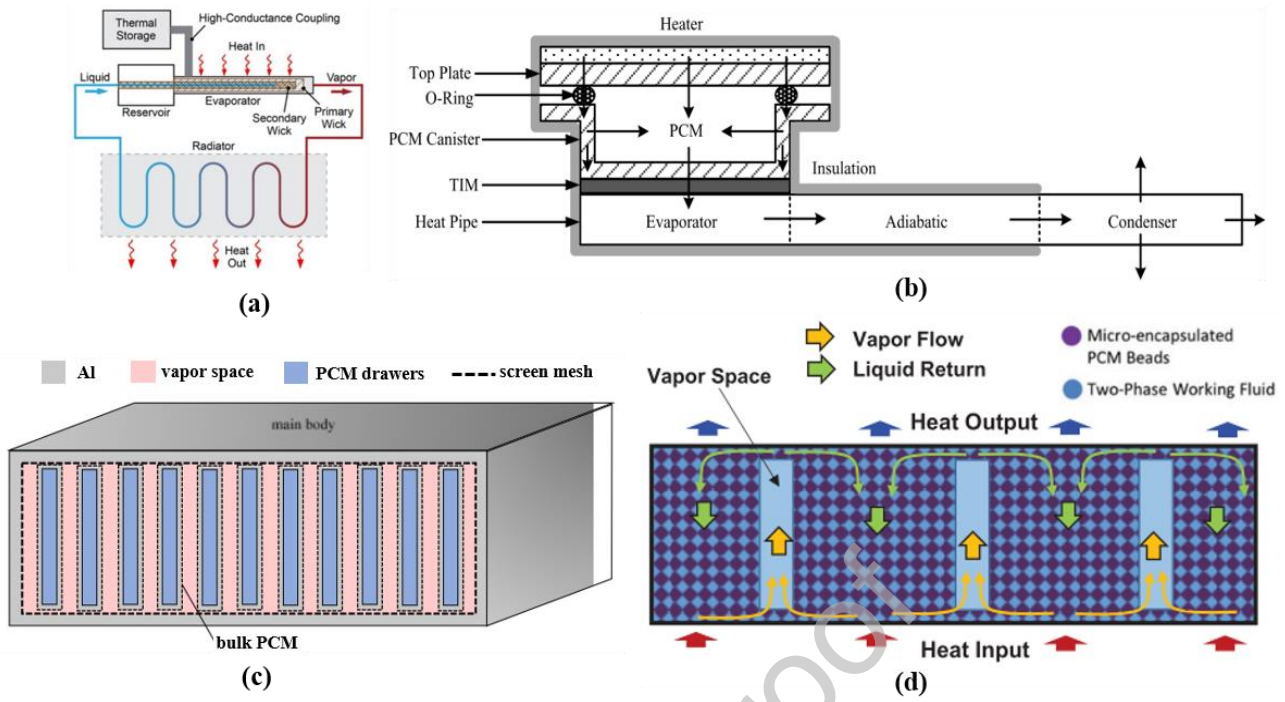


Fig. 21 PCMs in combination with other thermal control techniques [144, 145, 147, 149].

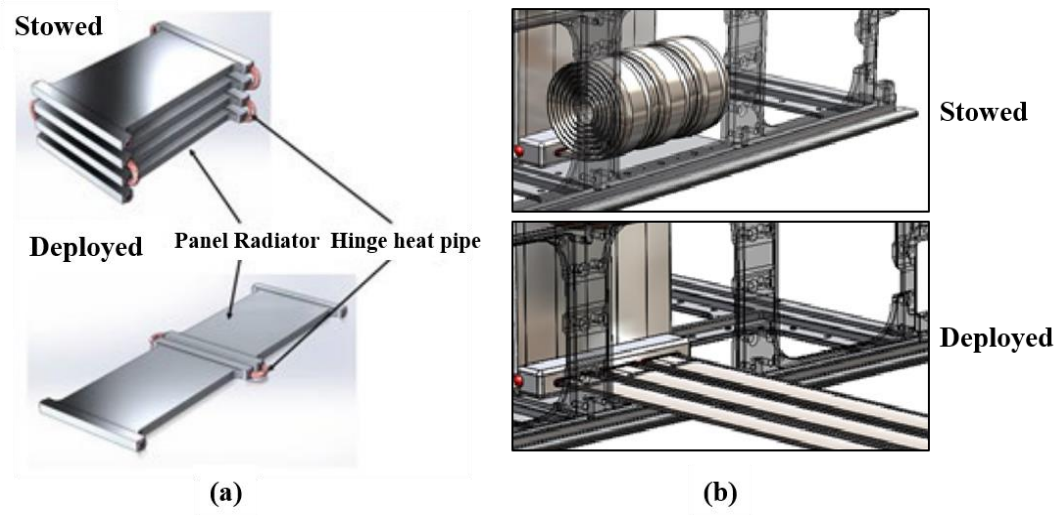


Fig. 22 Schematic of (a) the rigid panel deployable radiator and (b) the rollout deployable radiator [154].

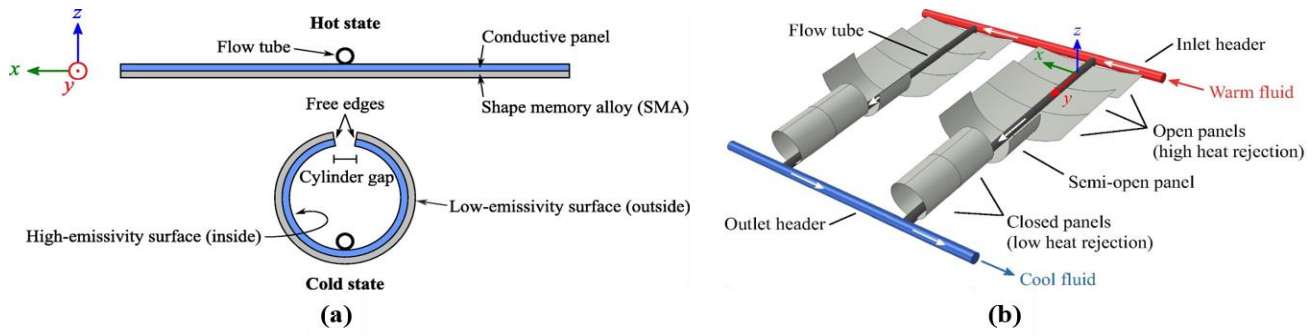


Fig. 23 (a) A conceptual illustration of the morphing design and (b) an array of radiator panels in a parallel flow configuration [156].

Journal Pre-proof

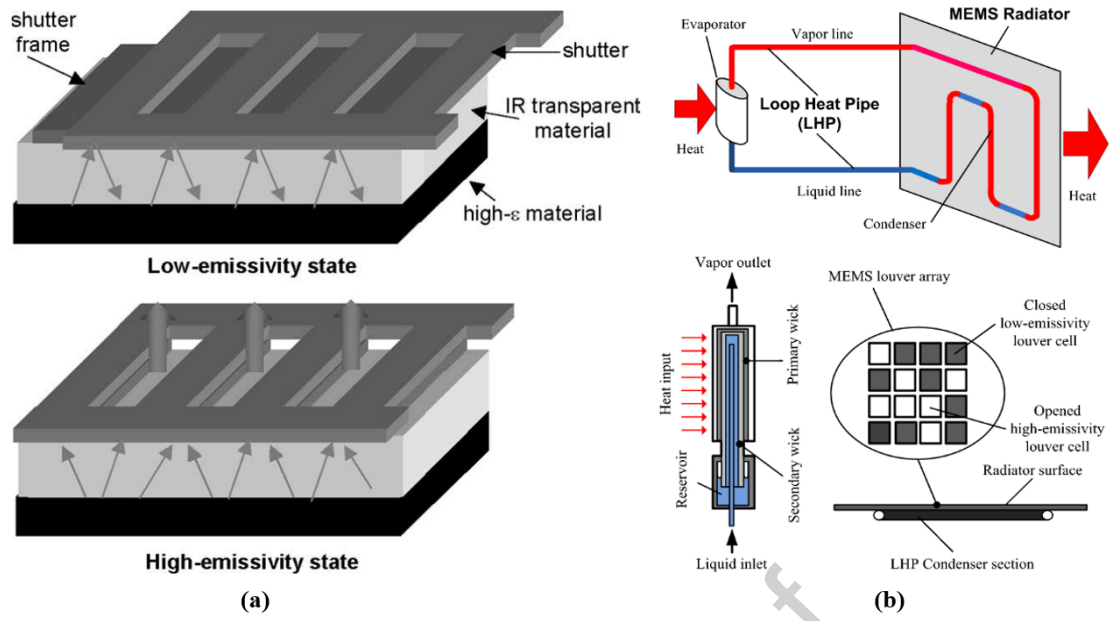


Fig. 24 MEMS-based variable emissivity radiator [162, 163].

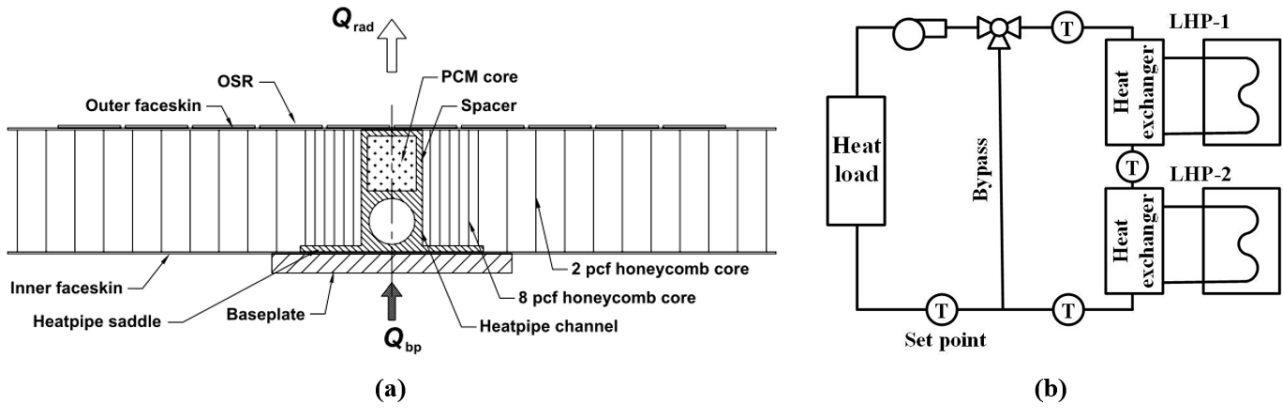


Fig. 25 Radiators combining with other thermal control devices [168, 169].

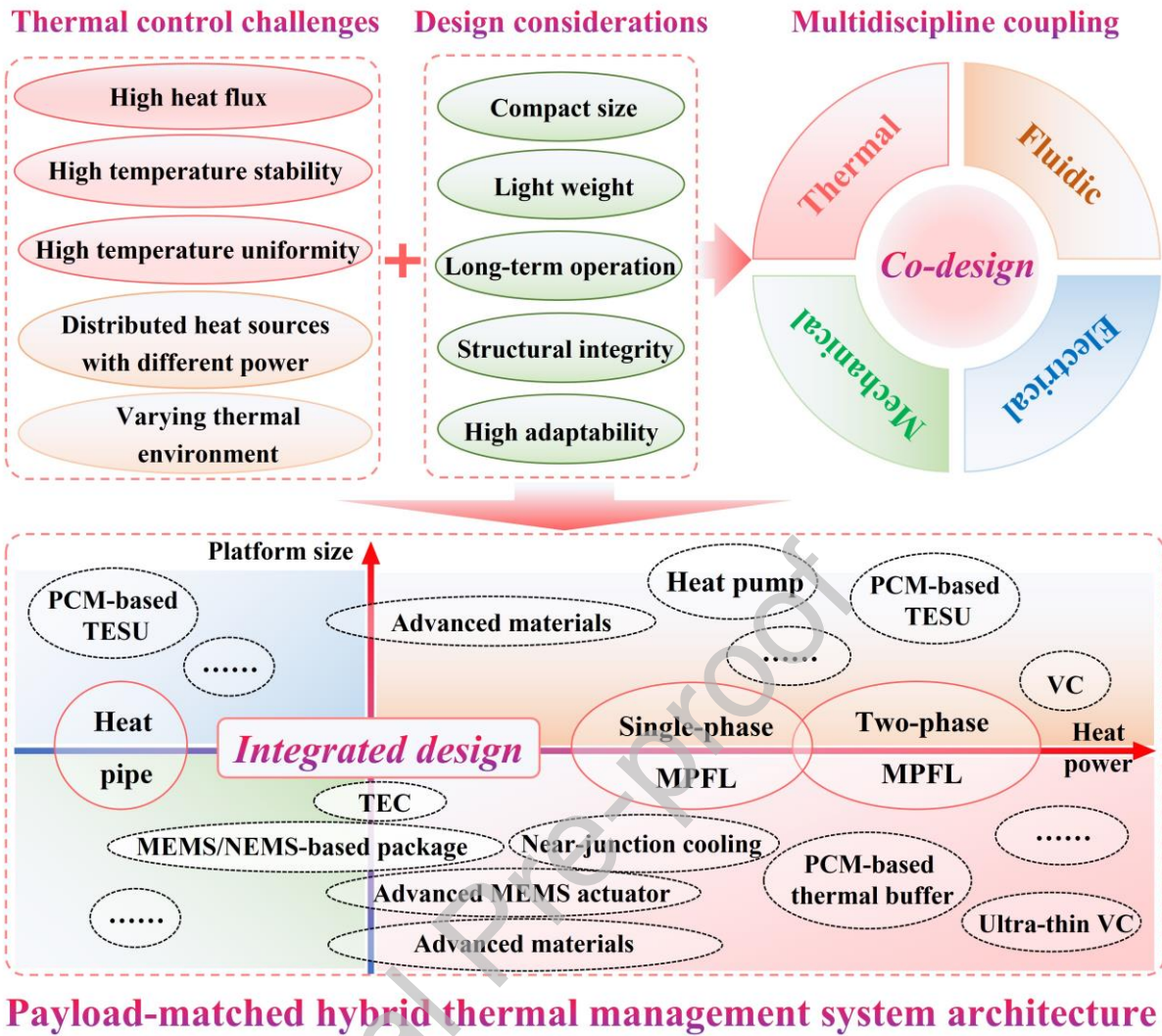


Fig. 26 Payload-matched hybrid thermal management system architecture.